INVESTIGATION OF THE ATMOSPHERIC OZONE FORMATION POTENTIALS OF SELECTED MINERAL SPIRITS SAMPLES

Final Report to
Safety-Kleen Corporation

by
William P. L. Carter, Dongmin Luo, and Irina L. Malkina

July 25, 1997

College of Engineering
Center for Environmental Research and Technology
University of California
Riverside, California 92521

97-AP-RT4V-001-FR

ABSTRACT

Environmental chamber experiments and computer model calculations were conducted to assess the atmospheric ozone formation potentials of four mineral spirits samples. Analyses of the four samples by high-resolution GC-MS, FIA type analysis, carbon number fractionation, and elemental composition indicated that they consisted primarily of C_8-C_{15} normal (5-26% by weight), branched (23-42%), and cyclic (44-52%) alkanes. Three of the samples were >98% alkane, while one sample also contained ~6% aromatics and ~2% olefins. The chamber experiments consisted of blacklight irradiations, in a dual ~5000-liter chamber, of simulated photochemical smog mixtures with and without the sample added. They employed two different reactive organic gas (ROG) surrogate mixtures to represent other organic pollutants in the atmosphere, and two different ROG/NO_x levels. All four samples inhibited OH radical levels in all experiments and inhibited rates of O_3 formation and NO oxidation in the simplified surrogate runs which are more sensitive to radical inhibition effects. However, the inhibition was somewhat less for the sample containing the aromatics and olefins than the samples consisting entirely of alkanes. The all-alkane mineral spirits had relatively small effects on ozone in the experiments using the more realistic ROG surrogate, while the aromatic and olefin-containing sample had a positive effect on ozone in the run with this surrogate at the higher NO_x levels, though it had no effect on the final ozone yield in the lower NO_x run. The results of the experiments with the all-alkane samples were similar to experiments with n-alkanes which were carried out in a previous program.

The analytical data were sufficient to determine the set of model species needed to calculate their ozone reactivities in environmental chamber and airshed simulations. However, the model underpredicted the O_3 inhibition in the runs with the simplified ROG surrogate. and overpredicted the O_3 reactivities in the runs with the more realistic surrogate. Much better simulations were obtained if the model represented the branched and cyclic alkane constituents as if they were normal alkanes. This is despite the fact that current estimation methods for atmospheric reactions of alkanes predict that branched and cyclic alkanes have mechanisms which are significantly more favorable for ozone formation than those for normal alkanes. This indicates that current reactivity scales [such as the Maximum Incremental Reactivity (MIR) scale] might be overestimating the ozone impacts of mineral spirits and similar petroleum-based mixtures by a factor of 2 or more. On the other hand, the model performed reasonably well in simulating the increase in reactivity caused by the presence of aromatics or alkenes in the sample, once it was suitably adjusted to correctly simulate all-alkane sample reactivities. It is concluded that the current methods for estimating mechanisms for the branched and cyclic alkanes are unsatisfactory and need to be studied. It is also concluded that more information is needed concerning the representativeness of the samples studied in this program to mineral spirits in general, and data are needed to improve our ability to model the atmospheric reactions of branched and cyclic alkanes.

ACKNOWLEDGEMENTS

The authors gratefully acknowledge Ms. Anne O'Donnell of the Safety-Kleen Corp. providing useful mineral spirits analysis data and for helpful discussions. Separate GC-MS analyses of the samples were also carried out by Dr Barbara Zielinska of Desert Research Institute (DRI). We also acknowledge Mr. Dennis Fitz for assistance in administering this program. Although this work was funded by the Safety-Kleen Corp, and includes data provided by Safety-Kleen and DRI, the opinions and conclusions expressed in this report are entirely those of the primary author, Dr. William P. L. Carter. Mention of trade names or commercial products do not constitute endorsement or recommendation for use.

TABLE OF CONTENTS

LIST OF TABLES

LIST OF FIGURES

INTRODUCTION

Many different types of volatile organic compounds (VOCs) are emitted into the atmosphere, each reacting at different rates and with different mechanisms. Because of this, VOCs can differ significantly in their effects on ozone formation, or their "reactivities". Therefore, VOC control strategies which take reactivity into account can potentially achieve ozone reductions in a more cost-effective manner than strategies which treat all non-exempt VOCs equally. Reactivity-based control strategies have already been implemented in the California Air Resources Board (CARB)'s Clean Fuel/Low Emissions Vehicle (CF/LEV) regulations (CARB, 1991, 1993), where reactivity adjustment factors are employed to place regulations of exhaust emissions from vehicles using alternative fuels on an equal ozone impact basis as those from vehicles using conventional gasoline. While reactivity-based control strategies have not yet been implemented for consumer product or other areas of stationary source VOC emissions, the possibility of developing such strategies is now under active consideration by the CARB staff.

Implementation of reactivity-based controls requires some means to quantify relative ozone impacts of different VOCs. This can be done using "reactivity scales", where each individual VOC is assigned a number which represents its ozone impact. However, as discussed in detail elsewhere (Carter 1991, 1994; CARB 1991, 1993), deriving such numbers is not a straightforward matter, and there are a number of uncertainties involved. One source of uncertainty in reactivity scales comes from the fact that ozone impacts of VOCs depend on the environment where the VOC is emitted. Therefore, no single reactivity scale will be applicable for all conditions. The California CF/LEV regulations utilize the "Maximum Incremental Reactivity" (MIR) scale, because it is based on quantifications of ozone impacts under conditions where VOCs have their greatest impact on ozone formation, but this is not the only scale that could be used (Carter, 1991, 1994; CARB, 1991, 1993). This will not be discussed further here except to note that given a chemical mechanism for a VOC its reactivity can be calculated for any type of scale that is deemed to be appropriate.

A second source of uncertainty comes from the complexity and uncertainties in the atmospheric processes by which emitted VOCs react to form ozone. This varies depending on the class of compound involved, and the extent to which experimental data are available for the compound(s) of interest or chemically similar species. Environmental chamber experiments play an essential role in addressing this source of uncertainty, since they provide the only means to assess as a whole all the many mechanistic factors which might affect reactivity, including the role of any reactive oxidation products formed which cannot be studied directly using currently available techniques. Because of this, control agencies and private sector groups have funded programs of environmental chamber studies to provide data needed to reduce uncertainties in reactivity assessments of the major classes of VOCs present in vehicle emissions

(Carter et al., 1993a, 1995a-c; 1997a), and selected individual VOCs of interest such as acetone (Carter et al, 1993b). A major CARB-funded study of selected species present in consumer product emissions is now underway (Carter, 1995a).

A third source of uncertainty is variability or uncertainty in the chemical composition of the VOC source being considered. This is not a factor when assessing reactivities of individual chemicals (such as, for example, acetone), but it can be significant when assessing reactivities of, for example, vehicle exhausts or mineral spirits. In the case of vehicle exhausts, methods have been developed for nearly complete speciation, and the primary source of uncertainty in this regard is variability, which can be quantified using statistical methods, and the chemical mechanistic uncertainties of the individual identified components (Carter et al, 1995d, and references therein). However, other mixtures cannot always be completely speciated, and thus compositional uncertainty may be a significant factor affecting estimates of their atmospheric reactivity.

Mineral spirits are petroleum distillate fractions which are widely used as solvents for cleaning and other applications, and methods to reliably quantify their atmospheric reactivity are of interest to companies, such as Safety-Kleen, which must cope with air quality regulations affecting their use. Unfortunately, reactivity estimates for mineral spirits are complicated with both significant compositional uncertainty, and also with uncertainty in the chemical mechanisms of their components. Although their composition vary, they typically consist of mixtures of normal, branched and cyclic alkanes in the C_8 - C_{15} range, with some samples also containing varying amounts of aromatics and small but non-negligible amounts of alkenes as well. Because of the large number of individual isomers they contain, it is rarely possible to unambiguously identify more than half the individual species present, even with extensive GC-MS analyses. While methods can be developed to estimate compositions of mineral spirit samples based on results of GC-MS analyses, GC carbon number fractionation, fluorescent indicator absorption (FIA) hydrocarbon type analyses, there will always exist a certain degree of uncertainty concerning the exact composition and the specific compounds involved.

Chemical mechanism uncertainty is also a non-negligible factor affecting estimates of mineral spirits reactivity. Although there are now data available to test chemical mechanisms for the C_8 - C_{15} n-alkanes (Carter et al., 1993a, 1995a,b, 1996) and for many of the most important aromatics (Carter et al., 1993a, 1995a,b, 1997a, Carter and Lurmann, 1991, and references therein), environmental chamber data are not available to test the estimated mechanisms for the branched or cyclic alkanes, which in many samples account for a substantial fraction of the mass present (see below). The only branched alkanes for which there are environmental chamber data of sufficient quality for mechanism evaluations are isobutane and isooctane (2,2,4-trimethylpentane), and in both cases the estimated mechanism performed poorly in predicting their reactivity, each for different reasons (Carter et al, 1993a, Carter, 1995a). However, the estimation methods may perform better in dealing with complex mixtures of branched and cyclic

compounds, where cancellation of errors may to some extent reduce the importance of uncertainties for any given compound. Nevertheless, even if we had confidence in our estimates of the composition of such a mineral spirits sample, there would still be significant uncertainty in estimates of their atmospheric reactivity.

To provide the information needed to assess whether current methods for estimating the composition and ozone formation potentials of these samples can accurately predict their actual ozone impacts, the Safety-Kleen Corporation contracted with the College of Engineering Center for Environmental Research and Technology (CE-CERT) at the University of California at Riverside to carry out an experimental and modeling study on the ozone formation potential of four selected mineral spirit samples. This involved using results of analyses of these samples to estimate their compositions, conducting environmental chamber experiments to measure the impacts on ozone formation and other measures of air quality in photochemical smog systems, and then using computer model simulations to assess whether predictions based on the estimated compositions and current atmospheric reaction mechanisms are consistent with the experimental results. The results of this study, and their implications concerning our current ability to estimate the ozone impacts of mineral spirit samples, are discussed in this report.

METHODS

Mineral Spirits Analysis

Analyses of the four mineral spirits samples were carried out by Safety-Kleen Corporation and by Dr. Barbara Zielinska of Desert Research Institute. The information they provided about the analyses they carried out is summarized below.

Data Provided by Safety-Kleen

The data provided by Safety-Kleen consisted of fluorescent indicator absorption (FIA) hydrocarbon type analyses, carbon number fractionation data by GC-FID, and high-resolution GC-MS. In addition, Safety-Kleen provided information concerning the specific gravities and an elemental analysis of the samples. The FIA hydrocarbon analysis was carried out using ASTM method D1319-95, "Hydrocarbon Types in Liquid Petroleum Products by Fluorescent Indicator Adsorption". The elemental analysis and density determinations were carried out using standard methods. Information provided by Safety-Kleen concerning the carbon number fraction and GC-MS methods is summarized below.

Carbon Number Fractionation by GC-FID. The relative percentages of hydrocarbons by carbon number were determined by high resolution gas chromatography with flame ionization detection (GC-FID). The n-alkane peaks were used to delineate the retention time segments assigned to each carbon number. The estimate of weight percent for each fraction was calculated from the area sum of that retention time span divided by the total area of the chromatogram. It should be noted that aromatics generally elute with retention times corresponding to saturated compounds with one higher carbon number, *e.g.*, toluene (C_7) elutes in the fraction attributed to C_8 species by this method. This needs to be taken into account when using such data for samples containing non-negligible amounts of aromatics.

The experimental parameters were as follows. Instrument: Hewlett-Packard Model 5890. Column: Supelco Cat. No. 2-4160 Petrocol™ DH, 100m x 0.25mm ID, 0.5µm film. Injector: 225°C, 1µL injected at a 100:1 split ratio. Detector: 300°C. Temperature Program: 5 min @ 60°C, 60→100 @ 5°/min, 2 min @ 100°, 100→200 @1.5°/min, 15 min @ 200°.

High Resolution GC-MS. High Resolution gas chromatography-mass spectroscopy (GC-MS) was utilized to provide information concerning the species present in the mineral spirits samples. The mass spectra of the separated components were used to identify or classify the species by a combination of library matching and spectral interpretation. Spectra which could be unambiguously identified were reported by name; typically these were the normal alkanes or (where applicable) individual aromatic species. Spectra in which the aliphatic ion series (29, 43, 57, 71, 85, ...) predominated were classified as

aliphatic hydrocarbons. Spectra in which the olefinic series (41, 55, 69, 83, 97, ...) predominated, indicating one degree of unsaturation, were classified as "alicyclic". These "alicyclic" compounds could be either cycloalkanes or olefins. Although no attempt was made to distinguish between them using this method, for three of the four samples studied the FIA data showed that the olefin content was negligible, indicating that these species are most likely cycloalkanes.

Quantitative estimates of component concentrations were obtained from the relative peak areas on the total ion current chromatogram (TIC). The TIC was divided into carbon number segments as for the GC-FID analysis (see discussion of results). Therefore, the GC-MS data allowed a type analysis within each carbon number fraction.

The experimental parameters were as follows: Instrument: Hewlett-Packard Model 5890 GC, Model 5970 MSD. Column: Restek Cat. No. 10244 Rtx™-5, 105m x 0.25mm ID, 0.5µm film thickness. Injector: 225°C, 1µL injected at a 100:1 split ratio. Interface: 250°C. Temperature Program: same as for GC-FID analysis. Scan Range: 20-300 amu.

Analyses Conducted by DRI

Portions of each of the four liquid mineral spirits samples were sent to Dr. Barbara Zielinska of Desert Research Institute (DRI) for GC-MS analysis and identification. The methods employed are similar to those of Safety-Kleen, and are summarized below. However, somewhat lower resolution GC method was employed, resulting in smaller number of components being separated for MS analysis. Analyses of the mass spectra of the major separated peaks were carried out by Dr. Zielinska, with assignments based on library spectra or experienced judgement.

The experimental parameters are follows: instrument: HP5890 series II GC with 5970 MSD; injection: splitless, 1µl; column: DB-5MS, 0.25µm film thickness, 60Mx0.25mm I.D. with ~0.5M megabore precolumn; temperatures: injection port 280C, transfer line 320C, initial temp 32C, final temp 280C, variable ramp rate; MSD scan mode: low mass 35, high mass 400.

Environmental Chamber Experiments

Overall Approach

The environmental chamber experiments consisted primarily of simultaneous irradiations of two model photochemical smog mixtures. The first is a "base case" experiment where a mixture of reactive organic gases (ROGs) representing those present in polluted atmospheres (the "ROG surrogate") is irradiated in the presence of oxides of nitrogen (NO_x) in air. The second is the "test" experiment which consists of irradiating the same base case mixture except that the mineral spirits sample whose reactivity is being assessed is added. The differences between the results of these experiments provide a measure

of the atmospheric impact of the test sample, and the difference relative to the amount added is a measure of its "incremental reactivity" (IR), which is quantified as discussed below.

To provide data concerning the reactivities of the samples under varying atmospheric conditions, three types of base case experiments were carried out:

1. Mini-Surrogate Experiments. This base case employed a simplified ROG surrogate and relatively low ROG/NO_x ratios. Low ROG/NO_x ratios represent "maximum incremental reactivity" (MIR) conditions, which are most sensitive to VOC effects. This is useful because it provides a sensitive test for the model, and also because it is most important that the model correctly predict a VOC sample's reactivity under conditions where the atmosphere is most sensitive to VOCs. The ROG mini-surrogate mixture employed consisted of ethene, n-hexane, and m-xylene. This same surrogate was employed in our previous studies (Carter et al, 1993a,b; 1995a,b.), and was found to provide a more sensitive test of the mechanism than the more complex surrogates which more closely represent atmospheric conditions (Carter et al, 1995b). This high sensitivity to mechanistic differences makes the mini-surrogate experiments most useful for mechanism evaluation.

2. Full Surrogate Experiments. This base case employed a more complex ROG surrogate under somewhat higher, though still relatively low, ROG/NO_x conditions. While less sensitive to some aspects of the VOCs reaction mechanism (Carter et al, 1995b), experiments with a more representative ROG surrogate are needed to evaluate the mechanism under conditions that more closely resemble the atmosphere. The ROG surrogate employed was the same as the 8-component "lumped molecule" surrogate as employed in our previous study (Carter et al., 1995b), and consists of n-butane, n-octane, ethene, propene, trans-2-butene, toluene, m-xylene, and formaldehyde. Calculations have indicated that use of this 8-component mixture will give essentially the same results in incremental reactivity experiments as actual ambient mixtures (Carter et al., 1995b).

3. Full Surrogate, low NO_x Experiments. This base case employs the same 8-component lumped molecule surrogate as the full surrogate experiments described above, except that lower NO_x levels (higher ROG/NO_x ratios) were employed to represent NO_x-limited conditions. Such experiments are necessary to assess the ability of the model to properly simulate reactivities under conditions where NO_x is low. The initial ROG and NO_x reactant concentrations were comparable to those employed in our previous studies (Carter et al. 1995b).

An appropriate set of control and characterization experiments necessary for assuring data quality and characterizing the conditions of the runs for mechanism evaluation were also carried out. These are discussed where relevant in the results or modeling methods sections.

Environmental Chamber

The environmental chamber system employed in this study was the CE-CERT "Dividable Teflon Chamber" (DTC) with a blacklight light source. This consists of two ~5000-liter 2-mil heat-sealed FEP Teflon reaction bags located adjacent to each other and fitted inside an 8'x8'x8' framework, and which uses two diametrically opposed banks of 32 Sylvania 40-W BL black lights as the light source. The lighting system in the DTC was found to provide so much intensity that only half the lights were used for irradiation. The unused black lights were covered with aluminum foil, and were used to bring the chamber up to the temperature it will encounter during the irradiation before the uncovered lights are turned on. (The light banks used were switched in the middle of the study, as discussed below.) The air conditioner for the chamber room was turned on before and during the experiments. Four air blowers which are located in the bottom of the chamber were used to help cool the chamber as well as mix the contents of the chamber. The CE-CERT DTC is very similar to the SAPRC DTC which is described in detail elsewhere (Carter et al, 1995b,e).

The DTC is designed to allow simultaneous irradiations of the base case and the test experiments under the same reaction conditions. Since the chamber is actually two adjacent FEP Teflon reaction bags, two mixtures can be simultaneously irradiated using the same light source and with the same temperature control system. These two reaction bags are referred to as the two "sides" of the chamber (Side A and Side B) in the subsequent discussion. The sides are interconnected with two ports, each with a box fan, which rapidly exchange their contents to assure that base case reactants have equal concentrations in both sides. In addition, a fan is located in each of the reaction bags to rapidly mix the reactants within each chamber. The ports connecting the two reactors can then be closed to allow separate injections and irradiations on each side. This design is optimized for carrying out incremental reactivity experiments such as those for this program.

Both of the Teflon reaction bags in the DTC chamber were replaced in the period between runs DTC-471 and DTC-472. The framework holding the reaction bags was modified somewhat so that the reaction bags would always be under slight positive pressure, so that any leakage that may occur would result in the chamber collapsing, rather than dilution of the contents with laboratory air. At the same time, the bank of blacklights used to irradiate the chamber were changed. This was done because of a loss of light intensity in the chamber, attributable to the aging of the lights which have been employed in essentially all runs since the chamber was constructed in early 1994. The set of lights used in the runs after DTC-471 had been rarely used previously, and this resulted in higher light intensities measured in the chamber in the later set of runs.

Experimental Procedures

The reaction bags were flushed with dry air produced by an AADCO air purification system for 14 hours (6pm-8am) on the nights before experiments. The continuous monitors were connected prior to

reactant injection and the data system began logging data from the continuous monitoring systems. The reactants were injected as described below (see also Carter et al, 1993a,, 1995e). The common reactants were injected in both sides simultaneously using a three-way (one inlet and two outlets connected to side A and B respectively) bulb of 2 liters in the injection line and were well mixed before the chamber was divided. The contents of each side were blown into the other using two box fans located between them. Mixing fans were used to mix the reactants in the chamber during the injection period, but these were turned off prior to the irradiation. The sides were then separated by closing the ports which connected them, after turning all the fans off to allow their pressures to equalize. After that, reactants for specific sides (the test sample in the case of reactivity experiments) were injected and mixed. The irradiation began by turning on the lights and proceeded for 6 hours. After the run, the contents of the chamber were emptied by allowing the bag to collapse, and it was then flushed with purified air. The contents of the reactors were vented into a fume hood.

The procedures for injecting the various types of reactants were as follows. The NO and NO_2 were prepared for injection using a high vacuum rack. Known pressure of NO, measured with MKS Baratron capacitance manometers, were expanded into Pyrex bulbs with known volumes, which were then filled with nitrogen (for NO) or oxygen (for NO2). The contents of the bulbs were then flushed into the chamber with AADCO air. The other gas reactants were prepared for injection either using a high vacuum rack or gas-tight syringes whose amounts were calculated. The gas reactants in a gas-tight syringe were usually diluted to 100-ml with nitrogen in a syringe. The volatile liquid reactants were injected, using a micro syringe, into a 1-liter Pyrex bulb equipped with stopcocks on each end and a port for the injection of the liquid. The port was then closed and one end of the bulb was attached to the injection port of the chamber and the other to a dry air source. The stopcocks were then opened, and the contents of the bulb were flushed into the chamber with a combination of dry air and heat gun for approximately 5 minutes. Formaldehyde was prepared in a vacuum rack system by heating paraformaldehyde in an evacuated bulb until the pressure corresponded to the desired amount of formaldehyde. The bulb was then closed and detached from the vacuum system and its contents were flushed into the chamber with dry air through the injection port.

Since the mineral spirits consist of many high boiling point components and may fractionate if not completely injected, a heated injection system was employed for injecting these samples. This consisted of a three way glass tube surrounded with heat tape. The desired amount of the liquid sample, measured using a microliter syringe, was injected into one port of the tube. The tube was then flushed with purified dry air at 2 liters per minute for about 15 minutes, and portion of the tube containing the sample was heated to approximately 200 °C. During this time the sample evaporated and passed into the chamber.

Analytical Methods

Ozone and nitrogen oxides (NO_x) were continuously monitored using commercially available continuous analyzers with Teflon sample lines inserted directly into the chambers. The sampling lines from each side of the chamber were connected to solenoids which switched from side to side every 10 minutes, so the instruments alternately collected data from each side. Ozone was monitored using a Dasibi 1003AH UV photometric ozone analyzer and NO and total oxides of nitrogen (including HNO_3 and organic nitrates) were monitored using a Teco Model 14B chemiluminescent NO/NO_x monitor. The output of these instruments, along with that from the temperature sensors and the and formaldehyde instrument, were attached to a computer data acquisition system, which recorded the data at 10 minutes intervals for ozone, NO and temperature (and at 15 minutes for formaldehyde), using 30 second averaging times. This yielded a sampling interval of 20 minutes for taking data from each side.

The Teco instrument and Dasibi CO analyzer were calibrated with a certified NO and CO source and CSI gas-phase dilution system. It was done prior to chamber experiment for each run. The NO_2 converter efficiency check was carried out in regular intervals. The Dasibi ozone analyzer was calibrated approximately every three months using a transfer standard, and was checked with an ozone generator set to 400 ppb for each experiment to assure that it worked properly. The details were discussed elsewhere (Carter et al, 1995e)

A Ratfisch model RS55 total carbon analyzer, employing flame ionization detection, was employed during run DTC-476 and those following (i.e., for the full surrogate but not the mini-surrogate runs). The instrument was calibrated with methane.

Organic reactants other than formaldehyde were measured by gas chromatography with FID detectors as described elsewhere (Carter et al. 1993a; 1995e). GC samples were taken for analysis at intervals from 20 minutes to 30 minutes either using 100 ml gas-tight glass syringes or by collecting the 100 ml sample from the chamber onto a Tenax-GC solid adsorbent cartridge. These samples were taken from ports directly connected to the chamber after injection and before irradiation and at regular intervals after irradiation. The sampling method employed for injecting the sample onto the GC column depended on the volatility or "stickiness" of the compound. For analysis of the more volatile species, which includes all the base ROG surrogate compounds employed in this study (except for formaldehyde), the contents of the syringe were flushed through a 2 ml or 3 ml stainless steel or 1/8’ Teflon tube loop and subsequently injected onto the column by turning a gas sample valve.

The GC systems employed for routine analyses during the chamber experiments lacked the resolution required to separate the many mineral spirits components, so no attempt was made to separately monitor them during the individual chamber runs. However, an indication of the total amount of mineral spirits vapors present in the chamber can be obtained from the integrated area under the entire mass of

overlapping GC peaks caused by the mineral spirits components. This major mass of mineral spirit component peaks was sufficiently well separated from the peaks for the base ROG surrogate components for this to be possible. This was calibrated in two ways: (1) by assuming that the per-carbon response for the mineral spirits components was the same as that measured around the same time period for n-octane, or (2) by injecting known amounts of the mineral spirits into the chamber. The amount of mineral spirits components (as ppm carbon) were calculated from the microliters sample injected, given the densities of the samples and the elemental analysis data provided by Safety-Kleen (see Results).

The calibrations for the GC analyses for most compounds were carried out by sampling from chambers or vessels of known volume into which known amounts of the reactants were injected, as described previously (Carter et al, 1995e).

Characterization Methods

Three temperature thermocouples for each chamber were used to monitor the chamber temperature, two of which were located in the sampling line of continuous analyzers to monitor the temperature in each side. The third one was located in the chamber to monitor chamber temperature. The temperature in these experiment was typically 21-25°C.

The light intensity in the DTC chamber was monitored by periodic NO_2 actinometry experiments utilizing the quartz tube method of Zafonte et al (1977), with the data analysis method modified as discussed by Carter et al. (1995e). The spectrum of the blacklight light source has been measured periodically using a LiCor LI-1200 spectra radiometer, and found not to vary significantly with time, being essentially the same as the general blacklight spectrum recommended by Carter et al (1995e) for use in modeling blacklight chamber experiments.

The dilution of the DTC chamber due to sampling is expected to be small because the flexible reaction bags can collapse as samples are withdrawn for analysis. However, some dilution occurs with the aging of reaction bags because of small leaks. Information concerning dilution in an experiment can be obtained from relative rates of decay of added VOCs which react with OH radicals with differing rate constants (Carter et al., 1993a; 1995e). Most experiments had a more reactive compound such as m-xylene and n-octane present either as a reactant or added in trace amounts to monitor OH radical levels. Trace amounts (~0.1 ppm) of n-butane were also added to experiments if needed to provide a less reactive compound for monitoring dilution. In addition, specific dilution check experiments such as CO experiments were carried out. Based on these results, the dilution rates were found to average ~0.5% per hour on both sides for the experiments prior to DTC-471. Because of the redesign of the system holding the reaction bags between DTC-471 and DTC-472, the dilution was assumed to be negligible in the chamber for the runs after DTC-471. This is consistent with the limited dilution data for the experiments with the chamber in this configuration.

Reactivity Data Analysis Methods

The results of the environmental chamber experiments are analyzed to yield two measures of reactivity for the mineral spirits samples. The first is the effect of the sample on the change in the quantity $[O_3]$-[NO], or $([O_3]_t$-$[NO]_t)$-$([O_3]_0$-$[NO]_0)$, which is abbreviated as $d(O_3$-NO) in the subsequent discussion. As discussed elsewhere (e.g., Johnson, 1983; Carter and Atkinson, 1987; Carter and Lurmann, 1990, 1991, Carter et al, 1993a, 1995a,b), this gives a direct measure of the amount of conversion of NO to NO_2 by peroxy radicals formed in the photooxidation reactions, which is the process that is directly responsible for ozone formation in the atmosphere. (Johnson calls it "smog produced" or "SP".) The incremental reactivity of the sample relative to this quantity, which is calculated for each hour of the experiment, is given by

$$IR[d(O_3\text{-NO})]_t^{VOC} = \frac{d(O_3\text{-NO})_t^{test} - d(O_3\text{-NO})_t^{base}}{[VOC]_0} \qquad (I)$$

where $d(O_3$-$NO)_t^{test}$ is the $d(O_3$-NO) measured at time t from the experiment where the test sample was added, $d(O_3$-$NO)_t^{base}$ is the corresponding value from the corresponding base case run, and $[VOC]_0$ is the amount of test sample added. The units used are ppm for O_3 and NO, and ppmC for $[VOC]_0$, so the incremental reactivity units are moles of O_3 formed and NO oxidized per mole carbon sample added. An estimated uncertainty for IR[$d(O_3$-NO)] is derived based on assuming an ~3% uncertainty or imprecision in the measured $d(O_3$-NO) values. This is consistent with the results of the side equivalency tests, where equivalent base case mixtures are irradiated on each side of the chamber.

Note that reactivity relative to $d(O_3$-NO) is essentially the same as reactivity relative to O_3 in experiments where O_3 levels are high, because under such conditions $[NO]_t^{base} \approx [NO]_t^{test} \approx 0$, so a change $d(O_3$-NO) caused by the test sample is due to the change in O_3 alone. However, $d(O_3$-NO) reactivity has the advantage that it provides a useful measure of the effect of the sample on processes responsible for O_3 formation even in experiments where O_3 formation is suppressed by relatively high NO levels.

The second measure of reactivity is the effect of the sample on integrated hydroxyl (OH) radical concentrations in the experiment, which is abbreviated as "IntOH" in the subsequent discussion. This is an important factor affecting reactivity because radical levels affect how rapidly all VOCs present, including the base ROG components, react to form ozone. If a compound is present in the experiment which reacts primarily with OH radicals, then the IntOH at time t can be estimated from

$$IntOH_t = \int_0^t [OH]_\tau \, d\tau = \frac{\ln\left(\frac{[tracer]_0}{[tracer]_t}\right) - D\,t}{kOH^{tracer}} , \qquad (II)$$

where $[tracer]_0$ and $[tracer]_t$ are the initial and time=t concentrations of the tracer compound, kOH^{tracer} is its OH rate constant, and D is the dilution rate in the experiments. The latter was found to be small and

was neglected in our analysis. The concentration of tracer at each hourly interval was determined by linear interpolation of the experimentally measured values. M-xylene was used as the OH tracer in these experiments because it is a base case component present in all incremental reactivity experiments, its OH rate constant is known (the value used was 2.36×10^{-11} cm^3 $molec^{-1}$ s^{-1} [Atkinson, 1989]), and it reacts sufficiently rapidly that its consumption rate can be measured with reasonable precision.

The effect of the mineral spirits sample on OH radicals can thus be measured by its IntOH incremental reactivity, which is defined as

$$IR[IntOH]_t = \frac{IntOH_t^{test} - IntOH_t^{base}}{[VOC]_0} \qquad \text{(III)}$$

where $IntOH_t^{test}$ and $IntOH_t^{base}$ are the IntOH values measured at time t in the added sample and the base case experiment, respectively. The results are reported in units of 10^6 min per ppm carbon. The uncertainties in IntOH and IR[IntOH] are estimated based on assuming an ~2% imprecision in the measurements of the m-xylene concentrations. This is consistent with the observed precision of results of replicate analyses of this compound.

Modeling Methods

General Atmospheric Photooxidation Mechanism

Ozone formation in photochemical smog is due to the gas-phase reactions of oxides of nitrogen (NO_x) and various reactive organic gases (ROGs) in sunlight. Various reaction schemes have been developed to represent these processes (e.g., Gery et al., 1988; Carter, 1990; Stockwell et al., 1990), but the one used as the starting point for this work was an updated version of the detailed SAPRC mechanism (Carter, 1990, 1995b; Carter et al., 1993b, 1997a). This is detailed in the sense that it explicitly represents a large number of different types of organic compounds, but it uses a condensed representation for most of their reactive products. The major characteristics of this mechanism are described by Carter (1990). The reactions of inorganics, CO, formaldehyde, acetaldehyde, peroxyacetyl nitrate, propionaldehyde, peroxypropionyl nitrate, glyoxal and its PAN analog, methyl glyoxal (model species 'MGLY"), and several other product compounds are represented explicitly. The reactions of unknown photoreactive products formed in the reactions of aromatic hydrocarbons are represented by model species whose yields and photolysis rate are adjusted based on fits of model simulations to environmental chamber experiments. A "chemical operator" approach is used to represent peroxy radical reactions. Generalized reactions with variable rate constants and product yields are used to represent the primary emitted alkane, alkene, aromatic, and other VOCs (with rate constants and product yields appropriate for the individual compounds being represented in each simulation). Most of the higher molecular weight oxygenated product species are represented using the "surrogate species" approach, where simpler molecules such as propionaldehyde or 2-butanone are used to represent the reactions of higher molecular weight analogues that are assumed to react similarly.

The mechanism of Carter (1990) was updated several times prior to this work. A number of changes were made to account for new kinetic and mechanistic information for certain classes of compounds as described by Carter et. al. (1993b) and Carter (1995b). Further modifications to the uncertain portions of the mechanisms for the aromatic hydrocarbons were made to satisfactorily simulate results of experiments carried out using differing light sources (Carter et al. 1997a). The latest version of the general mechanism is discussed by Carter et al. (1997a).

Representation of Normal, Branched, and Cyclic Alkanes

The results of the analyses of the mineral spirits indicate that their major components are normal, branched, and cyclic alkanes in the C_9-C_{14} range. Because of their importance in these samples, our current understanding of the atmospheric chemistry of alkanes, and the representation of their reactions in the model simulations, will be discussed in some detail. Much of this is taken from the discussion of Carter et al. (1996) concerning normal alkanes, and that report can be consulted for more information.

Atmospheric Reactions of Alkanes

The only significant gas-phase atmospheric reaction of alkanes is the reaction with OH radicals (Atkinson, 1989, 1990). Alkanes do not absorb light in the wavelength region provided by ground-level sunlight ($\lambda \geq 300$ nm) (Calvert and Pitts, 1966), and rate constants for their reactions with other reactive atmospheric species (e.g., O_3, NO_3 radicals, $O(^3P)$ atoms) are too low for them to be of significance (Atkinson and Carter, 1984; Atkinson, 1990, 1991). Rate constants for OH radical reactions have been measured for the n-alkanes up to C_{13}, and for various branched alkane isomers up to ~C_8. Based on this information, Atkinson (1987) developed a structure-estimation method which can be used to derive rate constants for other compounds which (for alkanes at least) is probably good to within ±50% (Kwok and Atkinson 1995). (This is based on assigning a group rate constant for each -CH_3, -CH_2-, and -CH- group, with corrections for the types of "neighbor" groups adjacent to each.) The OH radical rate constants used for the normal alkanes up to n-C_{13} were the experimentally-measured values reported by Atkinson (1989), while those used for n-C_{14+} and the branched and cyclic alkanes were estimated using the structure-reactivity estimates of Atkinson (1987).

The atmospheric reactions of ethane provide the simplest illustration of the general alkane mechanism. Its major reactions are as follows:

$$\cdot OH + CH_3CH_3 \rightarrow H_2O + CH_3CH_2\cdot \quad (1)$$

$$CH_3CH_2\cdot + O_2 \rightarrow CH_3CH_2OO\cdot \quad (2)$$

$$CH_3CH_2OO\cdot + NO \rightarrow CH_3CH_2O\cdot + NO_2 \quad (3a)$$

$$CH_3CH_2O\cdot + O_2 \rightarrow CH_3CHO + HO_2\cdot \quad (4a)$$

$$HO_2\cdot + NO \rightarrow NO_2 + \cdot OH \quad (5)$$

The net effect of these processes is the conversion of two molecules of NO to NO_2, the oxidation of ethane to acetaldehyde, and no net change in OH radical levels. The conversion of NO to NO_2 is the process directly responsible for ozone formation. Since acetaldehyde is a fairly reactive compound which also causes ozone formation, this means that ethane is a moderately efficient compound towards forming ozone once it reacts. Its relatively low overall reactivity is due primarily to its relatively low reaction rate, and not to its relatively efficient reaction mechanism.

In many respects the reactions of the higher alkanes are very similar to those shown above for ethane, but the larger radicals involved have available additional reaction routes which will affect the distribution of oxidized products formed, the number of molecules of NO converted to NO_2, and the effect of the overall processes on OH radical levels. The atmospheric reactions of higher molecular weight alkanes have been discussed in detail elsewhere (Carter and Atkinson, 1985; see also Atkinson, 1997), and only the major features will be summarized here. The initial reaction routes are directly analogous to those shown above, the primary process is abstraction by OH from a C-H bond forming an alkyl radical, which then reacts rapidly with O_2 to form a peroxy radical, which, in the presence of NO_x, reacts primarily with NO. Most (though not all — see below) proceed analogously to reactions (1-3a) above, giving rise to an alkoxy ($RO\cdot$) radical. However, higher molecular weight alkoxy radicals in general have two other types of possible reaction routes besides the O_2 reaction analogous to reaction (4a). One is decomposition via β-scission, whose net effect is formation of lower molecular weight oxidized products, and conversion of additional molecules of NO to NO_2. For example,

$$\begin{gathered} R'CH(O\cdot)R \rightarrow R'CHO + R\cdot \qquad (4b) \\ R\cdot + O_2 \rightarrow RO_2 \\ RO_2 + NO \rightarrow NO_2 + RO\cdot. \\ RO\cdot \rightarrow \rightarrow \text{(etc)} \end{gathered}$$

Another is isomerization via a 1,4-hydrogen shift to form polyfunctional oxygenates, and also cause additional NO to NO_2 conversions. For example,

$$\begin{gathered} RCH_2CH_2CH_2CH(O\cdot)R' \rightarrow RCH(\cdot)CH_2CH_2CH(OH)R' \qquad (4c) \\ RCH(\cdot)CH_2CH_2CH(OH)R' + O_2 \rightarrow RCH(OO\cdot)CH_2CH_2CH(OH)R' \\ RCH(OO\cdot)CH_2CH_2CH(OH)R' + NO \rightarrow RCH(O\cdot)CH_2CH_2CH(OH)R' + NO_2 \qquad (3a') \\ RCH(OO\cdot)CH_2CH_2CH(OH)R' + NO \rightarrow RCH(ONO_2)CH_2CH_2CH(OH)R'. \qquad (3b') \\ RCH(O\cdot)CH_2CH_2CH(OH)R' \rightarrow RCH(OH)CH_2CH_2C(\cdot)(OH)R' \\ RCH(OH)CH_2CH_2C(\cdot)(OH)R' + O_2 \rightarrow RCH(OH)CH_2CH_2C(=O)R' + HO_2 \\ HO_2 + NO \rightarrow NO_2 + HO\cdot. \end{gathered}$$

Decomposition processes (e.g., reaction 4b) tend to be relatively more important for the branched alkanes because radicals with substituents are more likely to split off. They are also more important in cyclic alkanes because they tend to relieve ring strain. Hydrogen shift isomerization processes (via a 6-member

ring transition state, e.g, reaction 4c) are more important with the n- and other longer-chain alkanes, and generally dominate over decomposition for those straight-chain radicals where such hydrogen shift isomerizations are possible. Both isomerization and decomposition have similar net effects on ozone formation in that they cause additional NO to NO_2 conversions compared to cases where the O_2 reaction (e.g, 4a) dominate. The main difference is that decomposition causes formation of lower molecular weight oxidized products, while isomerization is believed to form polyfunctional compounds which are more likely to undergo condensation. Isomerization may be relatively less important for cycloalkanes because of ring strain considerations; there is no information available concerning this.

If these were the only factors involved, then the higher alkanes would be relatively efficient ozone precursors because of the additional NO to NO_2 conversions. However, there is an additional factor which turns out to be even more important in affecting the overall ozone reactivity of these compounds. In the case of ethane and most other low molecular weight compounds, the reaction of NO with peroxy ($ROO\cdot$) radicals involves primarily formation of alkoxy radicals and NO_2, as shown in reaction (3a), above. Thus, no net loss of radicals or NO_x is involved. However, for the alkanes at least, it is now known that as the size of the peroxy radical increases, a competing process, alkyl nitrate formation via

$$ROO\cdot + NO \rightarrow RONO_2 \qquad (3b)$$

becomes increasingly important (Atkinson, 1990; Carter and Atkinson, 1985, 1989a). This can have a strong effect on the VOC's reactivity because it removes both radicals and NO_x from the system. As discussed above, if a VOC's reactions cause radical removal, it reduces the rate of ozone formation from all other VOCs, and, if sufficiently important, can more than compensate for the O_3 formed from the VOC's direct reactions. The NO_x removal effect of this process can also reduce the ultimate amount of O_3 which can be formed in environments where O_3 formation is NO_x-limited.

Thus, the $k_{3b}/(k_{3a}+k_{3b})$ ratio, or the "nitrate yield", tends to be the dominant factor affecting a high molecular weight alkane's reactivity. If sufficiently high, it would cause the alkane to have a lower incremental reactivity than ethane despite its higher atmospheric reaction rate and greater number of NO to NO_2 conversions, and it may even cause the alkane to have a negative effect on ozone.

The extent of alkyl nitrate formation via reactions such as (3b) has been quantified by measuring yields of alkyl nitrate isomers in the OH/NO_x/air reactions of various normal and branched alkanes. Such measurements have been made for all the n-alkanes from propane through n-octane, and for a few C_5 and C_6 branched alkanes (Carter and Atkinson, 1989a and references therein). Based on these data, Carter and Atkinson (1989a) derived a general estimation method for alkyl nitrate yields from reactions of NO with various alkanes. The yields were found to be dependent on both temperature and pressure, and increased monotonically with the number of carbons, though tending to level out for the larger radicals. Since n-

octane is the highest alkane for which alkyl nitrate yields have been measured, the nitrate yields for the higher alkanes, such as those important in mineral spirits, are extrapolations and therefore uncertain. The yields of nitrate isomers from neopentane and methyl butanes and methyl pentanes suggest that the nitrate yields from the reaction of NO with primary and tertiary peroxy radicals are respectively 2.5 and 3.3 times lower than those from the secondary peroxy radicals formed from n-alkanes, indicating lower overall nitrate yields, and thus higher ozone reactivity, for branched alkanes relative to n-alkanes of the same size. However, the extrapolation of data from the C_5 and C_6 branched alkanes to the C_{9+} components of mineral spirits is even more uncertain.

An additional uncertainty is the extent of nitrate formation in the reactions of NO with the oxidized peroxy radicals believed to be formed following the isomerization of the longer-chain alkoxy radicals, shown as Reaction (3b') above. Since all the data concerning nitrate formation in these reactions is based on measurements of the alkyl nitrates formed from the initially formed alkyl peroxy radicals, there is no information concerning these processes. If alkyl nitrate formation from these OH-substituted radicals were as important as from the initially formed ones, the total radical termination from nitrate-forming reactions from n-alkanes could be up to 75% higher in the case of the C_{12+} n-alkanes. However, the available environmental chamber data for n-octane (Carter et al, 1993a, 1995a,b) and n-C_{12} through n-C_{16} (Carter et al, 1996) indicated that radical inhibition by these compounds are significantly overpredicted if this is assumed. Therefore, nitrate formation from the oxidized radicals formed following isomerization (e.g. from Reaction (3b'), appears to be much less important than nitrate formation from the primarily formed radicals.

Representation of Alkanes in the Model

The alkane mechanisms for the model calculations were derived using the procedure described by Carter (1990). Given the structure of the molecule, a computer program is used to generate the sequence of reactions which could occur, then uses various estimation methods to derive branching ratios of competing processes, and then summed up NO to NO_2 conversions and total yields of organic nitrates and of the various types of oxygenated products. The program uses the estimation methods described by Carter and Atkinson (1985) to derive the branching ratios for the reaction of OH radicals at the various positions on the molecule and the various competing alkoxy radical reactions, and the extrapolations of Carter and Atkinson (1989a) were used to estimate the nitrate yields in the initially formed peroxy radicals. Alkyl nitrate formation from the reactions of NO with secondarily-formed peroxy radicals, such as the hydroxy-substituted radicals formed in the isomerization reactions is assumed to be negligible. Although the estimates for the branching ratios for the OH and alkoxy radical reactions used by this program are now superseded by more recent work Atkinson and Carter (1991), Kwok and Atkinson (1995) and Atkinson (1997), the updated methods do not give significantly different predictions for the major reactions involved in the photooxidations of the alkanes. In general, isomerizations are estimated to be the dominant reactions of the long-chain alkoxy radicals formed from the normal alkanes, while

decomposition generally tends be relatively more important for many of the radicals formed from branched and cyclic alkanes. The lumped higher aldehyde model species, RCHO, whose mechanism was based on that for propionaldehyde, is used to represent higher molecular weight products containing aldehyde groups, while the lumped higher ketone product, MEK, is used to represent most of the other high molecular weight oxygenate products.

No attempt was made to derive the mechanisms for all the possible branched and cyclic C_{9+} alkane isomers. Instead, a representative branched and cyclic alkane isomer was chosen for each carbon number, and it was assumed that all the other branched or cyclic alkane isomers with the same number of carbons had essentially the same overall mechanism. The choices of isomer to derive the general mechanisms were essentially arbitrary, being made prior to this work during the development of the current SAPRC detailed alkane mechanism (Carter, 1990).

Table 1 gives a summary of all the model species used to represent the alkane consisitutents in the mineral spirits samples, and shows the compounds used to derive the mechanisms for each of these species, along with their major mechanistic parameters. The complete mechanisms for these species are given in Appendix A. The most important mechanistic parameters in affecting atmospheric reactivity predictions for these alkane model species are overall nitrate ($RONO_2$) yields, numbers of NO to NO_2 conversions ($NO \rightarrow NO_2$) involved in the overall reactions, and yields of aldehyde products. Note that nitrate formation has an inhibiting effect on reactivity, while NO to NO_2 conversions and aldehyde formation have positive effects. The kinetic reactivity, or fraction of emitted VOC which reacts, is also shown on Table 1. As shown on the table, this is not a particularly important parameter affecting relative reactivities of these species, since they are all calculated to be 75-95% reacted in a one day scenario.

To give an indication of how these species differ in their predicted atmospheric ozone formation potentials, the table also shows the Maximum Incremental Reactivities (MIR's) calculated for these compounds. These were calculated on an ozone formed per gram basis using the "averaged conditions" MIR scenarios described by Carter (1994) and the updated mechanism given by Carter et al (1997a), and are shown relative to that for n-dodecane. (See also Appendix A for a listing of the mechanisms used.) These data show that the reactivities tend to decrease with the size of the molecule because of increasing nitrate yields, and the reactivities for branched and cyclic alkanes are calculated to be significantly greater, by factors of 2 to almost 5, than the normal alkanes. This is because of three factors: (1) these species are calculated to have somewhat lower nitrate yields because of increased numbers of tertiary hydrogens (which are more reactive towards OH radicals, and which form tertiary peroxy radicals which are estimated to have lower nitrate yields when they react with NO [Carter and Atkinson, 1989a]); (2)

Table 1. Summary of alkane model species and their major mechanistic parameters and relative ozone formation potentials.

Model Species	Kinetic React'y [a]	$RONO_2$ Yield [b]	O - NO_2 Convers. [c]	Alde-hyde Yields	MIR / n-C_{12} [d]	Compound used to Derive Mechanism [e]
Normal Alkanes						
N-C8	0.74	0.33	2.0	0.0	1.5	n-Octane [f]
N-C9	0.78	0.37	1.9	0.0	1.3	n-Nonane [f]
N-C10	0.82	0.40	1.9	0.0	1.2	n-Decane [f]
N-C11	0.85	0.41	1.8	0.0	1.1	n-Undecane [f]
N-C12	0.87	0.42	1.8	0.0	1.0	n-Dodecane [f]
N-C13	0.89	0.43	1.8	0.0	0.94	n-Tridecane [f]
N-C14	0.90	0.43	1.8	0.0	0.86	n-Tetradecane [f]
N-C15	0.91	0.43	1.8	0.0	0.85	n-Pentadecane [f]
Branched Alkanes						
BR-C8	0.73	0.25	2.3	0.4	2.6	4-Methyl Heptane
BR-C9	0.79	0.27	2.3	0.4	2.5	4-Ethyl Heptane
BR-C10	0.83	0.30	2.2	0.3	2.2	4-Propyl Heptane
BR-C11	0.87	0.25	2.8	0.2	2.5	3,5-Diethyl Heptane
BR-C12	0.89	0.27	2.8	0.4	2.6	2,6-Diethyl Octane
BR-C13	0.90	0.29	2.7	0.1	2.1	3,7-Diethyl Nonane
BR-C14	0.91	0.30	2.5	0.0	1.7	3,8-Diethyl Decane
BR-C15	0.92	0.31	2.5	0.0	1.6	3,9-Diethyl Undecane
Cyclo Alkanes						
ME-CYCC6	0.79	0.22	2.5	0.6	3.9	Methyl Cyclohexane [f]
CYC-C8	0.83	0.26	2.8	0.8	4.1	Ethyl Cyclohexane
CYC-C9	0.86	0.25	3.3	1.0	4.8	1-Ethyl-4-Methyl Cyclohexane
CYC-C10	0.89	0.27	3.1	0.8	3.8	1,3-Diethyl-Cyclohexane
CYC-C11	0.91	0.24	3.4	0.8	4.0	1,3-Diethyl-5-Methyl Cyclohexane
CYC-C12	0.92	0.25	3.2	0.7	3.6	1,3,5-Triethyl Cyclohexane
CYC-C13	0.93	0.27	2.9	0.6	3.1	1,3-Diethyl-5-Pentyl Cyclohxane
CYC-C14	0.94	0.28	2.7	0.5	2.7	1,3-Dipropyl-5-Ethyl Cyclohexane
CYC-C15	0.95	0.29	2.5	0.4	2.4	1,3,5-Tripropyl Cyclohexane

[a] Fraction of emitted VOC which reacts in a a 1-day maximum incremental reactivity (MIR) scenario (Carter, 1994).

[b] Total alkyl nitrate yield from all the RO2 + NO reactions.

[c] Total number of NO to NO2 conversions before radical termination or OH radical regeneratio

[d] Incremental reactivities (mass basis), relative to n-dodecane, calculated for the "averaged conditions", maximum incremental reactivity (MIR) scenario as described by Carter (1994), using the updated chemical mechanism given by Carter et al (1997) (see also Appendix A).

[e] The representative compounds used to derive the branched and cyclic alkanes were chosen at the time the SAPRC detailed alkane mechanism was developed (Carter, 1990), and may not necessarily reflect compounds present in mineral spirits samples.

[f] Explicit mechanism for this compound.

the relatively greater extent of alkoxy radical decomposition results in longer chains of consecutive reactions and thus more NO to NO_2 conversions; and (3) higher yields of products containing the reactive aldehyde group, as opposed to less reactive Δ-hydroxy ketones predicted from the n-alkanes, are predicted to be formed. Therefore, this mechanism predicts much higher ozone formation potentials for samples high in branched and cyclic alkanes, as opposed to those containing mostly normal alkanes.

It important to note that although the mechanisms derived for the C_{8+} normal alkanes have been evaluated and shown to perform reasonably well in simulating the ozone impacts of these compounds in environmental chamber experiments (Carter et al, 1996), this is not the case for the higher molecular weight branched and cyclic alkanes. The only branched alkanes for which environmental chamber data useful for mechanism evaluation are available are isobutane and isooctane (2,2,4-trimethylpentane), and in both cases the chamber data indicated that the mechanisms needed to be refined — with the model overpredicting the reactivity of the former, and underpredicting that of the latter (Carter et al, 1993a; 1995a). This means that the prediction that the C_{8+} branched and cyclic alkanes have significantly different reactivities than the normal alkanes may be in error.

For sensitivity testing purposes, simulations of the chamber experiments were carried out by representing the branched and cyclic alkanes with the same mechanism as used for the normal alkane with the same number of carbons.

Representation of Aromatics and Alkenes

As discussed below, the analysis of one of the mineral spirits samples indicates that it contains measurable amounts of aromatics and alkenes. Because of the high reactivities of these compounds compared to alkanes (see below), their reactions need to be represented in the model calculations. The atmospheric reactions of aromatics and alkenes (Atkinson, 1990; 1994, and references therein), and the methods used to represent them in model calculations (Carter, 1990, 1995b; Carter et al, 1993b, 1997a) are discussed in detail elsewhere. Table 2 lists the model species used to represent the aromatic and alkene and constituents identified in Sample "A", and indicates whether the compound was represented explicitly, or whether it was represented as having a mechanism of a similar, but lower molecular weight compound. In the case of the alkenes, the mechanisms were derived by analogy from those for propene and 1-butene (for the terminal alkenes) or from that of trans-2-butene (for the internal alkenes), except rate constants appropriate for a C_6 alkene were used, and overall organic nitrate yields in the OH reaction were estimated by assuming they were the same as an n-alkane with the same number of carbons (Carter et al, 1987; Carter, 1990). The specific reactions used for all these model species are listed in Appendix A.

Table 2 also shows the relative MIR ozone formation potentials for these species, for direct comparison for those shown on Table 1 for the alkane model species. It can be seen that the reactivities

Table 2.Summary of aromatic and alkene model species and their relative ozone formation potentials.

Model Species	Description	MIR / n-C_{12} [a]	Compound used to Derive Mechanism [b]
TOLUENE	Toluene	8.7	Toluene
M-XYLENE	m-Xylene	24.1	m-Xylene
O-XYLENE	o-Xylene	14.3	o-Xylene
P-XYLENE	p-Xylene	4.9	p-Xylene
I-C3-BEN	Cumene	3.2	Ethylbenzene
NAPHTHAL	Naphthalene	2.1	Naphthalene [c]
C9-BEN1	Monosubstituted C9 Alkylbenzenes	3.4	Ethylbenzene
C10-BEN1	Monosubstituted C10 Alkylbenzen	3.0	Ethylbenzene
C11-BEN1	Monosubstituted C11 Alkylbenzen	2.7	Ethylbenzene
C12-BEN1	Monosubstituted C12 Alkylbenzen	2.5	Ethylbenzene
C13-BEN1	Monosubstituted C13 Alkylbenzen	2.3	Ethylbenzene
C9-BEN2	Disubstituted C9 Alkylbenzenes	21.3	m-Xylene
C10-BEN2	Disubstituted C10 Alkylbenzenes	19.1	m-Xylene
C11-BEN2	Disubstituted C11 Alkylbenzenes	17.2	m-Xylene
C12-BEN2	Disubstituted C12 Alkylbenzenes	15.8	m-Xylene
C13-BEN2	Disubstituted C13 Alkylbenzenes	14.5	m-Xylene
C9-BEN3	Polysubstituted C9 Alkylbenzenes	23.3	1,3,5-Trimethylbenzene
C10-BEN3	Polysubstituted C10 Alkylbenzenes	20.9	1,3,5-Trimethylbenzene
C11-BEN3	Polysubstituted C11 Alkylbenzenes	18.9	1,3,5-Trimethylbenzene
C12-BEN3	Polysubstituted C12 Alkylbenzenes	17.3	1,3,5-Trimethylbenzene
C13-BEN3	Polysubstituted C13 Alkylbenzenes	15.9	1,3,5-Trimethylbenzene
C8-OLE1	C8 Terminal Alkenes	6.1	Propene, 1-Butene [d]
C9-OLE1	C9 Terminal Alkenes	5.0	Propene, 1-Butene [d]
C10-OLE1	C10 Terminal Alkenes	4.3	Propene, 1-Butene [d]
C11-OLE1	C11 Terminal Alkenes	3.8	Propene, 1-Butene [d]
C12-OLE1	C12 Terminal Alkenes	3.5	Propene, 1-Butene [d]
C13-OLE1	C13 Terminal Alkenes	3.1	Propene, 1-Butene [d]
C8-OLE2	C8 Internal Alkenes	12.4	trans-2-Butene [d]
C9-OLE2	C9 Internal Alkenes	10.8	trans-2-Butene [d]
C10-OLE2	C10 Internal Alkenes	9.5	trans-2-Butene [d]
C11-OLE2	C11 Internal Alkenes	8.6	trans-2-Butene [d]
C12-OLE2	C12 Internal Alkenes	7.8	trans-2-Butene [d]
C13-OLE2	C13 Internal Alkenes	7.1	trans-2-Butene [d]

[a] Incremental reactivities (mass basis), relative to n-dodecane, calculated for the "averaged conditions", maximum incremental reactivity (MIR) scenario as described by Carter (1994), using the updated chemical mechanism given by Carter et al (1997) (see also Appendix A).

[b] Except as noted, aromatic mechanisms derived based on fits to chamber data as discussed by

[c] Derived based on fits to chamber data as discussed by Carter et al (1987).

[d] Based on model simulations of 1-hexene experiments (Carter et al, 1987), the C8+ terminal and internal alkenes are assumed to have same organic nitrate yields in RO2+NO reaction as corresponding n-alkane. The other aspects of the mechanism are based on those for the compounds listed, as given by Carter (1995) and Carter et al. (1997).

for the most of these compounds are significantly higher than those for the alkanes. The main exceptions to this are naphthalene, the higher molecular weight monoalkyl benzenes, and the C_{10+} terminal alkenes, which have reactivities comparable to those for the cycloalkanes. The most reactive of the aromatics are the polysubstituted benzenes, and the most reactive alkenes are the lower molecular weight internal alkenes. Note that the assumed distribution of mono-, di- and polysubstituted aromatic isomers, and of terminal vs internal alkenes, can have a significant effect on the calculated reactivity contribution of these species.

Environmental Chamber Modeling Methods

The ability of the chemical mechanisms to appropriately simulate the atmospheric impacts of the mineral spirits samples was evaluated by conducting model simulations of the environmental chamber experiments from this study. This requires including in the model appropriate representations of chamber-dependent effects such as wall reactions and characteristics of the light source. The methods used are based on those discussed in detail by Carter and Lurmann (1990, 1991), updated as discussed by Carter et al. (1995c,e 1997a). The photolysis rates were derived from results of NO_2 actinometry experiments and measurements of the relative spectra of the light source. In the case of the blacklight light source used in these experiments, where the spectrum of the light source appears to be relatively constant, the general blacklight spectrum derived by Carter et al (1995e) was used. (Separate assignments of overall light intensities (as measured by NO_2 photolysis rates) were made for experiments prior to and after run DTC-472, when both the reactors and the light banks were changed.) The thermal rate constants were calculated using the temperatures measured during the experiments, with the small variations in temperature with time during the experiment being taken into account. The computer programs and modeling methods employed are discussed in more detail elsewhere (Carter et al, 1995e). The specific values of the chamber-dependent parameters used in the model simulations of the experiments for this study are given in Table A-4 in Appendix A.

The initial reactant concentrations used when modeling the experiments were based on the measured initial concentrations except for the components of the mineral spirits samples. These were derived based on the results of the composition analyses of the various samples, together with the total carbon concentration of sample injected. The amount of mineral spirits carbon injected into the chamber was calculated from the volume of sample injected as measured by a microliter syringe, and its density and elemental composition as provided by Safety-Kleen. The mineral spirits carbon concentration was calculated from the amount of carbon injected and the calculated volume of the reaction bag. The volume of the reaction bag was calculated from the measured NO_x concentrations and the moles of NO and NO_2 injected into both reaction bags (as determined by the pressure measured by a Baratron capacitance manometer in a flask of known volume), assuming that the volume of each reaction bag was equal. The volume of the chamber could also be measured by comparing amounts of gas-phase ROG surrogate components injected with their measured injections, and the results were consistent with the volumes

calculated from the NO_x injections. A comparison of the mineral spirits total carbon concentrations calculated in this way with results of total carbon or GC analyses is given in the Results section.

The mineral spirits components were represented in the model simulations using lumped model species whose rate constants and product yield parameters were weighted averages of the mixture of model species derived from the analyses of each sample. The all-alkane samples were represented using a single lumped $C_{10\text{-}15}$ model species, while the sample containing the aromatics and alkenes used three lumped species, one each for the alkane, aromatic, and alkene constituents. This type of lumping of species of similar kinetic reactivities has no significant effect on results of in box model or chamber simulations, and simplified integrating the data with the software employed. The reactions used for the lumped model species to represent each of the four samples are shown in Appendix A. As indicated above and in Appendix A, calculations were carried out both for the standard mechanisms for the branched and cyclic alkanes derived as indicated in Table 1, and also with a modified mechanism where the branched and cyclic alkanes were represented using the normal alkane with the same number of carbons. Appendix A shows the lumped alkane reactions derived using both these approaches for each of the samples.

Atmospheric Reactivity Simulations

To estimate the effects of emissions of the samples on ozone formation under conditions more representative of polluted urban atmospheres, incremental reactivities, defined as the change in O_3 caused by adding small amounts of the sample to the emissions, were calculated for ethane, the four mineral spirits samples, and the mixture representing the VOCs emitted from all sources. The modeling approach and scenarios is the same as used as described in detail elsewhere (Carter, 1994, Carter et al, 1993b, 1996, 1997b), and is only briefly summarized here.

The scenarios employed were those used by Carter (1994) to develop various reactivity scales to quantify impacts of VOCs on ozone formation in various environments. These were based on a series of single-day EKMA box model scenarios (EPA, 1984) derived by the EPA to represent 39 different urban ozone exceedence areas around the United States (Baugues, 1990). It was found that NO_x levels are the most important factor affecting differences in relative ozone impacts among VOCs, and that the ranges of relative reactivities in the various scales can be reasonably well represented by ranges in relative reactivities in three "averaged conditions" scenarios representing three different NO_x conditions. These scenarios were derived by averaging the inputs to the 39 EPA scenarios, except for the NO_x emissions. In the "Maximum Incremental Reactivity" (MIR) scenario, the NO_x inputs were adjusted such that the final O_3 level is most sensitive to changes in VOC emissions; in the "Maximum Ozone Incremental Reactivity" (MOIR) scenario the NO_x inputs were adjusted to yield the highest maximum O_3 concentration; and in the "Equal Benefit Incremental Reactivity" (EBIR) scenario the NO_x inputs were adjusted such that relative changes in VOC and NO_x emissions had equal effect on ozone formation. As discussed by Carter (1994),

there represent respectively the high, medium and low ranges of NO_x conditions which are of relevance when assessing VOC control strategies for reducing ozone.

The incremental reactivities depend on how the amount of VOC added and how the ozone impacts are quantified. In this work, the added VOC was quantified on a mass basis, since this is how VOCs are regulated. The ozone impacts can be quantified either in terms of ozone yield, or the peak ozone concentrations in the scenarios, or in terms of integrated ozone over the Federal standard of 0.12 ppm. The latter is defined as the sum of the hourly ozone concentrations for the hours when ozone exceeds the standard in the base case scenarios (Carter 1994a), and is designated as the $IntO_3>0.12$ in the tabulations of the results.

The compositions and mechanisms for the mineral spirits samples were the same as used in modeling the chamber data, as discussed above. The mechanisms for the other species were also the same as employed in the chamber simulations, except that the reactions representing chamber effects were removed, and the reactions for the full variety of VOCs emitted into the scenarios (Carter, 1994a) were included. Most of the emitted VOCs are not represented in the model explicitly, but are represented using lumped model species whose rate constants and product yield parameters are derived based on the mixture of compounds they represent. The rate constants and mechanistic parameters for the emitted species in the scenarios were the same as those used previously (Carter et al, 1993b), except for the aromatics, whose unknown photoreactive product yields were reoptimized in a manner analogous to that discussed above for toluene and m-xylene (Carter et al. 1997a). The mechanism listing in Appendix A gives the reactions of the model species used in the atmospheric simulations to represent various types of anthropogenic and biogenic emissions, indicating the types of compounds each is used to represent, and giving their rate constants and product yield parameters.

RESULTS AND DISCUSSION

Mineral Spirits Composition Analysis

Data Provided by Safety-Kleen

Safety-Kleen Corp. provided us with four mineral spirits samples for study, together with various information concerning the properties and compositions of these samples. The sample numbers, selected physical properties, elemental and FIA type analysis, and GC-FID carbon number fractionation data provided by Safety-Kleen is shown on Table 3. As indicated on the table, the four samples are designated by the codes "A" through "D", which will be used to identify them throughout the reminder of this report. Sample "A" is a Type I-B solvent with a relatively broad carbon number distribution centered around C_{11}, and (unlike the other samples) with some aromatic and olefin content; Sample "B" is a Type II-C, primarily alkane, solvent with a relatively broad carbon number distribution centered around C_{12}-C_{13}; and Samples "C" and "D" are also Type II-C, primarily alkane, solvents, but with narrower carbon number distributions centered around C_{12}. The elemental analysis indicates no significant amounts of elements other than carbon or hydrogen, with the weight percents corresponding to empirical formulas of $CH_{2.02\pm0.02}$.

As indicated above, Safety-Kleen also performed high-resolution GC-MS analyses of these four samples, with the MS patterns being used to classify the components as aliphatic, alicyclic, or aromatic, the retention times and MS patterns being used to identify the normal alkanes, and the retention times relative to the normal alkanes being used to estimate the carbon numbers of each of the components. Although no attempt was made to distinguish between cycloalkane or olefins for the peaks identified as "alicyclic", for Samples "B", "C", and "D", the FIA type analysis data indicate that they must primarily be cycloalkanes. A summary of the results of the Safety-Kleen GC-MS analyses are given in Table 4, The detailed data, including total ion chromatograms, and tabulations of retention-times, area percents, and assignments for all the separated peaks, are given in Appendix B.

Note that the Safety-Kleen analysis indicates that all four of these samples are dominated by branched and cyclic alkanes, with the normal alkanes being less than ~5% for Sample "B" and ~20-25% for the others, with the cyclic alkanes being ~40 to >50% by weight in all cases. Note also that Samples "C" and "D" have very similar compositions as well as carbon number distributions, though Sample "D" has a ~50% higher branched/cyclic alkane ratio. Note also that the GC-MS analysis for Sample "A" indicated a total aromatic contribution of 6.0%, in excellent agreement with the 6.5% contribution derived from the FIA type analysis data.

Table 3. Summary of the characteristics of the four mineral spirit samples used in this study.

A graphical comparison of the carbon number distributions derived by the GC-FID fractionation and carbon number and type distributions as derived by the GC-MS data is shown on Figure 1. It can be seen that there is reasonably good agreement with the fractionation derived by GC-MS and GC-FID. This tends to validate our implicit assumption that total ion current in the GC-MS analysis is at least approximately proportional to the weight fraction of the identified components in the GC-MS analyses.

Data Provided by DRI

As part of this project, samples of each of the four liquid mineral spirits samples were sent to Dr. Barbara Zielinska of Desert Research Institute (DRI) for analysis by GC-MS. The detailed results of these analyses are given in Appendix B, along with copies of the chromatograms which were provided. A summary of the relative amounts of the identified compounds are given in Table 5, and Figure 1 shows the carbon number distributions which correspond to the assignments provided by DRI.

Table 3. Summary of the characteristics of the four mineral spirits samples used in this

	Sample "A"	Sample "B"	Sample "C"	Sample "D"
Sample No.	93-0461	96-1077	96-1165	96-1177
ASTM D235-95 Type	I-B	II-C	II-C	II-C
Specific Gravity	0.7895	0.8063	0.7917	0.7935
Elemental Analysis (wt. %)				
Carbons	85.6	85.6	86.0	85.5
Hydrogens	14.5	14.6	14.7	14.5
Oxygens	0.1	-	0.2	-
FIA Type Analysis (vol. %)				
Alkanes	91.2	>98	>98	>98
Aromatics	6.4	-	-	-
Olefins	2.4	-	-	-
Carbon No. Fractionation (wt %)				
C8	0.4	-	-	-
C9	6.7	0.4	-	-
C10	29.3	4.3	1.3	0.1
C11	36.9	18.5	29.6	35.3
C12	21.9	31.6	53.5	53.8
C13	4.4	30.1	15.3	10.8
C14	0.1	12.6	0.4	-
C15	0.2	2.5	-	-
C16	0.1	0.1	-	-

Table 4. Summary of compositions of the minereal spirits samples from the GC-MS analyses provided by Safety-Kleen. [a]

nC	Sample "A"				Sample "B"			Sample "C"			Sample "D"		
	N-	Br-	Cyc-	Aro	N-	Br-	Cyc-	N-	Br-	Cyc-	N-	Br-	Cyc-
	Weight Percent [b]												
7	-	-	0.0	0.1	-	-	-	-	-	-	-	-	-
8	0.2	0.1	0.0	0.2	-	-	-	-	-	-	-	-	-
9	2.4	1.1	2.1	1.1	-	-	-	-	-	-	-	-	-
10	7.1	7.9	11.0	2.0	-	0.4	2.7	-	-	-	-	-	-
11	8.3	9.5	18.2	2.1	-	4.2	11.0	11.7	2.4	12.6	14.3	3.3	13.4
12	3.2	8.3	10.4	0.6	1.5	11.2	19.3	13.6	13.3	31.3	9.5	21.0	27.3
13	0.2	2.3	1.4	0.0	1.4	17.7	14.4	0.5	7.0	7.7	0.2	5.5	5.3
14	-	0.1	-	-	1.7	7.7	5.0	-	-	-	-	-	-
15	-	-	-	-	-	1.3	0.6	-	-	-	-	-	-
Tot	21.3	29.2	43.1	6.0	4.6	42.4	53.0	25.8	22.7	51.5	24.0	29.9	46.0
	Mix = 99.7				Mix = 100.0			Mix = 100.0			Mix = 100.0		
	Carbon Numbers												
	10.6	11.1	11.0	10.3	13.1	12.8	12.2	11.6	12.2	11.9	11.4	12.1	11.8
	Mix = 10.9				12.5			11.9			11.8		

[a] Type codes: N- = normal alkanes; Br- = branched alkanes (compounds identified as "aliphatic" which are not normal alkanes); Cyc = compounds identifed as "alicyclic", which are either alkenes or cycloalkanes; Aro = compounds identified as aromatics.

[b] Total ion current areas are assumed to be proportional to weight fractions.

Table 5. Summary of compositions of the minereal spirits samples from the GC-MS Analyses provided by DRI. [a]

nC	Sample "A"				Sample "B"			Sample "C"			Sample "D"		
	N-	Br-	Cyc-	Aro	N-	Br-	Cyc-	N-	Br-	Cyc-	N-	Br-	Cyc-
	Weight Percent												
9	-	2.0	4.6	1.6	-	0.4	0.6	-	-	-	-	-	-
10	10.7	3.5	28.4	6.1	-		15.8	-	0.3	9.8	-	-	11.1
11	-	7.9	2.9	-	-	8.0	10.9	-	3.5	12.0	-	-	36.2
12	-	-	5.4	-	-	12.7	8.0	43.3	9.7	5.4	9.4	16.3	5.5
13	-	-	1.8	-	-	21.0	4.7	-	1.2	2.2	-	1.8	1.1
14	-	-		-	1.3	2.4	2.4	-	-	-	-	-	-
Tot	10.7	13.4	43.1	7.7	1.3	44.6	42.3	43.3	14.7	29.4	9.4	18.2	53.9
	Mix = 74.8				Mix = 88.1			Mix = 87.4			Mix = 81.5		
	Carbon Numbers												
	10.0	10.4	10.3	9.8	14.0	12.4	11.2	12.0	11.8	11.0	12.0	12.1	10.9
	Mix = 10.2				Mix = 11.8			Mix = 11.6			Mix = 11.3		

[a] See Footnote [a] on Table 4, above.

[b] Total ion current areas are assumed to be proportional to weight fractions.

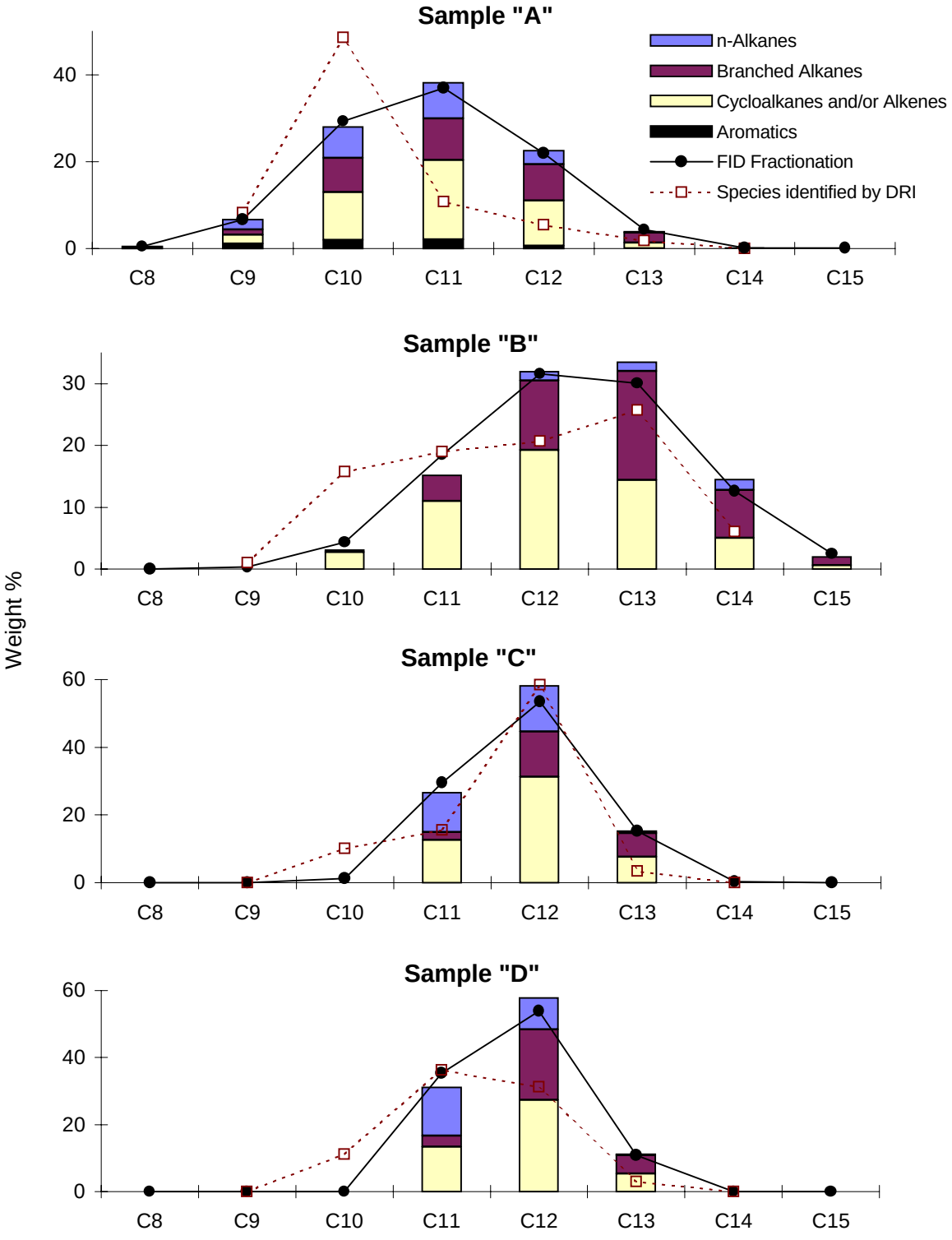

Figure 1. Plots of carbon number distributions derived using various methods for the four mineral spirits samples. (Data provided by Safety-Kleen except as

Note that the GC system used in the DRI analysis does not have the resolution as the system employed at Safety-Kleen, and therefore a smaller number of peaks were resolved and identified. (See example chromatograms in Appendix B.) In addition, identifications or classifications were attempted only for the major peaks, and some components were identified as oxygenated compounds, which is inconsistent with the elemental analysis data provided by Safety-Kleen. These unclassified or apparently misidentified peaks are not included in the summaries on Table 5, which is why the total area fractions add up to less than 100%. Several peaks were identified as olefins, but these are lumped with cycloalkanes for the purpose of the summary on Table 5, consistent with the treatment of these compounds by Safety-Kleen.

A comparison of the data on Tables 4 and 5, and the carbon number distributions on Figure 1, indicates that although the results of the DRI analyses are qualitatively similar to those from Safety-Kleen, there are some differences. The carbon number distributions from the DRI data are not consistent with the FID fractionation data for Samples "A", "B", and "D", and suggest that some significant high molecular weight compounds are not identified, or (in the case of Samples "A" and "B", possibly misidentified as lower molecular weight species. In addition, a number of normal alkane peaks were apparently buried by other peaks, and the large peak attributed to n-dodecane in Sample "C" is probably a mixture containing significant amounts of other compounds. Because of the inconsistencies with the higher resolution Safety-Kleen GC-MS and with the FID carbon number fractionation data, the DRI data were used for comparison purposes only.

Derived Compositions for Modeling

Because of its high resolution and consistency with the results of the elemental and type analysis data, the Safety-Kleen GC-MS data was used as the primary means for establishing the compositions of the mineral spirits for modeling, with the type analysis data used to provide necessary information concerning the contribution of olefins in the "alicyclic" species in Sample A. Tables B-1 through B-4 in Appendix B show the model species assigned to each of the peaks in the Safety-Kleen GC-MS peaks analysis, and the derived compositions in terms of weight fractions of model species are summarized in Table 6. The following assumptions were made in making these assignments:

1. The peak area in the total ion current GC-MS chromatograms was assumed to be proportional to weight percent,

2. The total peak areas of the GC-MS analyses were assumed to account for all the material in the sample.

3. Any peak labeled as "aliphatic" which was not also identified as a normal alkane was presumed to be a branched alkane.

4. Any peak labeled as "alicyclic" in samples where the FIA analysis indicated no significant olefins (i.e., Samples "B", "C", or "D") is assumed to be a cycloalkane.

Table 6. Compositions of the mineral spirits samples derived for modeling the chamber experiments.

Description	Model Species	Weight Percent A	B	C	D
Low reactivity components	INERT	0.17			
n-Octane	N-C8	0.20			
n-Nonane	N-C9	2.36			
n-Decane	N-C10	7.11			
n-Undecane	N-C11	8.29		11.71	14.33
n-Dodecane	N-C12	3.15	1.48	13.59	9.50
n-Tridecane	N-C13	0.23	1.40	0.53	0.21
n-Tetradecane	N-C14		1.71		
Branched C8 Alkanes	BR-C8	0.08			
Branched C9 Alkanes	BR-C9	1.10			
Branched C10 Alkanes	BR-C10	7.89	0.35		
Branched C11 Alkanes	BR-C11	9.52	4.16	2.38	3.33
Branched C12 Alkanes	BR-C12	8.27	11.18	13.30	21.05
Branched C13 Alkanes	BR-C13	2.26	17.69	6.99	5.55
Branched C14 Alkanes	BR-C14	0.10	7.71		
Branched C15 Alkanes	BR-C15		1.33		
Methylcyclohexane	ME-CYCC6	0.01			
Cyclic C8 Alkanes	CYC-C8	0.04			
Cyclic C9 Alkanes	CYC-C9	1.99			
Cyclic C10 Alkanes	CYC-C10	10.45	2.71		
Cyclic C11 Alkanes	CYC-C11	17.32	11.00	12.55	13.40
Cyclic C12 Alkanes	CYC-C12	9.90	19.28	31.26	27.32
Cyclic C13 Alkanes	CYC-C13	1.29	14.37	7.68	5.32
Cyclic C14 Alkanes	CYC-C14		5.04		
Cyclic C15 Alkanes	CYC-C15		0.59		
Toluene	TOLUENE	0.12			
o-Xylene	O-XYLENE	0.14			
m-Xylene	M-XYLENE	0.08			
p-Xylene	P-XYLENE	0.08			
Cumene	I-C3-BEN	0.02			
Naphthalene	NAPHTHAL	0.19			
Monosubstituted C9 Alkylbenzenes	C9-BEN1	0.05			
Monosubstituted C10 Alkylbenzenes	C10-BEN1	0.09			
Monosubstituted C11 Alkylbenzenes	C11-BEN1	0.10			
Monosubstituted C12 Alkylbenzenes	C12-BEN1	0.03			
Monosubstituted C13 Alkylbenzenes	C13-BEN1	0.00			
Disubstituted C9 Alkylbenzenes	C9-BEN2	0.24			
Disubstituted C10 Alkylbenzenes	C10-BEN2	0.44			
Disubstituted C11 Alkylbenzenes	C11-BEN2	0.52			
Disubstituted C12 Alkylbenzenes	C12-BEN2	0.16			
Disubstituted C13 Alkylbenzenes	C13-BEN2	0.01			
Polysubstituted C9 Alkylbenzenes	C9-BEN3	0.66			
Polysubstituted C10 Alkylbenzenes	C10-BEN3	1.23			
Polysubstituted C11 Alkylbenzenes	C11-BEN3	1.47			
Polysubstituted C12 Alkylbenzenes	C12-BEN3	0.45			
Polysubstituted C13 Alkylbenzenes	C13-BEN3	0.02			
C8 Terminal Alkenes	C8-OLE1	0.00			
C9 Terminal Alkenes	C9-OLE1	0.08			
C10 Terminal Alkenes	C10-OLE1	0.44			
C11 Terminal Alkenes	C11-OLE1	0.73			
C12 Terminal Alkenes	C12-OLE1	0.42			
C13 Terminal Alkenes	C13-OLE1	0.05			
C8 Internal Alkenes	C8-OLE2	0.00			
C9 Internal Alkenes	C9-OLE2	0.02			
C10 Internal Alkenes	C10-OLE2	0.11			
C11 Internal Alkenes	C11-OLE2	0.18			
C12 Internal Alkenes	C12-OLE2	0.10			
C13 Internal Alkenes	C13-OLE2	0.01			

5. Any peak labeled as "alicyclic" in a sample which FIA analysis indicates has non-negligible olefin content was assumed to be an olefin - cycloalkane mixture, with the olefin fraction being such that the total olefin content derived for the sample will agree with the FIA analysis. In the case of Sample "A", this corresponded to a ~5% olefin and ~95 cycloalkane split for each peak identified as "alicyclic".

6. The carbon numbers for unidentified "aliphatic" and "alicyclic" compounds were derived from their retention time by assuming they had the same carbon number as the nearest n-alkane with a greater retention time. This is the standard assumption for the GC fractionation method.

7. Carbon numbers for unidentified aromatics are assumed to be one less than would be derived for an "aliphatic" or "alicyclic" compound with the same retention time. This is consistent with the longer retention times for aromatics relative to alkanes, and with the identified aromatics found in Sample "A".

8. The xylene isomer with the longest retention time was assumed to be o-xylene. The other peak identified as "xylene" was assumed to be a 50-50 mix of m- and p- xylene.

9. The unidentified C_{8+} alkenes were arbitrarily assumed to be 80% terminal and ~80% internal alkenes. Previous analyses suggest that most of the olefins in these mixtures are terminal (O'Donnell, Safety-Kleen Corp., private communication, 1997).

10. The unidentified C_{9+} aromatics were assumed to be 5% 25%, and 70% mono-, di- and poly-alkylbenzenes, respectively. GC-MS analyses of other aromatic-containing mineral-spirits samples by Safety-Kleen indicated that the aromatics consisted primarily of polyalkylbenzenes, with ~20-30% dialkylbenzenes, and only small amounts of monoalkylbenzenes (O'Donnell, private communication, 1997).

Assumptions (1) and (2) seem to be reasonable in view of the fairly good agreement between the carbon number distribution derived by the GC-MS data with that derived by FID fractionation. Assumptions (3) and (4) are probably not uncertain, though unresolved peaks may contain contributions of compounds of another type. Although such compounds would be incorrectly classified, on the average such errors should cancel out. Assumption (5) is almost certainly incorrect for any particular "alicyclic" peak, which is probably either primarily cycloalkane or primarily olefin, but it is likely to give an appropriate aggregation for the mixture as a whole. Assumption (6) may lead to misassignments in some cases, particularly for compounds with retention times close to an n-alkane, and it might be possible to avoid it in some cases by analyzing the mass spectra to obtain the likely molecular weight. However, the misassignments are probably minor, and may cancel out in some cases. Assumption (7) is uncertain, but given that the reactivities of the aromatics are much less dependent on the size of the molecule as the number of substituents about the ring, the effect of this uncertainty is minor compared to the uncertainty inherent with Assumption (10). The assumed distributions for m- vs p- xylene (Assumption 8), terminal vs internal alkenes (Assumption 9), and type of aromatic isomer (Assumption 10) are uncertain and a significant source of uncertainty concerning the reactivity contributions of these species. However, these

uncertainties are only applicable for samples which FIA analysis indicate contain non-negligible aromatics or alkenes, or Sample "A" in the case of this study.

Table 6 shows the compositions of the mineral spirits which were derived using the above procedure. These were used for modeling the chamber experiments, except as indicated otherwise. These weight fractions were converted into mole or carbon fractions using the molecular weights and carbon numbers of the individual model species.

Environmental Chamber Experiments

Summary of Experiments

Table 7 gives a chronological listing of all the experiments carried out for this program. In addition to the reactivity experiments, whose results are discussed in the following section, control experiments were conducted to assure consistency with previous results, and side equivalency tests were conducted to assure that essentially equivalent results were obtained when equal mixtures were simultaneously irradiated in each of the dual reaction bags. Table 7 also includes characterization and control experiments carried out for other programs which are relevant to characterizing conditions of runs for this program. Relevant results of the control and characterization runs are summarized on the table, and are briefly discussed below.

As indicated on Table 7, the experiments for this program were conducted during two time periods. The first series (runs DTC-438 through DTC-444) were conducted in October and November of 1996. These consisted entirely of the mini-surrogate experiments, along with the associated characterization and control runs. The second series (runs DTC472-DTC488) were carried out in April and May of 1997, and consisted primarily of the full surrogate runs. Between the first and second series, experiments were conducted for other programs, including runs with a compound which caused apparent chamber contamination, as indicated by results of associated characterization and control runs. As a results of this, the reaction bags were replaced immediately prior to run DTC472. In addition, because the NO_2 actinometry experiments indicated that the light intensity had been degrading more rapidly than before, and the NO_2 photolysis rate had reached an unacceptably low value of 0.15 min^{-1}, the light banks were changed at the same time as the reaction bags were replaced. This resulted in the NO_2 photolysis rate increasing back to about 0.2 min^{-1}, which is more typical for most of the previous runs carried out in this chamber (see, for example, Carter et al, 1996, 1997a).

Except for the decline in the light intensity during the first series of experiments, the results of the characterization and control runs were as expected based on our previous experience with these and similar chambers in our laboratories (Carter et al. 1995b,e and references therein; Carter et al, 1997a). Good side equivalency was observed when equivalent surrogate - NO_x, propene - NO_x, or (for the first series of runs) n-butane - NO_x mixtures were simultaneously irradiated in the dual reactors. The results

Table 7. Chronological listing of the environmental chamber experiments carried out for this program.

RunID	Date	Title	Comments
DTC429	10/14/96	NO2 Actinometry	The NO_2 photolysis rate was measured using the quartz tube method was 0.18 min^{-1}, in good agreement with slightly downward trend of previous actinometry results in this chamber.
DTC431	10/16/96	Propene + NOx	Control run for comparison with other propene runs carried out in this and other chambers. The results were consistent with previous propene runs. Good side equivalency observed.
DTC434	10/21/96	n-Butane + NOx	Control run to measure the chamber radical source. Results were similar to those of the previous n-butane run, which was consistent with predictions of the standard chamber model. Run could not be modeled because of lack of n-butane data.
DTC435	10/22/96	pure air irradiation	After 6 hours of irradiation, approximately 24 ppb O_3 formed on side A and 22 on side B. Results are within the normal range, and were consistent with the predictions of the chamber effects model.
DTC436	10/23/96	Ozone decay	Measured O_3 decay rate was ~1% per hour, in good agreement with the default value used in the chamber model.
DTC438	10/30/96	Mini-Surrogate + Mineral Spirits "D"	20.8 ml mineral spirits "D" injected into side A. Results on Table 8. Very large inhibition in NO oxidation and ozone formation was observed. It was concluded that more useful data would be obtained using smaller amounts of mineral spirits injected.
DTC439	10/31/96	Mini-Surrogate + Mineral Spirits "D"	7 ml mineral spirits "D" injected into side B. Results on Table 8 and Figure 2.
DTC440	11/1/96	Mini-Surrogate + Mineral Spirits "C"	7 ml mineral spirits "C" injected into side A. Results on Table 8 and Figure 2.
DTC441	11/7/96	Mini-Surrogate + Mineral Spirits "B"	7 ml mineral spirits "B" injected into side B. Results on Table 8 and Figure 2.

Table 7 (continued)

RunID	Date	Title	Comments
DTC442	11/8/96	Mini-Surrogate + Mineral Spirits "A"	7 ml mineral spirits "A" injected into side A. Results on Table 8 and Figure 2.
DTC443	11/12/96	Propene + NOx	Control run for comparison with other propene runs carried out in this and other chambers. The results were consistent with previous propene runs. Good side equivalency observed.
DTC444	11/13/96	n-Butane + NOx	Control run to measure the chamber radical source. Results were in good agreement with predictions of the standard chamber model.
DTC445	11/14/96	Ozone dark decay	The ozone dark decay rate, after correction for dilution, was ~1.2%/hour on both sides, in good agreement with the standard chamber effects model. Dilution on both sides was ~0.5%/hour, within the normal range for these reactors.
DTC452	3/3/97	NO2 Actinometry	The NO_2 photolysis rate was measured using the quartz tube method was 0.18 min^{-1}, somewhat lower than predicted by the trend of previous actinometry results in this chamber.
DTC469	4/4/97	NO2 Actinometry	The NO_2 photolysis rate was measured using the quartz tube method was 0.15 min^{-1}, also lower than predicted by the trend of previous actinometry results, and suggesting a more rapid rate of decline in light intensity than was the case before run DTC429.
		New Reaction Bags Installed. Lights Changed	
DTC472	4/23/97	Propene + NOx	Control run for comparison with other propene runs carried out in this and other chambers. The results were consistent with previous propene runs, given the somewhat higher light intensity. Good side equivalency observed.

Table 7 (continued)

RunID	Date	Title	Comments
DTC473	4/24/97	n-Butane + NOx	Control run to measure the chamber radical source. Results for Side B were consistent with predictions of the standard chamber model. Radical source which fit data for Side B was ~45% higher, but within the normal range.
DTC474	4/25/97	Full Surrogate + NOx	Control run to evaluate side equivalency for full surrogate run. Good side equivalency observed. Slightly more ozone formed than predicted by model.
DTC475	4/28/97	NO2 Actinometry	The NO_2 photolysis rate was measured using the quartz tube method was 0.20 min^{-1}. This is higher than observed before the bags and lights were changed, but consistent with the light intensity measurements in the chamber around the time of DTC-300.
DTC476	4/29/97	Full Surrogate + Mineral Spirits "D"	15 ml mineral spirits "D" injected into side A. Results on Table 8 and Figure 3.
DTC477	4/30/97	Low NOx Full Surrogate + Mineral Spirits "D"	15 ml mineral spirits "D" injected into side B. Results on Table 8 and Figure 4.
DTC478	5/1/97	Full Surrogate +Mineral Spirits "C"	15 ml mineral spirits "C" injected into side A. Results on Table 8 and Figure 3.
DTC479	5/2/97	Low NOx Full Surrogate + Mineral Spirits "C"	15 ml mineral spirits "C" injected into side A. Results on Table 8 and Figure 4.
DTC480	5/5/97	Full Surrogate +Mineral Spirits "B"	15 ml mineral spirits "B" injected into side A. Results on Table 8 and Figure 3.
DTC481	5/6/97	Low NOx Full Surrogate + Mineral Spirits "B"	15 ml mineral spirits "B" injected into side B. Results on Table 8 and Figure 4.
DTC482	5/7/97	n-Butane + NOx	Control run to measure the chamber radical source. Essentially the same results as DTC473, with Side A having a slightly higher apparent radical source.

Table 7 (continued)

RunID	Date	Title	Comments
DTC483	5/8/97	Propene + NOx	Control run for comparison with other propene runs carried out in this and other chambers. Slightly more O_3 formation than DTC472, probably because of slightly higher initial propene. Good side equivalency observed.
DTC484	5/9/97	NO2 Actinometry	The NO_2 photolysis rate was measured using the quartz tube method was 0.22 min^{-1}, in reasonably good agreement with the previous determination.
DTC485	5/11/97	Ozone Dark Decay	Approximately 0.3 ppm O_3 injected. The O_3 dark decay rate on each side was ~6.3%/hour, about 4 times greater than usual for Teflon reaction bags. However, no dilution information was obtained because of improper CO injection.
DTC486	5/12/97	Full Surrogate + Mineral Spirits "A"	15 ml mineral spirits "A" injected into side A. Results on Table 8 and Figure 3.
DTC487	5/13/97	Low NOx Full Surrogate + Mineral Spirits "A"	15 ml mineral spirits "A" injected into side B. Results on Table 8 and Figure 4.
DTC488	5/15/97	Full Surrogate + NOx	Control run to evaluate side equivalency for full surrogate run. Good side equivalency observed. Slightly more ozone formed than predicted by the model.
DTC490	5/19/97	NO2 Actinometry	The NO2 photolysis rate was measured using the quartz tube method was 0.20 min-1, in good agreement with the previous determination, and indicating that the light intensity is relatively sTable 8uring this period.
DTC499	6/2/97	Ozone Dark Decay	Approximately 1 ppm O_3 injected. The O_3 dark decay rate on each side, after correction for dilution of ~0.2%/hour, was only ~0.3%/hour, which is lower than the usual O3 dark decay rate for Teflon bag reactors.

of the n-butane - NO_x experiments, which are highly sensitive to the magnitude of the chamber radical source assumed in the model (see Table A-4 in Appendix A), were sufficiently well simulated by the model to indicate that the model was appropriately representing this effect for these runs. The n-butane - NO_x runs carried out during the second series indicated a slightly higher chamber radical input rate for side B relative to side A. However, this difference was not important in affecting the results of the full surrogate reactivity experiments conducted during this period, as indicated both by simulation sensitivity runs, and by results of the surrogate - NO_x side equivalency experiment.

Results of The Reactivity Experiments

Summaries of the conditions and results of the incremental reactivity experiments are given on Table 8. Except for run DTC438, where a relatively large amount of sample "D" was added to assess its approximate reactivity range, all experiments of the same base ROG and NO_x type had the same amount of mineral spirits sample added. This allows for more direct comparison of results. However, because of variations in temperature control in the laboratory, the average temperatures for mini-surrogate runs DTC441 and DTC442 were somewhat lower than for the other mini-surrogate runs, resulting in slightly lower base-case ozone formation in those experiments. The conditions were better duplicated in the full surrogate experiments, as shown on Table 8.

A comparison of the amounts of mineral spirits components injected as determined by GC total peak area integration, total carbon analyzer, and calculated amount injected is also shown on Table 8. It can be seen that these measures did not agree perfectly, but they were all of the same magnitude, and the discrepancies between them were not systematic. There was only a slight difference between the GC total peak area analysis when calibrated based on n-octane and aromatic response factors, or when calibrated based on amounts of liquid mineral spirits injected into known volumes. The GC total peak areas measured were somewhat higher than the calculated amounts injected in the runs and the full surrogate experiments employing Samples "C" (for low NO_x) and "D", but lower for the full surrogate runs with Samples "A" and "B". The mineral spirits levels as determined by the total hydrocarbon analyzer, which was not used during the mini-surrogate runs, are consistently 25-30% lower than the value calculated based on the amount injected.

For modeling purposes, it was assumed that the amounts of mineral spirits components present in the chamber were as indicated based on the calculated amount injected. This could be an overestimate if the mineral spirits were not completely evaporated into the chamber. However, the total per-carbon GC peak area calibration factors obtained from calibrations based on the calculated amounts injected agreed quite well with those obtained for n-octane and other compounds, indicating that the samples were completely injected when the calibrations were carried out, where the same injection procedures were used. The lower THC readings may be due to losses of the compounds on the sample lines or calibration problems, but this has not been completely investigated. Nevertheless, the possibility that the amounts

Table 8. Summary of conditions and results of the incremental reactivity experiments.

Run ID	Samp.	Conditions		Base Mix [a]		Sample Injected (ppmC) [b]				t=6 d(O_3-NO) (ppm)			t=5 IntOH (10^{-6} min)		
	ID	T (K)	k1 [c]	NOx	ROG	THC	GC		Calc	Base	Test	IR [d]	Base	Test	IR
Mini-Surrogate															
DTC-438(A)	D	296	0.17	0.36	5.5	-	6.0	6.5	5.4	0.50	0.21	-0.055	9	3	-1.1
DTC-442(A)	A	294	0.17	0.34	5.2	-	2.0	2.5	1.8	0.40	0.31	-0.049	12	7	-0.9
DTC-441(B)	B	294	0.17	0.35	5.5	-	2.4	2.0	1.8	0.40	0.26	-0.076	9	5	-0.6
DTC-440(A)	C	296	0.17	0.36	5.4	-	2.2	2.5	1.8	0.50	0.32	-0.099	12	7	-1.0
DTC-439(B)	D	297	0.17	0.35	5.5	-	1.9	2.1	1.8	0.51	0.36	-0.084	10	7	-0.6
High NO_x Full Surrogate															
DTC-486(A)	A	298	0.21	0.31	4.7	2.8	2.2	2.6	3.7	0.66	0.72	0.017	24	15	-1.9
DTC-480(A)	B	298	0.21	0.30	4.4	2.5	3.0	2.5	3.7	0.66	0.66	-0.001	26	14	-2.7
DTC-478(A)	C	297	0.21	0.32	4.8	2.6	3.5	3.8	3.7	0.67	0.66	-0.003	24	14	-2.2
DTC-476(A)	D	298	0.21	0.32	4.6	2.8	3.9	4.3	3.7	0.66	0.68	0.004	25	14	-2.4
Low NO_x Full Surrogate															
DTC-487(B)	A	298	0.21	0.13	4.4	2.7	2.2	2.6	3.7	0.43	0.43	-0.001	26	13	-2.9
DTC-481(B)	B	298	0.21	0.13	4.6	2.5	2.5	2.1	3.7	0.42	0.42	0.000	26	14	-2.7
DTC-479(B)	C	297	0.21	0.15	4.9	2.8	4.1	4.5	3.7	0.44	0.46	0.005	27	15	-2.4
DTC-477(B)	D	297	0.21	0.14	5.0	3.0	4.4	4.8	3.7	0.43	0.43	0.001	26	14	-2.3

[a] Initial NOx in ppm and base ROG surrogate in ppmC.

[b] Methods for determining total gas-phase ppmC of mineral spirits components: THC = difference in total hydrocarbon analyzer reading between base and added sample sides. GC = determined from area under overlapping GC peaks attributed to mineral spirits components. Number on right is determined from separate calibrations for each sample and number on left is determined from average per-carbon response for n-hexane, n-octane, toluene, and m-xylene. Calc = calculated from microliters of sample injected and volume of the chamber, as determined from NOx injections. The amount calculated from the microliters injected was used in the reactivity analysis and model simulations.

[c] NO_2 photolysis rate in min^{-1} assigned from results of NO_2 actinometry experiments carried out around the same time.

[d] Incremental reactivity, relative to ppmC sample injected, as calculated from amount injected.

of mineral spirits assumed to be present in the model calculations may be ~25% high cannot be entirely ruled out.

Plots of d(O_3-NO) data and d(O_3-NO) and IntOH incremental reactivity results from comparable mini-surrogate, and high and low NO_x full surrogate runs are shown on Figures 2-4, respectively. Results of model calculations, discussed in the following section, are also shown. For comparison purposes, Figures 2-4 also show results for the most closely comparable experiment previously carried out for n-dodecane (Carter et al, 1996). Note, however, that the full surrogate n-dodecane runs had slightly lower NO_x than the full surrogate runs for this program, so the base case conditions are not exactly the same in those cases. Also, the amount of test compound added was somewhat less.

Table 8 and Figure 2 show that all four mineral spirits samples, like n-dodecane and the other higher n-alkanes (Carter et al, 1996), significantly inhibit NO oxidation, O_3 formation, and integrated OH radical levels in the mini-surrogate experiments. In the first mini-surrogate experiment with the larger amount of sample added, DTC438, the amount of inhibition was so great that very little ozone was formed [with the d(O_3-NO) yield essentially reflecting only NO oxidation], and the IntOH levels were suppressed to levels which were almost too low to measure. Consequently, the subsequent mini-surrogate experiments were carried out with 1/3 as much mineral spirits sample added.

Each of the three all-alkane mineral spirits samples (Samples "B", "C", and "D") caused essentially the same amount of d(O_3-NO) and IntOH inhibition in the mini-surrogate experiments, to within the experimental variability. The inhibition of IntOH by sample "A" was also essentially the same as that for the others, but Sample "A" caused somewhat less d(O_3-NO) inhibition than the all-alkane samples, indicating the likely effect of the presence of reactive aromatic and alkene components. The d(O_3-NO) and IntOH inhibition caused by the all-alkane mineral spirits samples is somewhat less than seen in the most closely comparable n-dodecane run, though the differences are not great. Note, however, that the amount of n-dodecane added is somewhat less than the amount of sample added in the mineral spirits runs, and model calculations indicate that inhibition by alkanes relative to the amount added (i.e., negative incremental reactivities) tends to increase as the amount added is reduced (Carter et al., 1993a).

Table 8 and Figure 2 show that the addition of the all-alkane samples also causes significant OH radical inhibition in the higher NO_x full surrogate runs, and also slightly inhibits the initial NO oxidation rate [i.e., the d(O_3-NO) formation in the early parts of the runs]. On the other hand, they cause essentially no change in the final O_3 [or d(O_3-NO)] levels. These results are similar to the data observed for n-dodecane, though there was some slight O_3 inhibition at the end of the run, and the intOH inhibition was slightly higher. Sample "A" had somewhat less IntOH inhibition, and had a positive effect on the final ozone in the experiment. This higher NO_x full surrogate experiment showed the greatest differences

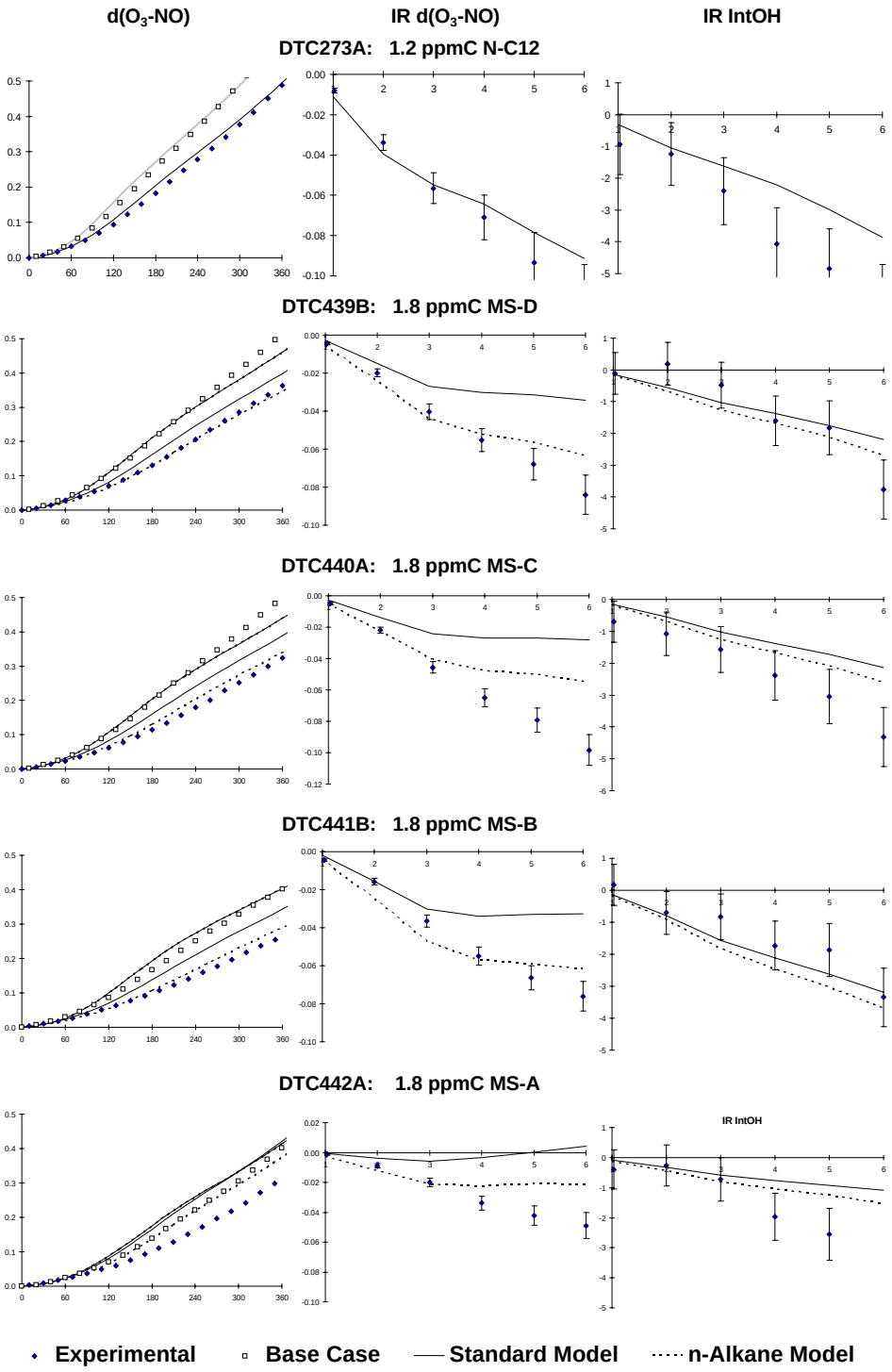

Figure 2. Plots of selected results of incremental reactivity experiments using the mini-surrogate. Previous results from a comparable n-dodecane run are shown for comparison.

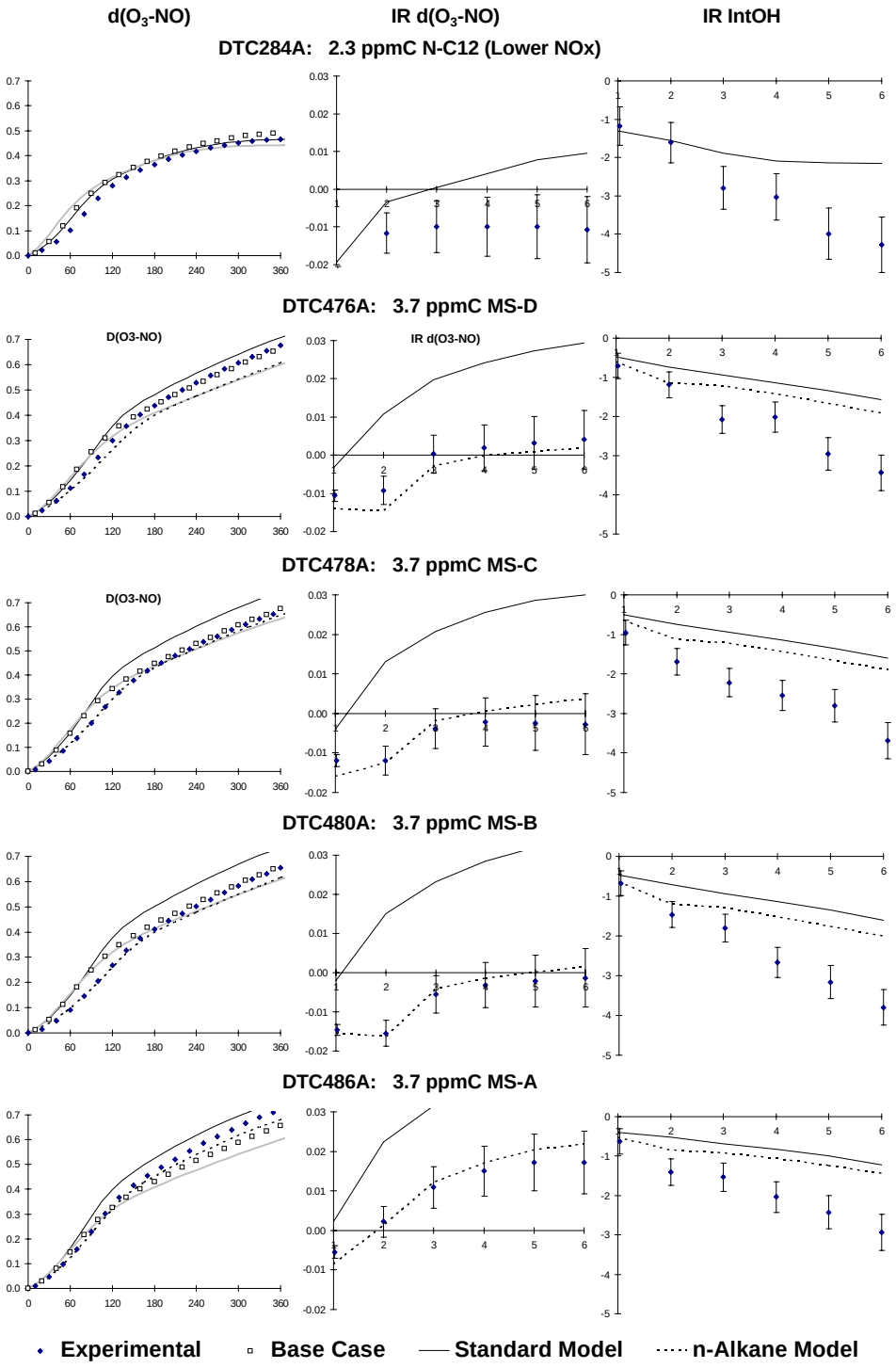

Figure 3. Plots of selected results of incremental reactivity experiments using the high NO_x full surrogate. Previous results from a comparable n-dodecane run are shown for comparison.

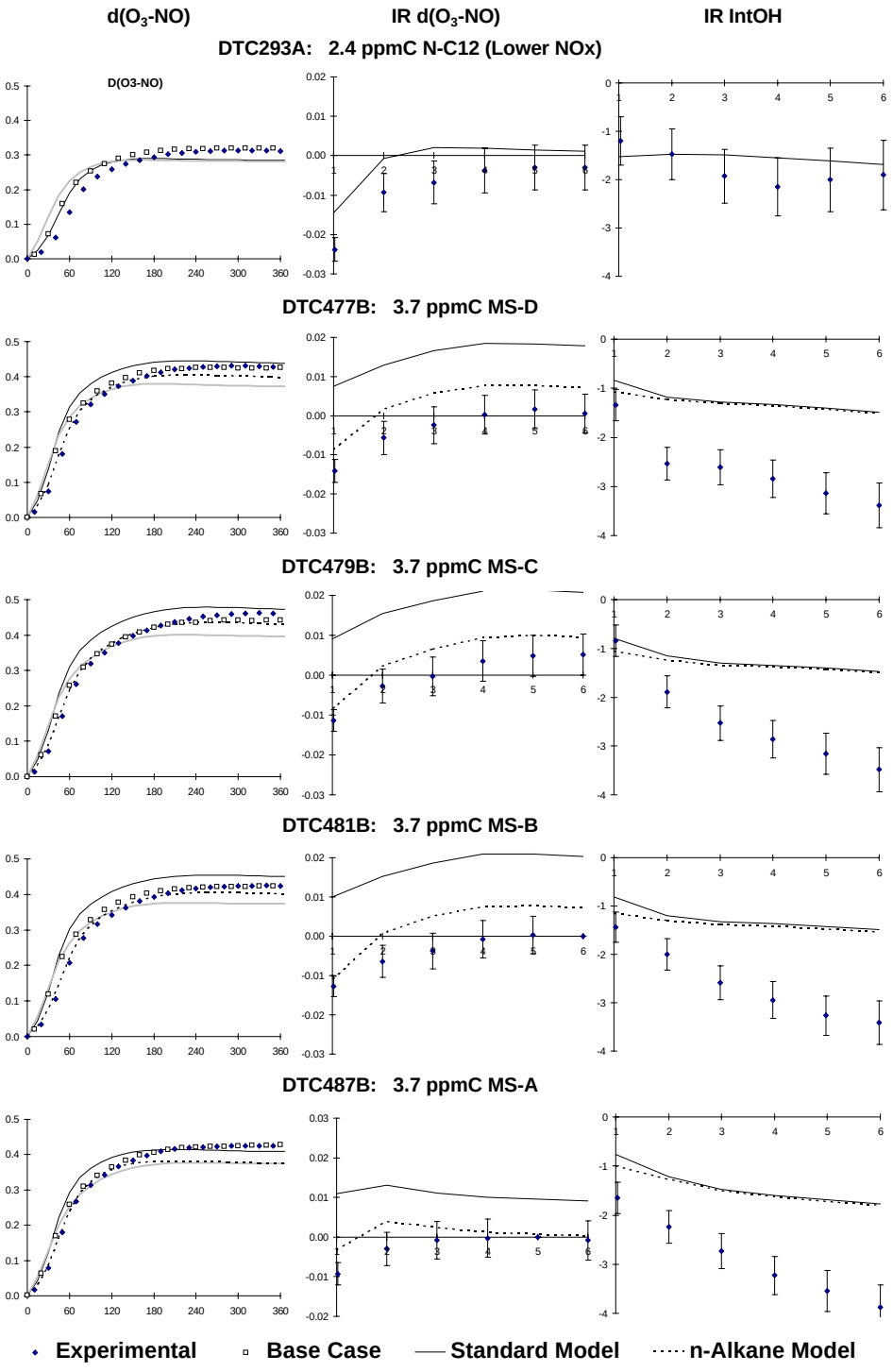

Figure 4. Plots of selected results of incremental reactivity experiments using the low NO_x full surrogate. Previous results from a comparable n-dodecane run are shown for comparison.

between sample "A" and the all-alkane samples than the other two types of reactivity experiments employed in this study.

The fact that the mineral spirits cause large inhibitions of d(O_3-NO) in the mini-surrogate runs yet have only small or (in the case of Sample "A") positive effects on d(O_3-NO) in the full surrogate runs is consistent with results observed with other compounds (Carter et al, 1995b, 1996, unpublished results from this laboratory). This is due to the fact that ozone formation and NO oxidation tend to be much more sensitive to radical inhibition (and initiation) effects in the mini-surrogate runs than in runs with the full surrogate (Carter et al, 1995b). This is because the full surrogate contains radical initiating species such as formaldehyde and trans-2-butene which are not present in the mini-surrogate. Ozone formation and NO oxidation in full surrogate runs tend to be more sensitive to the NO to NO_2 conversions in the test compounds, which have a positive effect on ozone formation. In the case of the higher alkanes, the positive effect of the relatively large number of NO to NO_2 conversions is not enough to counter the negative effect due to radical termination caused by nitrate formation in the mini-surrogate runs, but in the full surrogate runs, where the effect of radical termination is relatively less important, the two effects more closely balance, resulting in small net effects of the alkane samples on d(O_3-NO) reactivities.

Finally, Table 8 and Figure 3 show that all the samples cause significant OH radical inhibition in the low NO_x full surrogate runs, slightly slow down the initial NO oxidation rate, but have essentially no effect on final ozone formation. The results for the most comparable n-dodecane experiment is very similar, despite its lower NO_x levels and lower amount of test compound added. Unlike the higher NO_x full surrogate runs, the results of the run with Sample "A" did not appear to be significantly different than the runs with n-dodecane or the all-alkane samples.

Results of Model Simulations of the Reactivity Experiments

Figures 2-4 also show results of model simulations of these experiments. The solid lines show calculations using the compositions shown in Table 6 and the estimated mechanisms for all the components, as discussed above and indicated in Tables 1 and 2 and Appendix A. These are referred to as the "standard" model calculations in the subsequent discussion. The figures show that the standard model gives moderately good fits to the n-dodecane runs, with the data shown for the three runs on these figures being representative of the fits to the full set of higher n-alkane runs given by Carter et al (1996). The figures also show that the standard model performs very poorly in simulating the mineral spirits runs, significantly underpredicting the d(O_3-NO) inhibition in the mini-surrogate runs, and significantly overpredicting their d(O_3-NO) reactivities in both the higher and low NO_x full surrogate runs.

The possibility that the model discrepancies could be due to an uncertainty in the assumed amounts of mineral spirits components present in the chamber needs to be considered. As indicated above, the amounts of mineral spirits present in the chamber assumed in the model calculations could be

high by ~25%. However, assuming ~25% less mineral spirits present in the experiments has only a relatively small effect on the results of the model simulations, not nearly enough to account for the significant discrepancies which are observed. The GC and total hydrocarbon data indicate that it is unlikely that the amount of mineral spirits components assumed in the model simulations could be in high by more than ~25%.

The fact that the standard model can simulate reasonably well the d(O_3-NO) reactivities for the n-alkanes indicates that the significant overprediction of reactivity (or underprediction of inhibition) for the all-alkane mineral spirits samples is almost certainly due to problems with the branched and/or cyclic alkane mechanisms. The GC-MS data indicate that the these are major components of all these samples, with the n-alkanes being no more than ~25% by weight (see Table 4). As discussed above, although the mechanisms used for these compounds represent our best current estimates, they are based on application of estimation techniques derived from a very limited data set of low molecular weight compounds. Clearly these mechanisms are not applicable to at least some of the C_{10+} compounds which are dominant in these samples.

Figures 2-4 show that the data for the all-alkane samples look qualitatively much more like the data and model for the n-dodecane runs than the model predictions for those runs. This suggests that assuming that branched and cyclic alkanes react with essentially the same mechanisms as normal alkanes may result in a model which performs better in simulating these experiments. The effect of making this assumption, i.e., using the mechanism of an n-alkane with the same number of carbons to represent each of the branched and cyclic alkanes in the samples, are shown as the dotted lines on Figures 2-4. These calculations are referred to as the "n-alkane" model in the subsequent discussion. The figures show that this n-alkane model indeed gives significantly better fits of the model simulations of the mineral spirits samples, not only for the all-alkane samples, but for the aromatic and olefin containing sample "A" as well.

Although the n-alkane model performs significantly better than the standard model in fitting the mineral spirit reactivity data, some discrepancies still exist. In particular, the n-alkane model tends to underpredict the O_3 inhibition at the latter stages of the mini-surrogate runs, and underpredicts the inhibition of IntOH in the full surrogate runs. This underprediction of IntOH inhibition in full surrogate runs is also observed in the simulations of many of the n-alkane experiments (Carter et al, 1996), and may be a problem with the general mechanism, rather than the use of n-alkane mechanisms to represent branched and cyclic compounds. Note that the model discrepancies in all cases tend towards the n-alkane model *overpredicting* reactivity (underpredicting inhibition), which is opposite of what one would expect based on the fact that the standard mechanisms predict that a normal alkane model should *underpredict* reactivities of branched and cyclic alkane-containing samples.

Note that in addition to performing reasonably well in approximately simulating the d(O_3-NO) reactivities of the all-alkane samples, the n-alkane model also correctly predicts the reactivity differences between sample "A" and the all-alkane samples. In particular, it correctly predicts that the samples are most different in the higher NO_x full surrogate experiment, and predicts the d(O_3-NO) reactivities reasonably well in all those runs. This means that although the mechanisms and in some cases isomeric assignments for the aromatics and (particularly) the higher molecular weight alkenes have significant uncertainties, the model performs reasonably well in predicting the effects the presence of these high-reactivity compounds have on the overall reactivity this particular sample.

Atmospheric Reactivity Calculations

Since incremental reactivities in environmental chamber experiments are not necessarily the same as those in the atmosphere (Carter and Atkinson, 1989b; Carter et al, 1995b), atmospheric reactivity simulations are needed to assess the atmospheric implications of our results. Table 9 shows the relative ozone impacts, in terms of ozone formed per gram of mixture or compound added, calculated for various types of atmospheric conditions for each of the four samples, for both the standard and the n-alkane model. For comparison purposes, the relative impacts of ethane, the compound the EPA has used as the basis for determining VOC exemptions (Dimitriades, 1996), and of n-dodecane, the n-alkane with the most similar molecular weight to the average for most of the samples, are also shown. The ozone impacts are quantified both in terms of peak ozone (ozone yield) and in terms of integrated ozone over the Federal standard of 0.12 ppm ($IntO_3$>0.12). The ozone impacts are shown relative to the ozone impact caused by increasing the mass emissions of all VOCs, so the numbers shown are the relative effects of controlling emissions of the mixture or compound compared to controlling emissions of VOCs from all sources equally. The relative reactivities are shown for the Maximum Incremental Reactivity (MIR), the Maximum Ozone Incremental Reactivity (MOIR), and the Equal Benefit Incremental Reactivity (EBIR) scenarios, and statistics indicating the distributions of relative reactivities are shown for the 39 "Base Case" scenarios. These represent respectively the high NO_x conditions where O_3 is most sensitive to VOCs, the moderate NO_x conditions which are most favorable for ozone formation, the low NO_x conditions where NO_x control is equally effective in reducing O_3 as VOC control, and the distribution of scenarios developed by the EPA to represent various ozone non-attainment areas around the United States (Baugues, 1990). These provide an indication how relative reactivities vary with varying NO_x and with other scenario conditions.

The data on Table 9 show that the reactivities calculated using the all-alkane model are 2 - 4 times lower than those calculated using the standard mechanism for the all-alkane samples, and 1.6 - 2.5 times lower for the aromatic and alkene-containing sample. Given the fits to the chamber data, the predictions of the n-alkane model is considered to be a more reliable indication of the actual ozone impacts of these samples. This indicates that use of the standard mechanism would result in overpredictions of ozone

Table 9. Summary of calculated reactivities (gram basis) for ethane, n-dodecane, and the mineral spirits samples, relative to the total of all VOC emissions.

impacts of the all-alkane samples by at least a factor of two, with a slightly lower overprediction in the case of samples containing aromatics and alkenes.

The reactivities calculated for Samples B-D are very similar to those for n-dodecane. The alkane model predicts the samples are slightly more reactive than n-dodecane because of the lower n-alkanes in the samples, and the fact that the nitrate yields, the main factor affecting the decline in reactivity as the size of the n-alkane increases, tends to level off at the highest carbon number. The relative reactivities of n-dodecane and the n-alkane samples are calculated to vary significantly with environmental conditions, being up to ~40% of the average of all emissions in some scenarios, having negative effects on ozone in others. In addition, the n-alkane and n-alkane mixture reactivities are lower when ozone is calculated by integrated ozone over the standard as opposed to ozone yield, with $IntO_3$>0.12 reactivities being comparable to those for ethane in most of the scenarios. The variation of n-alkane reactivity with scenario

Table 9. Summary of calculated reactivities (gram basis) for ethane, n-dodecane, and the mineral spirit samples, relative to total of all VOC emissions..

Scenario	Ethane	n-C_{12}	Sample "A"		Sample "B"		Sample "C"		Sample "D"	
			Std.	n-Alk	Std.	n-Alk	Std.	n-Alk	Std.	n-Alk
					O_3 Yield Relative Reactivities					
Averaged Conditions										
MIR	0.08	0.14	0.54	0.34	0.40	0.16	0.38	0.16	0.38	0.16
MOIR	0.15	0.29	0.71	0.45	0.62	0.31	0.60	0.32	0.60	0.32
EBIR	0.19	0.28	0.77	0.40	0.72	0.29	0.68	0.29	0.68	0.29
39 Base Case										
Max	0.27	0.41	0.89	0.54	0.88	0.43	0.83	0.44	0.84	0.44
Avg+St.Dev	0.21	0.37	0.83	0.52	0.79	0.39	0.75	0.40	0.75	0.40
Average	0.17	0.25	0.74	0.40	0.68	0.28	0.64	0.28	0.64	0.28
Avg-St.Dev	0.13	0.14	0.65	0.29	0.57	0.16	0.53	0.16	0.53	0.16
Min	0.05	-0.10	0.50	0.07	0.34	-0.05	0.32	-0.06	0.32	-0.06
					IntO_3 >0.12 Relative Reactivities					
Averaged Conditions										
MIR	0.07	0.13	0.53	0.33	0.39	0.14	0.36	0.15	0.36	0.15
MOIR	0.10	0.16	0.58	0.35	0.46	0.17	0.43	0.18	0.43	0.18
EBIR	0.12	0.11	0.62	0.28	0.53	0.12	0.48	0.12	0.48	0.12
39 Base Case										
Max	0.19	0.21	0.68	0.38	0.63	0.23	0.57	0.23	0.57	0.23
Avg+St.Dev	0.14	0.19	0.64	0.38	0.57	0.21	0.52	0.21	0.52	0.21
Average	0.11	0.11	0.60	0.29	0.50	0.12	0.46	0.12	0.46	0.12
Avg-St.Dev	0.09	0.02	0.55	0.21	0.43	0.04	0.39	0.03	0.40	0.03
Min	0.05	-0.18	0.49	0.02	0.33	-0.18	0.30	-0.18	0.30	-0.18

conditions, and their reactivities relative to ethane, are discussed in detail by Carter et al (1996), and that discussion is also applicable to the sample reactivities when calculated by the model which best fits the chamber data.

As expected, Sample A is calculated to have higher atmospheric reactivities than the all-alkane samples, due to the role of the aromatic and alkene impurities. Although the standard model predicts that the presence of the non-alkane components increases the reactivity of this sample by only ~10-30% compared to the all-alkane samples, the all-alkane model predicts that the increase is greater, with the increase in O_3 yield reactivities ranging from 20% to a factor of 2, and the increase in $IntO_3$>0.12 reactivities ranging from 50% to over a factor of two. The greater difference is expected because the n-alkane mechanism assumes lower reactivities for the alkane components, and thus a greater reactivity difference between them and alkenes and aromatics.

CONCLUSIONS AND RECOMMENDATIONS

The objective of this program was to assess whether current methods for assessing the compositions and ozone formation potentials for mineral spirits could be used to predict the ozone impact for several representative mineral spirits samples. The results indicated that with high resolution GC-MS techniques, combined with FIA type analysis GC fractionation and elemental analysis data, it is possible to characterize their compositions reasonably well in terms of the model species currently used to assess ozone reactivities in airshed model calculations. However, the current model performs poorly in simulating the environmental chamber results, and probably overpredicts the atmospheric reactivities of these samples by at least a factor of two. This is apparently due to problems with the estimated atmospheric reaction mechanisms derived for the C_{9+} branched and/or cyclic alkane constituents, which represent ~70-95% of the mass of these samples. The model based on current estimates predict that these compounds are 2-3 times more reactive than the corresponding n-alkanes, but the chamber data for all four samples are much better simulated if the branched and cyclic alkanes are represented as if they were n-alkanes. This is inconsistent with our current understanding of the atmospheric chemistry of alkanes.

The discrepancies between chamber data and model predictions are unlikely to be due to problems in characterizing compositions of these samples. The type analysis data indicate that all samples contain ~90-100% alkanes, and the GC-MS data, from two different laboratories, indicate that the n-alkanes are not the primary constituents. Thus there can be no doubt that the branched and cyclic alkanes are the major components in these samples. Although the analytical data are not able to distinguish the particular isomers present, the current modeling approach represents all branched or cyclic isomers with a given carbon number using a single representative model species, so additional information concerning the exact distribution would not have been used in any case. Given the large numbers of possible isomers possible for C_{9+} branched and cyclic alkane, the obviously large number of such isomers in these samples, this is probably the only practical approach at the present time.

Although the chemical mechanisms currently used for the $C_{\leq 8}$ and C_{12+} normal alkanes have been shown to perform reasonably well in simulating the results of environmental chamber experiments (Carter et al, 1993a, 1995a,b, 1996), the assumed mechanisms for C_{9+} branched and cyclic alkanes have not been adequately evaluated. The only relevant information concern as-yet-unreported chamber data on reactivity experiments with n-hexylcyclohexane and n-octylcyclohexane, which were carried out under funding from the Aluminum Association. The results indicated that these n-alkylcyclohexanes, like the mineral spirits samples studied in this program, are better simulated by n-alkane models than the by standard mechanisms assumed for C_{12} and C_{14} cycloalkanes, or even by the mechanisms derived explicitly for these n-alkylcyclohexanes (unpublished results from this laboratory). It is clear that our current methods for

estimating the atmospheric reaction mechanisms of branched and cyclic alkanes need to be revised. This would require considerably more information concerning the atmospheric reactions of these compounds than is currently available, including basic laboratory studies concerning the branching ratios of the competing processes, as well as environmental chamber studies on effects of structure on overall atmospheric reactivity.

Despite the apparent problems with the alkane mechanism, the results of this program tend to validate the prediction that samples containing measurable amounts of aromatics and alkenes will have greater ozone impacts than samples where these are not detected. Once the model for the alkane constituents was modified to be consistent with the data for the all-alkane samples, the model performed reasonably well in simulating the apparent effect of the presence of these constituents. This is despite the fact that somewhat arbitrary assumptions concerning relative amounts of aromatic and olefin isomers which were calculated to have quite different reactivities. Improved identification of aromatic isomers, and information on the ratio of internal vs terminal alkenes present, would reduce the uncertainties in this regard. Although the somewhat arbitrary assumptions employed concerning isomeric distributions of aromatics and alkenes seemed to work reasonably well in the case of Sample "A", it is not known whether they would work as well with other samples, particularly those with higher aromatic or olefin content.

The results of this program, as well as the available preliminary data concerning alkylcyclohexanes, suggests that all the C_{9+} alkane constituents in mineral spirits samples should be represented as if they were normal alkanes when estimating their atmospheric ozone impacts. This method gives predictions which are more consistent with the chamber data than using the current estimation methods for representing branched and cyclic alkanes, at least for the four samples which were studied in this program. This would mean that the maximum incremental reactivities (MIR)'s of mineral spirits samples would be about half of what is currently predicted. This could make a significant difference if reactivity-based control strategies, such as being considered in California, are adopted. However, the representativeness of these four samples to the full range of mineral spirits or similar samples being subject to VOC regulations is highly uncertain. Chamber data with a wider variety of spirits samples, including those with varying levels of aromatic and alkene constituents, as well as all-alkane samples with widely varying ratios of branched to cyclic alkanes and with differing derivations, are necessary to determine the general applicability of the results of this study to mineral spirits in general.

REFERENCES

Atkinson, R. (1987): "A Structure-Activity Relationship for the Estimation of Rate Constants for the Gas-Phase Reactions of OH Radicals with Organic Compounds," Int. J. Chem. Kinet., 19, 799-828.

Atkinson, R. (1989): "Kinetics and Mechanisms of the Gas-Phase Reactions of the Hydroxyl Radical with Organic Compounds," J. Phys. Chem. Ref. Data, Monograph no 1.

Atkinson, R. (1990): "Gas-Phase Tropospheric Chemistry of Organic Compounds: A Review," Atmos. Environ., 24A, 1-24.

Atkinson, R. (1991): "Kinetics and Mechanisms of the Gas-Phase Reactions of the NO_3 Radical with Organic Compounds," J. Phys. Chem. Ref. Data, 20, 459-507.

Atkinson, R. (1994): "Gas-Phase Tropospheric Chemistry of Organic Compounds," J. Phys. Chem. Ref. Data, Monograph No. 2.

Atkinson, R. (1997): "Gas Phase Tropospheric Chemistry of Volatile Organic Compounds: 1. Alkanes and Alkenes," J. Phys. Chem. Ref. Data, 26, 215-290.

Atkinson, R. and W. P. L. Carter (1992): "Reactions of Alkoxy Radicals under Atmospheric Conditions: The Relative Importance of Decomposition versus Reaction with O_2," J. Atm. Chem., 13, 195-210.

Atkinson, R. and W. P. L. Carter (1984): "Kinetics and Mechanisms of the Gas-Phase Reactions of Ozone with Organic Compounds under Atmospheric Conditions," Chem. Rev. 1984, 437-470.

Baugues, K. (1990): "Preliminary Planning Information for Updating the Ozone Regulatory Impact Analysis Version of EKMA," Draft Document, Source Receptor Analysis Branch, Technical Support Division, U. S. Environmental Protection Agency, Research Triangle Park, NC, January.

Calvert, J. G., and J. N. Pitts, Jr. (1966): Photochemistry, John Wiley and Sons, New York.

CARB (1991): "Proposed Reactivity Adjustment Factors for Transitional Low-Emissions Vehicles — Staff Report and Technical Support Document," California Air Resources Board, Sacramento, CA, September 27, 1991.

CARB (1993): "Proposed Regulations for Low-Emission Vehicles and Clean Fuels — Staff Report and Technical Support Document," California Air Resources Board, Sacramento, CA, August 13, 1990. See also Appendix VIII of "California Exhaust Emission Standards and Test Procedures for 1988 and Subsequent Model Passenger Cars, Light Duty Trucks and Medium Duty Vehicles," as last amended September 22, 1993. Incorporated by reference in Section 1960.1 (k) of Title 13, California Code of Regulations.

Carter, W. P. L. (1990): "A Detailed Mechanism for the Gas-Phase Atmospheric Reactions of Organic Compounds," Atmos. Environ., 24A, 481-518.

Carter, W. P. L. (1991): "Development of Ozone Reactivity Scales for Volatile Organic Compounds", EPA-600/3-91/050, August.

Carter, W. P. L. (1994): "Development of Ozone Reactivity Scales for Volatile Organic Compounds," J. Air & Waste Manage. Assoc., 44, 881-899.

Carter, W. P. L. (1995a): "Investigation of Atmospheric Reactivities of Selected Stationary Source VOCs," Research Proposal to the California Air Resources Board, October 3.

Carter, W. P. L. (1995b): "Computer Modeling of Environmental Chamber Measurements of Maximum Incremental Reactivities of Volatile Organic Compounds," Atmos. Environ., 29, 2513-2517.

Carter, W. P. L., and R. Atkinson (1985): "Atmospheric Chemistry of Alkanes", J. Atmos. Chem., 3, 377-405, 1985.

Carter, W. P. L., A. M. Winer, R. Atkinson, S. E. Heffron, M. P. Poe, and M. A. Goodman (1987): "Atmospheric Photochemical Modeling of Turbine Engine Fuels. Phase II. Computer Model Development," Report on USAF Contract no. F08635-83-0278, Engineering and Services Laboratory, Air Force Engineering and Services Center, Tyndall Air Force Base, Florida, August.

Carter, W. P. L. and R. Atkinson (1987): "An Experimental Study of Incremental Hydrocarbon Reactivity," Environ. Sci. Technol., 21, 670-679

Carter, W. P. L. and R. Atkinson (1989a): "Alkyl Nitrate Formation from the Atmospheric Photooxidation of Alkanes; a Revised Estimation Method," J. Atm. Chem. 8, 165-173.

Carter, W. P. L. and R. Atkinson (1989b): "A Computer Modeling Study of Incremental Hydrocarbon Reactivity", Environ. Sci. Technol., 23, 864.

Carter, W. P. L., and F. W. Lurmann (1990): "Evaluation of the RADM Gas-Phase Chemical Mechanism," Final Report, EPA-600/3-90-001.

Carter, W. P. L. and F. W. Lurmann (1991): "Evaluation of a Detailed Gas-Phase Atmospheric Reaction Mechanism using Environmental Chamber Data," Atm. Environ. 25A, 2771-2806.

Carter, W. P. L., J. A. Pierce, I. L. Malkina, D. Luo and W. D. Long (1993a): "Environmental Chamber Studies of Maximum Incremental Reactivities of Volatile Organic Compounds," Report to Coordinating Research Council, Project No. ME-9, California Air Resources Board Contract No. A032-0692; South Coast Air Quality Management District Contract No. C91323, United States Environmental Protection Agency Cooperative Agreement No. CR-814396-01-0, University Corporation for Atmospheric Research Contract No. 59166, and Dow Corning Corporation. April 1.

Carter, W. P. L, D. Luo, I. L. Malkina, and J. A. Pierce (1993b): "An Experimental and Modeling Study of the Photochemical Ozone Reactivity of Acetone," Final Report to Chemical Manufacturers Association Contract No. KET-ACE-CRC-2.0. December 10.

Carter, W. P. L., J. A. Pierce, D. Luo, and I. L. Malkina (1995a): "Environmental Chamber Study of Maximum Incremental Reactivities of Volatile Organic Compounds," Atmos. Environ. 29, 2499-2511.

Carter, W. P. L., D. Luo, I. L. Malkina, and J. A. Pierce (1995b): "Environmental Chamber Studies of Atmospheric Reactivities of Volatile Organic Compounds. Effects of Varying ROG Surrogate and NO_x," Final report to Coordinating Research Council, Inc., Project ME-9, California Air Resources Board, Contract A032-0692, and South Coast Air Quality Management District, Contract C91323. March 24.

Carter, W. P. L., D. Luo, I. L. Malkina, and J. A. Pierce (1995c): "Environmental Chamber Studies of Atmospheric Reactivities of Volatile Organic Compounds. Effects of Varying Chamber and Light Source," Final report to National Renewable Energy Laboratory, Contract XZ-2-12075, Coordinating Research Council, Inc., Project M-9, California Air Resources Board, Contract A032-0692, and South Coast Air Quality Management District, Contract C91323, March 26.

Carter, W. P. L., J. M. Norbeck, A. Venkatram, M. J. Barth, R. Hariharan, T. D. Durbin, S. E. Belinski, R. Fitzgerald, and P. G. Stein (1995d): "Atmospheric Process Evaluation of Mobile Source Emissions," Final Report to National Renewable Energy Laboratory, Midwest Research Institute Contract No. XCC-4-14161-01, June.

Carter, W. P. L., D. Luo, I. L. Malkina, and D. Fitz (1995e): "The University of California, Riverside Environmental Chamber Data Base for Evaluating Oxidant Mechanism. Indoor Chamber Experiments through 1993," Report submitted to the U. S. Environmental Protection Agency, EPA/AREAL, Research Triangle Park, NC., March 20..

Carter, W. P. L., D. Luo, and I. L. Malkina (1996): "Investigation of the Atmospheric Ozone Formation Potentials of C_{12} - C_{16} n-alkanes," Report to the Aluminum Association, Contract AA1345, October 28.

Carter, W. P. L., D. Luo, and I. L. Malkina (1997a): "Environmental Chamber Studies for Development of an Updated Photochemical Mechanism for VOC Reactivity Assessment," Draft final report to California Air Resources Board Contract 92-345, Coordinating Research Council Project M-9, and National Renewable Energy Laboratory Contract ZF-2-12252-07. March 10.

Carter, W. P. L., D. Luo, and I. L. Malkine (1997b): "Investigation of the Atmospheric Ozone Formation Potential of Propylene Glycol," Report to Philip Morris, USA, May 2.

EPA (1984): "Guideline for Using the Carbon Bond Mechanism in City-Specific EKMA," EPA-450/4-84-005, February.

Gery, M. W., G. Z. Whitten, and J. P. Killus (1988): "Development and Testing of the CBM-IV For Urban and Regional Modeling,", EPA-600/ 3-88-012, January.

Johnson, G. M. (1983): "Factors Affecting Oxidant Formation in Sydney Air," in "The Urban Atmosphere -- Sydney, a Case Study." Eds. J. N. Carras and G. M. Johnson (CSIRO, Melbourne), pp. 393-408.

Kwok, E. S. C., and R. Atkinson (1995): "Estimation of Hydroxyl Radical Reaction Rate Constants for Gas-Phase Organic Compounds Using a Structure-Reactivity Relationship: An Update," Atmos. Environ 29, 1685-1695.

Pitts, J. N., Jr., E. Sanhueza, R. Atkinson, W. P. L. Carter, A. M. Winer, G. W. Harris, and C. N. Plum (1984): "An Investigation of the Dark Formation of Nitrous Acid in Environmental Chambers," Int. J. Chem. Kinet., 16, 919-939.

Stockwell, W. R., P. Middleton, J. S. Chang, and X. Tang (1990): "The Second Generation Regional Acid Deposition Model Chemical Mechanism for Regional Air Quality Modeling," J. Geophys. Res. 95, 16343- 16376.

Tuazon, E. C., R. Atkinson, C. N. Plum, A. M. Winer, and J. N. Pitts, Jr. (1983): "The Reaction of Gas-Phase N_2O_5 with Water Vapor," Geophys. Res. Lett. 10, 953-956.

Zafonte, L., P. L. Rieger, and J. R. Holmes (1977): "Nitrogen Dioxide Photolysis in the Los Angeles Atmosphere," Environ. Sci. Technol. 11, 483-487.

APPENDIX A
LISTING OF THE CHEMICAL MECHANISM

The chemical mechanism used in the environmental chamber and atmospheric model simulations discussed in this report is given in Tables A-1 through A-4. Table A-1 lists the species used in the mechanism, Table A-2 gives the reactions and rate constants, Table A-3 gives the parameters used to calculate the rates of the photolysis reactions, and Table A-4 gives the values and derivations of the chamber-dependent parameters used when modeling the environmental chamber experiments. Footnotes to Table A-2 indicate the format used for the reaction listing.

Table A-1. List of species in the chemical mechanism used in the model simulations for this study.

Name	Description
Constant Species.	
O2	Oxygen
M	Air
H2O	Water
Active Inorganic Species.	
O3	Ozone
NO	Nitric Oxide
NO2	Nitrogen Dioxide
NO3	Nitrate Radical
N2O5	Nitrogen Pentoxide
HONO	Nitrous Acid
HNO3	Nitric Acid
HNO4	Peroxynitric Acid
HO2H	Hydrogen Peroxide
Active Radical Species and Operators.	
HO2.	Hydroperoxide Radicals
RO2.	Operator to Calculate Total Organic Peroxy Radicals
RCO3.	Operator to Calculate Total Acetyl Peroxy Radicals
Active Reactive Organic Product Species.	
CO	Carbon Monoxide
HCHO	Formaldehyde
CCHO	Acetaldehyde
RCHO	Lumped C3+ Aldehydes
ACET	Acetone
MEK	Lumped Ketones

Table A-1, (continued)

Name	Description
PHEN	Phenol
CRES	Cresols
BALD	Aromatic aldehydes (e.g., benzaldehyde)
GLY	Glyoxal
MGLY	Methyl Glyoxal
BACL	Biacetyl or other lumped α-dicarbonyls, including α-keto esters
AFG1	Reactive Aromatic Fragmentation Products from benzene and naphthalene
AFG2	Other Reactive Aromatic Fragmentation Products
AFG3	Aromatic Fragmentation Products used in adjusted m-xylene mechanism
RNO3	Organic Nitrates
NPHE	Nitrophenols
ISOPROD	Lumped isoprene product species
PAN	Peroxy Acetyl Nitrate
PPN	Peroxy Propionyl Nitrate
GPAN	PAN Analogue formed from Glyoxal
PBZN	PAN Analogues formed from Aromatic Aldehydes
-OOH	Operator Representing Hydroperoxy Groups
Non-Reacting Species	
CO2	Carbon Dioxide
-C	"Lost Carbon"
-N	"Lost Nitrogen"
H2	Hydrogen
Steady State Species and Operators.	
HO.	Hydroxyl Radicals
O	Ground State Oxygen Atoms
O*1D2	Excited Oxygen Atoms
RO2-R.	Peroxy Radical Operator representing NO to NO_2 conversion with HO_2 formation.
RO2-N.	Peroxy Radical Operator representing NO consumption with organic nitrate formation.
RO2-NP.	Peroxy Radical Operator representing NO consumption with nitrophenol formation
R2O2.	Peroxy Radical Operator representing NO to NO_2 conversion.
CCO-O2.	Peroxy Acetyl Radicals
C2CO-O2.	Peroxy Propionyl Radicals
HCOCO-O2.	Peroxyacyl Radical formed from Glyoxal
BZ-CO-O2.	Peroxyacyl Radical formed from Aromatic Aldehydes
HOCOO.	Intermediate formed in Formaldehyde + HO_2 reaction
BZ-O.	Phenoxy Radicals
BZ(NO2)-O.	Nitratophenoxy Radicals
HOCOO.	Radical Intermediate formed in the HO_2 + Formaldehyde system.
(HCHO2)	Excited Criegee biradicals formed from $=CH_2$ groups
(CCHO2)	Excited Criegee biradicals formed from $=CHCH_3$ groups
(RCHO2)	Excited Criegee biradicals formed from =CHR groups, where R not CH_3
(C(C)CO2)	Excited Criegee biradicals formed from $=C(CH_3)_2$ groups

Table A-1, (continued)

Name	Description
(C(R)CO2)	Excited Criegee biradicals formed from $=C(CH_3)R$ or CR_2 groups
(BZCHO2)	Excited Criegee biradicals formed from styrenes
(C:CC(C)O2)	Excited Criegee biradicals formed from isoprene
(C:C(C)CHO2)	Excited Criegee biradicals formed from isoprene
(C2(O2)CHO)	Excited Criegee biradicals formed from isoprene products
(HOCCHO2)	Excited Criegee biradicals formed from isoprene products
(HCOCHO2)	Excited Criegee biradicals formed from isoprene products
(C2(O2)COH)	Excited Criegee biradicals formed from isoprene products
Primary Organics Represented explicitly	
CH4	Methane
ETHANE	Ethane
N-C4	n-Butane
N-C6	n-Hexane
N-C8	n-Octane
N-C9	n-Nonane
N-C10	n-Decane
N-C11	n-Undecane
N-C12	n-Dodecane
N-C13	n-Tridecane
N-C14	n-Tetradecane
N-C15	n-Pentadecane
BR-C8	Branched C_8 Alkanes
BR-C9	Branched C_9 Alkanes
BR-C10	Branched C_{10} Alkanes
BR-C11	Branched C_{11} Alkanes
BR-C12	Branched C_{12} Alkanes
BR-C13	Branched C_{13} Alkanes
BR-C14	Branched C_{14} Alkanes
BR-C15	Branched C_{15} Alkanes
ME-CYCC6	Methylcyclohexane
CYC-C8	Cyclic C_8 Alkanes
CYC-C9	Cyclic C_9 Alkanes
CYC-C10	Cyclic C_{10} Alkanes
CYC-C11	Cyclic C_{11} Alkanes
CYC-C12	Cyclic C_{12} Alkanes
CYC-C13	Cyclic C_{13} Alkanes
CYC-C14	Cyclic C_{14} Alkanes
CYC-C15	Cyclic C_{15} Alkanes
TOLUENE	Toluene
C2-BENZ	Ethylbenzene

Table A-1, (continued)

Name	Description
O-XYLENE	o-Xylene
M-XYLENE	m-Xylene
P-XYLENE	p-Xylene
135-TMB	1,3,5-Trimethylbenzene
ETHE	Ethene
PROPENE	Propene
T-2-BUTE	trans-2-Butene
C8-OLE1	C_8 Terminal Alkenes
C9-OLE1	C_9 Terminal Alkenes
C10-OLE1	C_{10} Terminal Alkenes
C11-OLE1	C_{11} Terminal Alkenes
C12-OLE1	C_{12} Terminal Alkenes
C13-OLE1	C_{13} Terminal Alkenes
C8-OLE2	C_8 Internal Alkenes
C9-OLE2	C_9 Internal Alkenes
C10-OLE2	C_{10} Internal Alkenes
C11-OLE2	C_{11} Internal Alkenes
C12-OLE2	C_{12} Internal Alkenes
C13-OLE2	C_{13} Internal Alkenes
ISOP	Isoprene
APIN	α-Pinene
UNKN	Unknown biogenics.

Lumped species used to represent the Base ROG mixture in the EKMA model simulations.

ALK1	Alkanes and other saturated compounds with $k_{OH} < 10^4$ ppm^{-1} min^{-1}.
ALK2	Alkanes and other saturated compounds with $k_{OH} \geq 10^4$ ppm^{-1} min^{-1}.
ARO1	Aromatics with $k_{OH} < 2x10^4$ ppm^{-1} min^{-1}.
ARO2	Aromatics with $k_{OH} \geq 2x10^4$ ppm^{-1} min^{-1}.
OLE2	Alkenes (other than ethene) with $k_{OH} < 7x10^4$ ppm^{-1} min^{-1}.
OLE3	Alkenes with $k_{OH} \geq 7x10^4$ ppm^{-1} min^{-1}.

Lumped Species used to Represent the Components of the Mineral Spirits Samples

MS-A-ALK	Lumped Alkanes in Sample "A"
MS-A-ARO	Lumped Aromatics in Sample "A"
MS-A-OLE	Lumped Alkenes in Sample "A"
MS-B-ALK	Lumped Alkanes in Sample "B"
MS-C-ALK	Lumped Alkanes in Sample "C"
MS-D-ALK	Lumped Alkanes in Sample "D"

Table A-2. List of reactions in the chemical mechanism used in the model simulations for this study.

Rxn. Label	Kinetic Parameters [a] k(300)	A	Ea	B	Reactions [b]
Inorganic Reactions					
1	(Phot. Set = NO2)				NO2 + HV = NO + O
2	6.00E-34	6.00E-34	0.00	-2.30	O + O2 + M = O3 + M
3A	9.69E-12	6.50E-12	-0.24	0.00	O + NO2 = NO + O2
3B	1.55E-12	(Falloff Kinetics)			O + NO2 = NO3 + M
	k0 =	9.00E-32	0.00	-2.00	
	kINF =	2.20E-11	0.00	0.00	
		F= 0.60	n= 1.00		
4	1.88E-14	2.00E-12	2.78	0.00	O3 + NO = NO2 + O2
5	3.36E-17	1.40E-13	4.97	0.00	O3 + NO2 = O2 + NO3
6	2.80E-11	1.70E-11	-0.30	0.00	NO + NO3 = 2 NO2
7	1.92E-38	3.30E-39	-1.05	0.00	NO + NO + O2 = 2 NO2
8	1.26E-12	(Falloff Kinetics)			NO2 + NO3 = N2O5
	k0 =	2.20E-30	0.00	-4.30	
	kINF =	1.50E-12	0.00	-0.50	
		F= 0.60	n= 1.00		
9	5.53E+10	9.09E+26	22.26	0.00	N2O5 + #RCON8 = NO2 + NO3
10	1.00E-21	(No T Dependence)			N2O5 + H2O = 2 HNO3
11	4.17E-16	2.50E-14	2.44	0.00	NO2 + NO3 = NO + NO2 + O2
12A	(Phot. Set = NO3NO)				NO3 + HV = NO + O2
12B	(Phot. Set = NO3NO2)				NO3 + HV = NO2 + O
13A	(Phot. Set = O3O3P)				O3 + HV = O + O2
13B	(Phot. Set = O3O1D)				O3 + HV = O*1D2 + O2
14	2.20E-10	(No T Dependence)			O*1D2 + H2O = 2 HO.
15	2.92E-11	1.92E-11	-0.25	0.00	O*1D2 + M = O + M
16	4.81E-12	(Falloff Kinetics)			HO. + NO = HONO
	k0 =	7.00E-31	0.00	-2.60	
	kINF =	1.50E-11	0.00	-0.50	
		F= 0.60	n= 1.00		
17	(Phot. Set = HONO)				HONO + HV = HO. + NO
18	1.13E-11	(Falloff Kinetics)			HO. + NO2 = HNO3
	k0 =	2.60E-30	0.00	-3.20	
	kINF =	2.40E-11	0.00	-1.30	
		F= 0.60	n= 1.00		
19	1.03E-13	6.45E-15	-1.65	0.00	HO. + HNO3 = H2O + NO3
21	2.40E-13	(No T Dependence)			HO. + CO = HO2. + CO2
22	6.95E-14	1.60E-12	1.87	0.00	HO. + O3 = HO2. + O2
23	8.28E-12	3.70E-12	-0.48	0.00	HO2. + NO = HO. + NO2
24	1.37E-12	(Falloff Kinetics)			HO2. + NO2 = HNO4
	k0 =	1.80E-31	0.00	-3.20	
	kINF =	4.70E-12	0.00	-1.40	
		F= 0.60	n= 1.00		
25	7.92E+10	4.76E+26	21.66	0.00	HNO4 + #RCON24 = HO2. + NO2
27	4.61E-12	1.30E-12	-0.75	0.00	HNO4 + HO. = H2O + NO2 + O2
28	2.08E-15	1.10E-14	0.99	0.00	HO2. + O3 = HO. + 2 O2
29A	1.73E-12	2.20E-13	-1.23	0.00	HO2. + HO2. = HO2H + O2
29B	5.00E-32	1.90E-33	-1.95	0.00	HO2. + HO2. + M = HO2H + O2
29C	3.72E-30	3.10E-34	-5.60	0.00	HO2. + HO2. + H2O = HO2H + O2 + H2O
29D	2.65E-30	6.60E-35	-6.32	0.00	HO2. + HO2. + H2O = HO2H + O2 + H2O
30A	1.73E-12	2.20E-13	-1.23	0.00	NO3 + HO2. = HNO3 + O2
30B	5.00E-32	1.90E-33	-1.95	0.00	NO3 + HO2. + M = HNO3 + O2
30C	3.72E-30	3.10E-34	-5.60	0.00	NO3 + HO2. + H2O = HNO3 + O2 + H2O
30D	2.65E-30	6.60E-35	-6.32	0.00	NO3 + HO2. + H2O = HNO3 + O2 + H2O
31	(Phot. Set = H2O2)				HO2H + HV = 2 HO.
32	1.70E-12	3.30E-12	0.40	0.00	HO2H + HO. = HO2. + H2O
33	9.90E-11	4.60E-11	-0.46	0.00	HO. + HO2. = H2O + O2
Peroxy Radical Operators					
B1	7.68E-12	4.20E-12	-0.36	0.00	RO2. + NO = NO
B2	2.25E-11	(Falloff Kinetics)			RCO3. + NO = NO
	k0 =	5.65E-28	0.00	-7.10	
	kINF =	2.64E-11	0.00	-0.90	
		F= 0.27	n= 1.00		
B4	1.04E-11	(Falloff Kinetics)			RCO3. + NO2 = NO2
	k0 =	2.57E-28	0.00	-7.10	
	kINF =	1.20E-11	0.00	-0.90	
		F= 0.30	n= 1.00		
B5	4.90E-12	3.40E-13	-1.59	0.00	RO2. + HO2. = HO2. + RO2-HO2-PROD
B6	4.90E-12	3.40E-13	-1.59	0.00	RCO3. + HO2. = HO2. + RO2-HO2-PROD
B8	1.00E-15	(No T Dependence)			RO2. + RO2. = RO2-RO2-PROD
B9	1.09E-11	1.86E-12	-1.05	0.00	RO2. + RCO3. = RO2-RO2-PROD

Table A-2 (continued)

Rxn. Label	Kinetic Parameters [a] k(300)	A	Ea	B	Reactions [b]
B10	1.64E-11	2.80E-12	-1.05	0.00	RCO3. + RCO3. = RO2-RO2-PROD
B11	(Same k as for RO2.)				RO2-R. + NO = NO2 + HO2.
B12	(Same k as for RO2.)				RO2-R. + HO2. = -OOH
B13	(Same k as for RO2.)				RO2-R. + RO2. = RO2. + 0.5 HO2.
B14	(Same k as for RO2.)				RO2-R. + RCO3. = RCO3. + 0.5 HO2.
B19	(Same k as for RO2.)				RO2-N. + NO = RNO3
B20	(Same k as for RO2.)				RO2-N. + HO2. = -OOH + MEK + 1.5 -C
B21	(Same k as for RO2.)				RO2-N. + RO2. = RO2. + 0.5 HO2. + MEK + 1.5 -C
B22	(Same k as for RO2.)				RO2-N. + RCO3. = RCO3. + 0.5 HO2. + MEK + 1.5 -C
B15	(Same k as for RO2.)				R2O2. + NO = NO2
B16	(Same k as for RO2.)				R2O2. + HO2. =
B17	(Same k as for RO2.)				R2O2. + RO2. = RO2.
B18	(Same k as for RO2.)				R2O2. + RCO3. = RCO3.
B23	(Same k as for RO2.)				RO2-XN. + NO = -N
B24	(Same k as for RO2.)				RO2-XN. + HO2. = -OOH
B25	(Same k as for RO2.)				RO2-XN. + RO2. = RO2. + 0.5 HO2.
B26	(Same k as for RO2.)				RO2-XN. + RCO3. = RCO3. + HO2.
G2	(Same k as for RO2.)				RO2-NP. + NO = NPHE
G3	(Same k as for RO2.)				RO2-NP. + HO2. = -OOH + 6 -C
G4	(Same k as for RO2.)				RO2-NP. + RO2. = RO2. + 0.5 HO2. + 6 -C
G5	(Same k as for RO2.)				RO2-NP. + RCO3. = RCO3. + HO2. + 6 -C
Excited Criegee Biradicals					
RZ1	(fast)				(HCHO2) = 0.7 HCOOH + 0.12 "HO. + HO2. + CO" + 0.18 "H2 + CO2"
RZ2	(fast)				(CCHO2) = 0.25 CCOOH + 0.15 "CH4 + CO2" + 0.6 HO. + 0.3 "CCO-O2. + RCO3." + 0.3 "RO2-R. + HCHO + CO + RO2."
RZ3	(fast)				(RCHO2) = 0.25 CCOOH + 0.15 CO2 + 0.6 HO. + 0.3 "C2CO-O2. + RCO3." + 0.3 "RO2-R. + CCHO + CO + RO2." + 0.55 -C
RZ4	(fast)				(C(C)CO2) = HO. + R2O2. + HCHO + CCO-O2. + RCO3. + RO2.
RZ5	(fast)				(C(R)CO2) = HO. + CCO-O2. + CCHO + R2O2. + RCO3. + RO2.
RZ6	(fast)				(CYCCO2) = 0.3 "HO. + C2CO-O2. + R2O2. + RCO3. + RO2." + 0.3 RCHO + 4.2 -C
RZ8	(fast)				(BZCHO2) = 0.5 "BZ-O. + R2O2. + CO + HO."
ISZ1	(fast)				(C:CC(C)O2) = HO. + R2O2. + HCHO + C2CO-O2. + RO2. + RCO3.
ISZ2	(fast)				(C:C(C)CHO2) = 0.75 RCHO + 0.25 ISOPROD + 0.5 -C
MAZ1	(fast)				(C2(O2)CHO) = HO. + R2O2. + HCHO + HCOCO-O2. + RO2. + RCO3.
M1Z1	(fast)				(HOCCHO2) = 0.6 HO. + 0.3 "CCO-O2. + RCO3." + 0.3 "RO2-R. + HCHO + CO + RO2." + 0.8 -C
M2Z1	(fast)				(HCOCHO2) = 0.12 "HO2. + 2 CO + HO." + 0.74 -C + 0.51 "CO2 + HCHO"
M2Z2	(fast)				(C2(O2)COH) = HO. + MGLY + HO2. + R2O2. + RO2.
Organic Product Species					
B7	(Phot. Set = CO2H)				-OOH + HV = HO2. + HO.
B7A	1.81E-12	1.18E-12	-0.25	0.00	HO. + -OOH = HO.
B7B	3.71E-12	1.79E-12	-0.44	0.00	HO. + -OOH = RO2-R. + RO2.
C1	(Phot. Set = HCHONEWR)				HCHO + HV = 2 HO2. + CO
C2	(Phot. Set = HCHONEWM)				HCHO + HV = H2 + CO
C3	9.76E-12	1.13E-12	-1.29	2.00	HCHO + HO. = HO2. + CO + H2O
C4	7.79E-14	9.70E-15	-1.24	0.00	HCHO + HO2. = HOCOO.
C4A	1.77E+02	2.40E+12	13.91	0.00	HOCOO. = HO2. + HCHO
C4B	(Same k as for RO2.)				HOCOO. + NO = -C + NO2 + HO2.
C9	6.38E-16	2.80E-12	5.00	0.00	HCHO + NO3 = HNO3 + HO2. + CO
C10	1.57E-11	5.55E-12	-0.62	0.00	CCHO + HO. = CCO-O2. + H2O + RCO3.
C11A	(Phot. Set = CCHOR)				CCHO + HV = CO + HO2. + HCHO + RO2-R. + RO2.
C12	2.84E-15	1.40E-12	3.70	0.00	CCHO + NO3 = HNO3 + CCO-O2. + RCO3.
C25	1.97E-11	8.50E-12	-0.50	0.00	RCHO + HO. = C2CO-O2. + RCO3.
C26	(Phot. Set = RCHO)				RCHO + HV = CCHO + RO2-R. + RO2. + CO + HO2.
C27	2.84E-15	1.40E-12	3.70	0.00	NO3 + RCHO = HNO3 + C2CO-O2. + RCO3.
C38	2.23E-13	4.81E-13	0.46	2.00	ACET + HO. = R2O2. + HCHO + CCO-O2. + RCO3. + RO2.

Table A-2 (continued)

Rxn. Label	Kinetic Parameters [a] k(300)	A	Ea	B	Reactions [b]
C39	(Phot. Set = ACET-93C)				ACET + HV = CCO-O2. + HCHO + RO2-R. + RCO3. + RO2.
C44	1.16E-12	2.92E-13	-0.82	2.00	MEK + HO. = H2O + 0.5 "CCHO + HCHO + CCO-O2. + C2CO-O2." + RCO3. + 1.5 "R2O2. + RO2."
C57	(Phot. Set = KETONE)				MEK + HV + #0.1 = CCO-O2. + CCHO + RO2-R. + RCO3. + RO2.
C95	2.07E-12	2.19E-11	1.41	0.00	RNO3 + HO. = NO2 + 0.155 MEK + 1.05 RCHO + 0.48 CCHO + 0.16 HCHO + 0.11 -C + 1.39 "R2O2. + RO2."
C58A	(Phot. Set = GLYOXAL1)				GLY + HV = 0.8 HO2. + 0.45 HCHO + 1.55 CO
C58B	(Phot. Set = GLYOXAL2)				GLY + HV + #0.029 = 0.13 HCHO + 1.87 CO
C59	1.14E-11	(No T Dependence)			GLY + HO. = 0.6 HO2. + 1.2 CO + 0.4 "HCOCO-O2. + RCO3."
C60	(Same k as for CCHO)				GLY + NO3 = HNO3 + 0.6 HO2. + 1.2 CO + 0.4 "HCOCO-O2. + RCO3."
C68A	(Phot. Set = MEGLYOX1)				MGLY + HV = HO2. + CO + CCO-O2. + RCO3.
C68B	(Phot. Set = MEGLYOX2)				MGLY + HV + 0.107 = HO2. + CO + CCO-O2. + RCO3.
C69	1.72E-11	(No T Dependence)			MGLY + HO. = CO + CCO-O2. + RCO3.
C70	(Same k as for CCHO)				MGLY + NO3 = HNO3 + CO + CCO-O2. + RCO3.
G7	1.14E-11	(No T Dependence)			HO. + AFG1 = HCOCO-O2. + RCO3.
G8	(Phot. Set = ACROLEIN)				AFG1 + HV + #0.029 = HO2. + HCOCO-O2. + RCO3.
U2OH	1.72E-11	(No T Dependence)			HO. + AFG2 = C2CO-O2. + RCO3.
U2HV	(Phot. Set = ACROLEIN)				AFG2 + HV = HO2. + CO + CCO-O2. + RCO3.
G46	2.63E-11	(No T Dependence)			HO. + PHEN = 0.15 RO2-NP. + 0.85 RO2-R. + 0.2 GLY + 4.7 -C + RO2.
G51	3.60E-12	(No T Dependence)			NO3 + PHEN = HNO3 + BZ-O.
G52	4.20E-11	(No T Dependence)			HO. + CRES = 0.15 RO2-NP. + 0.85 RO2-R. + 0.2 MGLY + 5.5 -C + RO2.
G57	2.10E-11	(No T Dependence)			NO3 + CRES = HNO3 + BZ-O. + -C
G30	1.29E-11	(No T Dependence)			BALD + HO. = BZ-CO-O2. + RCO3.
G31	(Phot. Set = BZCHO)				BALD + HV + #0.05 = 7 -C
G32	2.61E-15	1.40E-12	3.75	0.00	BALD + NO3 = HNO3 + BZ-CO-O2.
G58	3.60E-12	(No T Dependence)			NPHE + NO3 = HNO3 + BZ(NO2)-O.
G59	(Same k as for BZ-O.)				BZ(NO2)-O. + NO2 = 2 -N + 6 -C
G60	(Same k as for RO2.)				BZ(NO2)-O. + HO2. = NPHE
G61	(Same k as for BZ-O.)				BZ(NO2)-O. = NPHE
C13	(Same k as for RCO3.)				CCO-O2. + NO = CO2 + NO2 + HCHO + RO2-R. + RO2.
C14	(Same k as for RCO3.)				CCO-O2. + NO2 = PAN
C15	(Same k as for RCO3.)				CCO-O2. + HO2. = -OOH + CO2 + HCHO
C16	(Same k as for RCO3.)				CCO-O2. + RO2. = RO2. + 0.5 HO2. + CO2 + HCHO
C17	(Same k as for RCO3.)				CCO-O2. + RCO3. = RCO3. + HO2. + CO2 + HCHO
C18	6.50E-04	(Falloff Kinetics)			PAN = CCO-O2. + NO2 + RCO3.
	k0 =	4.90E-03	23.97	0.00	
	kINF =	4.00E+16	27.08	0.00	
		F= 0.30	n= 1.00		
C28	(Same k as for RCO3.)				C2CO-O2. + NO = CCHO + RO2-R. + CO2 + NO2 + RO2.
C29	8.40E-12	(No T Dependence)			C2CO-O2. + NO2 = PPN
C30	(Same k as for RCO3.)				C2CO-O2. + HO2. = -OOH + CCHO + CO2
C31	(Same k as for RCO3.)				C2CO-O2. + RO2. = RO2. + 0.5 HO2. + CCHO + CO2
C32	(Same k as for RCO3.)				C2CO-O2. + RCO3. = RCO3. + HO2. + CCHO + CO2
C33	6.78E-04	1.60E+17	27.97	0.00	PPN = C2CO-O2. + NO2 + RCO3.
C62	(Same k as for RCO3.)				HCOCO-O2. + NO = NO2 + CO2 + CO + HO2.
C63	(Same k as for RCO3.)				HCOCO-O2. + NO2 = GPAN
C65	(Same k as for RCO3.)				HCOCO-O2. + HO2. = -OOH + CO2 + CO
C66	(Same k as for RCO3.)				HCOCO-O2. + RO2. = RO2. + 0.5 HO2. + CO2 + CO
C67	(Same k as for RCO3.)				HCOCO-O2. + RCO3. = RCO3. + HO2. + CO2 + CO
C64	(Same k as for PAN)				GPAN = HCOCO-O2. + NO2 + RCO3.
G33	(Same k as for RCO3.)				BZ-CO-O2. + NO = BZ-O. + CO2 + NO2 + R2O2. + RO2.
G43	3.53E-11	1.30E-11	-0.60	0.00	BZ-O. + NO2 = NPHE
G44	(Same k as for RO2.)				BZ-O. + HO2. = PHEN
G45	1.00E-03	(No T Dependence)			BZ-O. = PHEN
G34	8.40E-12	(No T Dependence)			BZ-CO-O2. + NO2 = PBZN
G36	(Same k as for RCO3.)				BZ-CO-O2. + HO2. = -OOH + CO2 + PHEN
G37	(Same k as for RCO3.)				BZ-CO-O2. + RO2. = RO2. + 0.5 HO2. + CO2 + PHEN

Table A-2 (continued)

Rxn. Label	Kinetic Parameters [a] k(300)	A	Ea	B	Reactions [b]
G38	(Same k as for RCO3.)				BZ-CO-O2. + RCO3. = RCO3. + HO2. + CO2 + PHEN
G35	2.17E-04	1.60E+15	25.90	0.00	PBZN = BZ-CO-O2. + NO2 + RCO3.
IPOH	3.36E-11	(No T Dependence)			ISOPROD + HO. = 0.293 CO + 0.252 CCHO + 0.126 HCHO + 0.041 GLY + 0.021 RCHO + 0.168 MGLY + 0.314 MEK + 0.503 RO2-R. + 0.21 CCO-O2. + 0.288 C2CO-O2. + 0.21 R2O2. + 0.713 RO2. + 0.498 RCO3. + -0.112 -C
IPO3	7.11E-18	(No T Dependence)			ISOPROD + O3 = 0.02 CCHO + 0.04 HCHO + 0.01 GLY + 0.84 MGLY + 0.09 MEK + 0.66 (HCHO2) + 0.09 (HCOCHO2) + 0.18 (HOCCHO2) + 0.06 (C2(O2)CHO) + 0.01 (C2(O2)COH) + -0.39 -C
IPHV	(Phot. Set = ACROLEIN)				ISOPROD + HV + 0.0036 = 0.333 CO + 0.067 CCHO + 0.9 HCHO + 0.033 MEK + 0.333 HO2. + 0.7 RO2-R. + 0.267 CCO-O2. + 0.7 C2CO-O2. + 0.7 RO2. + 0.967 RCO3. + -0.133 -C
IPN3	1.00E-15	(No T Dependence)			ISOPROD + NO3 = 0.643 CO + 0.282 HCHO + 0.85 RNO3 + 0.357 RCHO + 0.925 HO2. + 0.075 C2CO-O2. + 0.075 R2O2. + 0.925 RO2. + 0.075 RCO3. + 0.075 HNO3 + -2.471 -C
Hydrocarbon Species Represented Explicitly					
	8.71E-15	6.25E-13	2.55	2.00	METHANE + HO. = RO2-R. + HCHO + RO2.
	2.74E-13	1.28E-12	0.92	2.00	ETHANE + HO. = RO2-R. + CCHO + RO2.
	2.56E-12	1.36E-12	-0.38	2.00	N-C4 + HO. = 0.076 RO2-N. + 0.924 RO2-R. + 0.397 R2O2. + 0.001 HCHO + 0.571 CCHO + 0.14 RCHO + 0.533 MEK + -0.076 -C + 1.397 RO2.
	5.63E-12	1.35E-11	0.52	0.00	N-C6 + HO. = 0.185 RO2-N. + 0.815 RO2-R. + 0.738 R2O2. + 0.02 CCHO + 0.105 RCHO + 1.134 MEK + 0.186 -C + 1.738 RO2.
	8.76E-12	3.15E-11	0.76	0.00	N-C8 + HO. = 0.333 RO2-N. + 0.667 RO2-R. + 0.706 R2O2. + 0.002 RCHO + 1.333 MEK + 0.998 -C + 1.706 RO2.
	1.02E-11	2.17E-11	0.45	0.00	N-C9 + HO. = 0.373 RO2-N. + 0.627 RO2-R. + 0.673 R2O2. + 0.001 RCHO + 1.299 MEK + 1.934 -C + 1.673 RO2.
	1.17E-11	2.47E-11	0.45	0.00	N-C10 + HO. = 0.397 RO2-N. + 0.603 RO2-R. + 0.659 R2O2. + 0.001 RCHO + 1.261 MEK + 2.969 -C + 1.659 RO2.
	1.33E-11	2.81E-11	0.45	0.00	N-C11 + HO. = 0.411 RO2-N. + 0.589 RO2-R. + 0.654 R2O2. + 0.001 RCHO + 1.241 MEK + 3.975 -C + 1.654 RO2.
	1.43E-11	3.02E-11	0.45	0.00	N-C12 + HO. = 0.42 RO2-N. + 0.58 RO2-R. + 0.644 R2O2. + 0.001 RCHO + 1.223 MEK + 5.004 -C + 1.644 RO2.
	1.61E-11	3.40E-11	0.45	0.00	N-C13 + HO. = 0.427 RO2-N. + 0.573 RO2-R. + 0.638 R2O2. + 0.001 RCHO + 1.211 MEK + 6.022 -C + 1.638 RO2.
	1.67E-11	3.64E-11	0.47	0.00	N-C14 + HO. = 0.431 RO2-N. + 0.569 RO2-R. + 0.634 R2O2. + 0.001 RCHO + 1.202 MEK + 7.033 -C + 1.634 RO2.
	8.65E-12	1.20E-11	0.19	0.00	BR-C8 + HO. = 0.244 RO2-N. + 0.002 RO2-XN. + 0.753 RO2-R. + 0.803 R2O2. + 0.352 RCHO + 1.204 MEK + 0.906 -C + 1.803 RO2.
	1.06E-11	1.29E-11	0.12	0.00	BR-C9 + HO. = 0.271 RO2-N. + 0.002 RO2-XN. + 0.727 RO2-R. + 0.804 R2O2. + 0.002 HCHO + 0.059 CCHO + 0.303 RCHO + 1.167 MEK + 1.949 -C + 1.804 RO2.
	1.20E-11	1.55E-11	0.15	0.00	BR-C10 + HO. = 0.301 RO2-N. + 0.002 RO2-XN. + 0.696 RO2-R. + 0.775 R2O2. + 0.004 CCHO + 0.328 RCHO + 1.139 MEK + 2.945 -C + 1.775 RO2.
	1.45E-11	1.26E-11	-0.08	0.00	BR-C11 + HO. = 0.246 RO2-N. + 0.754 RO2-R. + 1.273 R2O2. + 0.021 HCHO + 0.054 CCHO + 0.09 RCHO + 1.862 MEK + 1.922 -C + 2.273 RO2.
	1.59E-11	1.49E-11	-0.04	0.00	BR-C12 + HO. = 0.267 RO2-N. + 0.733 RO2-R. + 1.35 R2O2. + 0.002 HCHO + 0.422 CCHO + 0.012 RCHO + 1.647 MEK + 3.192 -C + 2.351 RO2.
	1.73E-11	(No T Dependence)			BR-C13 + HO. = 0.285 RO2-N. + 0.715 RO2-R. + 1.226 R2O2. + 0.002 HCHO + 0.008 CCHO + 0.111 RCHO + 1.819 MEK + 3.943 -C + 2.226 RO2.
	1.87E-11	1.97E-11	0.03	0.00	BR-C14 + HO. = 0.298 RO2-N. + 0.702 RO2-R. + 1.122 R2O2. + 0.002 HCHO + 0.003 RCHO + 1.82 MEK + 5.223 -C + 2.122 RO2.
	2.01E-11	2.22E-11	0.06	0.00	BR-C15 + HO. = 0.31 RO2-N. + 0.69 RO2-R. + 1.103 R2O2. + 0.001 HCHO + 0.003 RCHO + 1.79 MEK + 6.285 -C + 2.103 RO2.

Table A-2 (continued)

Rxn. Label	Kinetic Parameters [a] k(300)	A	Ea	B	Reactions [b]
	1.03E-11	1.34E-11	0.16	0.00	ME-CYCC6 + HO. = 0.216 RO2-N. + 0.784 RO2-R. + 0.928 R2O2. + 0.092 HCHO + 0.001 CCHO + 0.466 RCHO + 0.987 MEK + 0.003 CO + 0.046 CO2 + 0.432 -C + 1.928 RO2.
	1.23E-11	1.44E-11	0.09	0.00	CYC-C8 + HO. = 0.265 RO2-N. + 0.735 RO2-R. + 1.282 R2O2. + 0.186 HCHO + 0.293 CCHO + 0.347 RCHO + 0.811 MEK + 0.01 CO + 0.185 CO2 + 1.424 -C + 2.282 RO2.
	1.41E-11	1.29E-11	-0.05	0.00	CYC-C9 + HO. = 0.247 RO2-N. + 0.753 RO2-R. + 1.782 R2O2. + 0.278 HCHO + 0.25 CCHO + 0.457 RCHO + 1.022 MEK + 0.264 CO2 + 1.263 -C + 2.782 RO2.
	1.61E-11	1.41E-11	-0.08	0.00	CYC-C10 + HO. = 0.267 RO2-N. + 0.733 RO2-R. + 1.596 R2O2. + 0.211 HCHO + 0.37 CCHO + 0.175 RCHO + 1.151 MEK + 0.006 CO + 0.208 CO2 + 2.37 -C + 2.596 RO2.
	1.79E-11	1.33E-11	-0.17	0.00	CYC-C11 + HO. = 0.238 RO2-N. + 0.762 RO2-R. + 1.89 R2O2. + 0.226 HCHO + 0.368 CCHO + 0.159 RCHO + 1.53 MEK + 0.001 CO + 0.184 CO2 + 2.068 -C + 2.89 RO2.
	1.99E-11	1.47E-11	-0.18	0.00	CYC-C12 + HO. = 0.251 RO2-N. + 0.749 RO2-R. + 1.722 R2O2. + 0.202 HCHO + 0.392 CCHO + 0.136 RCHO + 1.408 MEK + 0.001 CO + 0.166 CO2 + 3.55 -C + 2.722 RO2.
	2.13E-11	1.68E-11	-0.14	0.00	CYC-C13 + HO. = 0.267 RO2-N. + 0.001 RO2-XN. + 0.732 RO2-R. + 1.469 R2O2. + 0.129 HCHO + 0.216 CCHO + 0.25 RCHO + 1.391 MEK + 0.001 CO + 0.107 CO2 + 4.682 -C + 2.469 RO2.
	2.27E-11	1.90E-11	-0.11	0.00	CYC-C14 + HO. = 0.281 RO2-N. + 0.001 RO2-XN. + 0.718 RO2-R. + 1.277 R2O2. + 0.077 HCHO + 0.097 CCHO + 0.329 RCHO + 1.359 MEK + 0.001 CO + 0.066 CO2 + 5.835 -C + 2.277 RO2.
	2.42E-11	2.12E-11	-0.08	0.00	CYC-C15 + HO. = 0.293 RO2-N. + 0.002 RO2-XN. + 0.705 RO2-R. + 1.128 R2O2. + 0.041 HCHO + 0.023 CCHO + 0.38 RCHO + 1.312 MEK + 0.001 CO + 0.038 CO2 + 7.02 -C + 2.128 RO2.
	5.91E-12	1.81E-12	-0.70	0.00	TOLUENE + HO. = 0.085 BALD + 0.26 CRES + 0.118 GLY + 0.964 MGLY + 0.259 AFG2 + 0.74 RO2-R. + 0.26 HO2. + 0.681 -C + 0.74 RO2.
	7.10E-12	(No T Dependence)			C2-BENZ + HO. = 0.085 BALD + 0.26 CRES + 0.118 GLY + 0.199 MGLY + 0.181 AFG2 + 0.74 RO2-R. + 0.26 HO2. + 4.207 -C + 0.74 RO2.
	2.36E-11	(No T Dependence)			M-XYLENE + HO. = 0.04 BALD + 0.18 CRES + 0.108 GLY + 1.599 MGLY + 0.461 AFG2 + 0.82 RO2-R. + 0.18 HO2. + 0.063 -C + 0.82 RO2.
	1.37E-11	(No T Dependence)			O-XYLENE + HO. = 0.04 BALD + 0.18 CRES + 0.108 GLY + 0.805 MGLY + 0.582 AFG2 + 0.82 RO2-R. + 0.18 HO2. + 2.083 -C + 0.82 RO2.
	1.43E-11	(No T Dependence)			P-XYLENE + HO. = 0.04 BALD + 0.18 CRES + 0.108 GLY + 0.168 MGLY + 0.15 AFG2 + 0.82 RO2-R. + 0.18 HO2. + 5.289 -C + 0.82 RO2.
	5.75E-11	(No T Dependence)			135-TMB + HO. = 0.03 BALD + 0.18 CRES + 1.164 MGLY + 0.61 AFG2 + 0.82 RO2-R. + 0.18 HO2. + 2.207 -C + 0.82 RO2.
	8.43E-12	1.96E-12	-0.87	0.00	ETHENE + HO. = RO2-R. + RO2. + 1.56 HCHO + 0.22 CCHO
	1.68E-18	9.14E-15	5.13	0.00	ETHENE + O3 = HCHO + (HCHO2)
	2.18E-16	4.39E-13	4.53	2.00	ETHENE + NO3 = R2O2. + RO2. + 2 HCHO + NO2
	7.42E-13	1.04E-11	1.57	0.00	ETHENE + O = RO2-R. + HO2. + RO2. + HCHO + CO
	2.60E-11	4.85E-12	-1.00	0.00	PROPENE + HO. = RO2-R. + RO2. + HCHO + CCHO
	1.05E-17	5.51E-15	3.73	0.00	PROPENE + O3 = 0.6 HCHO + 0.4 CCHO + 0.4 (HCHO2) + 0.6 (CCHO2)
	9.74E-15	4.59E-13	2.30	0.00	PROPENE + NO3 = R2O2. + RO2. + HCHO + CCHO + NO2
	4.01E-12	1.18E-11	0.64	0.00	PROPENE + O = 0.4 HO2. + 0.5 RCHO + 0.5 MEK + -0.5 -C
	6.30E-11	1.01E-11	-1.09	0.00	T-2-BUTE + HO. = RO2-R. + RO2. + 2 CCHO
	1.95E-16	6.64E-15	2.10	0.00	T-2-BUTE + O3 = CCHO + (CCHO2)
	3.92E-13	1.10E-13	-0.76	2.00	T-2-BUTE + NO3 = R2O2. + RO2. + 2 CCHO + NO2
	2.34E-11	2.26E-11	-0.02	0.00	T-2-BUTE + O = 0.4 HO2. + 0.5 RCHO + 0.5 MEK + 0.5 -C
	3.66E-11	6.84E-12	-1.00	0.00	C8-OLE1 + HO. = 0.67 RO2-R. + 0.33 RO2-N. + RO2. + 0.67 HCHO + 0.67 RCHO + 3.67 -C
	1.14E-17	3.36E-15	3.39	0.00	C8-OLE1 + O3 = 0.6 HCHO + RCHO + 2.8 -C + 0.4 (HCHO2) + 0.6 (CCHO2)
	1.30E-14	6.55E-12	3.71	0.00	C8-OLE1 + NO3 = R2O2. + RO2. + HCHO + RCHO + 4 -C + NO2

Table A-2 (continued)

Rxn. Label	Kinetic Parameters [a] k(300)	A	Ea	B	Reactions [b]
	4.22E-12	1.25E-11	0.65	0.00	C8-OLE1 + O = 0.4 HO2. + 0.5 RCHO + 0.5 MEK + 4.5 -C
	3.66E-11	6.84E-12	-1.00	0.00	C9-OLE1 + HO. = 0.63 RO2-R. + 0.37 RO2-N. + RO2. + 0.63 HCHO + 0.63 RCHO + 4.63 -C
	1.14E-17	3.36E-15	3.39	0.00	C9-OLE1 + O3 = 0.6 HCHO + RCHO + 3.8 -C + 0.4 (HCHO2) + 0.6 (CCHO2)
	1.30E-14	6.55E-12	3.71	0.00	C9-OLE1 + NO3 = R2O2. + RO2. + HCHO + RCHO + 5 -C + NO2
	4.22E-12	1.25E-11	0.65	0.00	C9-OLE1 + O = 0.4 HO2. + 0.5 RCHO + 0.5 MEK + 5.5 -C
	3.66E-11	6.84E-12	-1.00	0.00	C10-OLE1 + HO. = 0.6 RO2-R. + 0.4 RO2-N. + RO2. + 0.6 HCHO + 0.6 RCHO + 5.6 -C
	1.14E-17	3.36E-15	3.39	0.00	C10-OLE1 + O3 = 0.6 HCHO + RCHO + 4.8 -C + 0.4 (HCHO2) + 0.6 (CCHO2)
	1.30E-14	6.55E-12	3.71	0.00	C10-OLE1 + NO3 = R2O2. + RO2. + HCHO + RCHO + 6 -C + NO2
	4.22E-12	1.25E-11	0.65	0.00	C10-OLE1 + O = 0.4 HO2. + 0.5 RCHO + 0.5 MEK + 6.5 -C
	3.66E-11	6.84E-12	-1.00	0.00	C11-OLE1 + HO. = 0.59 RO2-R. + 0.41 RO2-N. + RO2. + 0.59 HCHO + 0.59 RCHO + 6.59 -C
	1.14E-17	3.36E-15	3.39	0.00	C11-OLE1 + O3 = 0.6 HCHO + RCHO + 5.8 -C + 0.4 (HCHO2) + 0.6 (CCHO2)
	1.30E-14	6.55E-12	3.71	0.00	C11-OLE1 + NO3 = R2O2. + RO2. + HCHO + RCHO + 7 -C + NO2
	4.22E-12	1.25E-11	0.65	0.00	C11-OLE1 + O = 0.4 HO2. + 0.5 RCHO + 0.5 MEK + 7.5 -C
	3.66E-11	6.84E-12	-1.00	0.00	C12-OLE1 + HO. = 0.58 RO2-R. + 0.42 RO2-N. + RO2. + 0.58 HCHO + 0.58 RCHO + 7.58 -C
	1.14E-17	3.36E-15	3.39	0.00	C12-OLE1 + O3 = 0.6 HCHO + RCHO + 6.8 -C + 0.4 (HCHO2) + 0.6 (CCHO2)
	1.30E-14	6.55E-12	3.71	0.00	C12-OLE1 + NO3 = R2O2. + RO2. + HCHO + RCHO + 8 -C + NO2
	4.22E-12	1.25E-11	0.65	0.00	C12-OLE1 + O = 0.4 HO2. + 0.5 RCHO + 0.5 MEK + 8.5 -C
	3.66E-11	6.84E-12	-1.00	0.00	C13-OLE1 + HO. = 0.57 RO2-R. + 0.43 RO2-N. + RO2. + 0.57 HCHO + 0.57 RCHO + 8.57 -C
	1.14E-17	3.36E-15	3.39	0.00	C13-OLE1 + O3 = 0.6 HCHO + RCHO + 7.8 -C + 0.4 (HCHO2) + 0.6 (CCHO2)
	1.30E-14	6.55E-12	3.71	0.00	C13-OLE1 + NO3 = R2O2. + RO2. + HCHO + RCHO + 9 -C + NO2
	4.22E-12	1.25E-11	0.65	0.00	C13-OLE1 + O = 0.4 HO2. + 0.5 RCHO + 0.5 MEK + 9.5 -C
	6.56E-11	1.22E-11	-1.00	0.00	C8-OLE2 + HO. = 0.67 RO2-R. + 0.33 RO2-N. + RO2. + 1.34 RCHO + 2.33 -C
	2.68E-16	7.68E-15	2.00	0.00	C8-OLE2 + O3 = RCHO + 2 -C + (RCHO2)
	3.92E-13	1.10E-13	-0.76	2.00	C8-OLE2 + NO3 = R2O2. + RO2. + 2 RCHO + 2 -C + NO2
	3.00E-11	(No T Dependence)			C8-OLE2 + O = 0.4 HO2. + 0.5 RCHO + 0.5 MEK + 4.5 -C
	6.56E-11	1.22E-11	-1.00	0.00	C9-OLE2 + HO. = 0.63 RO2-R. + 0.37 RO2-N. + RO2. + 1.26 RCHO + 3.37 -C
	2.68E-16	7.68E-15	2.00	0.00	C9-OLE2 + O3 = RCHO + 3 -C + (RCHO2)
	3.92E-13	1.10E-13	-0.76	2.00	C9-OLE2 + NO3 = R2O2. + RO2. + 2 RCHO + 3 -C + NO2
	3.00E-11	(No T Dependence)			C9-OLE2 + O = 0.4 HO2. + 0.5 RCHO + 0.5 MEK + 5.5 -C
	6.56E-11	1.22E-11	-1.00	0.00	C10-OLE2 + HO. = 0.6 RO2-R. + 0.4 RO2-N. + RO2. + 1.2 RCHO + 4.4 -C
	2.68E-16	7.68E-15	2.00	0.00	C10-OLE2 + O3 = RCHO + 4 -C + (RCHO2)
	3.92E-13	1.10E-13	-0.76	2.00	C10-OLE2 + NO3 = R2O2. + RO2. + 2 RCHO + 4 -C + NO2
	3.00E-11	(No T Dependence)			C10-OLE2 + O = 0.4 HO2. + 0.5 RCHO + 0.5 MEK + 6.5 -C
	6.56E-11	1.22E-11	-1.00	0.00	C11-OLE2 + HO. = 0.59 RO2-R. + 0.41 RO2-N. + RO2. + 1.18 RCHO + 5.41 -C
	2.68E-16	7.68E-15	2.00	0.00	C11-OLE2 + O3 = RCHO + 5 -C + (RCHO2)
	3.92E-13	1.10E-13	-0.76	2.00	C11-OLE2 + NO3 = R2O2. + RO2. + 2 RCHO + 5 -C + NO2
	3.00E-11	(No T Dependence)			C11-OLE2 + O = 0.4 HO2. + 0.5 RCHO + 0.5 MEK + 7.5 -C
	6.56E-11	1.22E-11	-1.00	0.00	C12-OLE2 + HO. = 0.58 RO2-R. + 0.42 RO2-N. + RO2. + 1.16 RCHO + 6.42 -C
	2.68E-16	7.68E-15	2.00	0.00	C12-OLE2 + O3 = RCHO + 6 -C + (RCHO2)
	3.92E-13	1.10E-13	-0.76	2.00	C12-OLE2 + NO3 = R2O2. + RO2. + 2 RCHO + 6 -C + NO2
	3.00E-11	(No T Dependence)			C12-OLE2 + O = 0.4 HO2. + 0.5 RCHO + 0.5 MEK + 8.5 -C
	6.56E-11	1.22E-11	-1.00	0.00	C13-OLE2 + HO. = 0.57 RO2-R. + 0.43 RO2-N. + RO2. + 1.14 RCHO + 7.43 -C
	2.68E-16	7.68E-15	2.00	0.00	C13-OLE2 + O3 = RCHO + 7 -C + (RCHO2)
	3.92E-13	1.10E-13	-0.76	2.00	C13-OLE2 + NO3 = R2O2. + RO2. + 2 RCHO + 7 -C + NO2
	3.00E-11	(No T Dependence)			C13-OLE2 + O = 0.4 HO2. + 0.5 RCHO + 0.5 MEK + 9.5 -C

Table A-2 (continued)

Rxn. Label	Kinetic Parameters [a] k(300)	A	Ea	B	Reactions [b]
Lumped Mineral Spirits Components (Standard Model) [c]					
	1.53E-11	(No T Dependence)			MS-A-ALK + HO. = 0.293 RO2-N. + 0.707 RO2-R. + 1.293 R2O2. + 0.1 HCHO + 0.204 CCHO + 0.128 RCHO + 1.397 MEK + 0.001 CO + 0.085 CO2 + 2.968 -C + 2.293 RO2.
	4.24E-11	(No T Dependence)			MS-A-ARO + HO. = 0.809 RO2-R. + 0.186 HO2. + 0.005 RO2-NP. + 3.336 -C + 0.036 BALD + 0.006 PHEN + 0.18 CRES + 0.039 GLY + 1.148 MGLY + 0.011 AFG1 + 0.814 RO2. + 0.515 AFG2
	4.24E-11	(No T Dependence)			MS-A-OLE + HO. = 0.593 RO2-R. + 0.407 RO2-N. + RO2. + 0.474 HCHO + 0.712 RCHO + 6.356 -C
	6.27E-17	(No T Dependence)			MS-A-OLE + O3 = 0.48 HCHO + RCHO + 5.64 -C + 0.32 (HCHO2) + 0.48 (CCHO2) + 0.2 (RCHO2)
	8.88E-14	(No T Dependence)			MS-A-OLE + NO3 = R2O2. + RO2. + 0.8 HCHO + 1.2 RCHO + 6.6 -C + NO2
	9.37E-12	(No T Dependence)			MS-A-OLE + O = 0.4 HO2. + 0.5 RCHO + 0.5 MEK + 7.5 -C
	1.84E-11	(No T Dependence)			MS-B-ALK + HO. = 0.273 RO2-N. + 0.727 RO2-R. + 1.436 R2O2. + 0.098 HCHO + 0.223 CCHO + 0.13 RCHO + 1.549 MEK + 0.001 CO + 0.081 CO2 + 3.424 -C + 2.436 RO2.
	1.73E-11	(No T Dependence)			MS-C-ALK + HO. = 0.298 RO2-N. + 0.702 RO2-R. + 1.353 R2O2. + 0.103 HCHO + 0.244 CCHO + 0.093 RCHO + 1.446 MEK + 0.001 CO + 0.084 CO2 + 3.772 -C + 2.353 RO2.
	1.70E-11	(No T Dependence)			MS-D-ALK + HO. = 0.295 RO2-N. + 0.705 RO2-R. + 1.352 R2O2. + 0.094 HCHO + 0.258 CCHO + 0.083 RCHO + 1.468 MEK + 0.001 CO + 0.077 CO2 + 3.715 -C + 2.352 RO2.
Lumped Mineral Spirits Components (n-Alkane Model) [c,d]					
	1.53E-11	(No T Dependence)			MS-A-ALK + HO. = 0.411 RO2-N. + 0.589 RO2-R. + 0.654 R2O2. + 0.001 RCHO + 1.241 MEK + 3.975 -C + 1.654 RO2.
	1.84E-11	(No T Dependence)			MS-B-ALK + HO. = 0.42 RO2-N. + 0.58 RO2-R. + 0.644 R2O2. + 0.001 RCHO + 1.223 MEK + 5.004 -C + 1.644 RO2.
	1.73E-11	(No T Dependence)			MS-C-ALK + HO. = 0.42 RO2-N. + 0.58 RO2-R. + 0.644 R2O2. + 0.001 RCHO + 1.223 MEK + 5.004 -C + 1.644 RO2.
	1.70E-11	(No T Dependence)			MS-D-ALK + HO. = 0.42 RO2-N. + 0.58 RO2-R. + 0.644 R2O2. +
Lumped Species used in EKMA Simulations [e]					
A1OH	3.46E-12	2.56E-12	-0.18	0.00	ALK1 + HO. = 0.911 RO2-R. + 0.074 RO2-N. + 0.005 RO2-XN. + 0.011 HO2. + 0.575 R2O2. + 1.564 RO2. + 0.065 HCHO + 0.339 CCHO + 0.196 RCHO + 0.322 ACET + 0.448 MEK + 0.024 CO + 0.025 GLY + 0.051 -C
A2OH	9.14E-12	5.12E-12	-0.35	0.00	ALK2 + HO. = 0.749 RO2-R. + 0.249 RO2-N. + 0.002 RO2-XN. + 0.891 R2O2. + 1.891 RO2. + 0.029 HCHO + 0.048 CCHO + 0.288 RCHO + 0.028 ACET + 1.105 MEK + 0.043 CO + 0.018 CO2 + 1.268 -C
B1OH	5.87E-12	(No T Dependence)			ARO1 + HO. = 0.742 RO2-R. + 0.258 HO2. + 0.742 RO2. + 0.015 PHEN + 0.244 CRES + 0.08 BALD + 0.124 GLY + 0.681 MGLY + 0.11 AFG1 + 0.244 AFG2 + 1.857 -C
B2OH	3.22E-11	1.20E-11	-0.59	0.00	ARO2 + HO. = 0.82 RO2-R. + 0.18 HO2. + 0.82 RO2. + 0.18 CRES + 0.036 BALD + 0.068 GLY + 1.02 MGLY + 0.532 AFG2 + 2.588 -C
O2OH	3.17E-11	2.22E-12	-1.59	0.00	OLE2 + HO. = 0.858 RO2-R. + 0.142 RO2-N. + RO2. + 0.858 HCHO + 0.252 CCHO + 0.606 RCHO + 1.267 -C
O2O3	1.08E-17	1.42E-15	2.91	0.00	OLE2 + O3 = 0.6 HCHO + 0.635 RCHO + 0.981 -C + 0.4 (HCHO2) + 0.529 (CCHO2) + 0.071 (RCHO2)

Table A-2 (continued)

Rxn. Label	Kinetic Parameters [a] k(300)	A	Ea	B	Reactions [b]
O2N3	1.16E-14	1.99E-13	1.69	0.00	OLE2 + NO3 = R2O2. + RO2. + HCHO + 0.294 CCHO + 0.706 RCHO + 1.451 -C + NO2
O2OA	4.11E-12	4.51E-12	0.06	0.00	OLE2 + O = 0.4 HO2. + 0.5 RCHO + 0.5 MEK + 1.657 -C
O3OH	6.23E-11	4.54E-12	-1.56	0.00	OLE3 + HO. = 0.861 RO2-R. + 0.139 RO2-N. + RO2. + 0.24 HCHO + 0.661 CCHO + 0.506 RCHO + 0.113 ACET + 0.086 MEK + 0.057 BALD + 0.848 -C
O3O3	1.70E-16	1.77E-15	1.40	0.00	OLE3 + O3 = 0.203 HCHO + 0.358 CCHO + 0.309 RCHO + 0.061 MEK + 0.027 BALD + 0.976 -C + 0.076 (HCHO2) + 0.409 (CCHO2) + 0.279 (RCHO2) + 0.158 (C(C)CO2 + 0.039 (C(R)CO2 + 0.04 (BZCHO2)
O3N3	1.07E-12	3.19E-13	-0.72	0.00	OLE3 + NO3 = R2O2. + RO2. + 0.278 HCHO + 0.767 CCHO + 0.588 RCHO + 0.131 ACET + 0.1 MEK + 0.066 BALD + 0.871 -C + NO2
O3OA	2.52E-11	8.66E-12	-0.64	0.00	OLE3 + O = 0.4 HO2. + 0.5 RCHO + 0.5 MEK + 2.205 -C + 0.001 RCHO + 1.223 MEK + 5.004 -C + 1.644 RO2.
Reactions used to Represent Chamber-Dependent Processes [f]					
O3W	(varied)	(No T Dependence)			O3 =
N25I	(varied)	(No T Dependence)			N2O5 = 2 NOX-WALL
N25S	(varied)	(No T Dependence)			N2O5 + H2O = 2 NOX-WALL
NO2W	(varied)	(No T Dependence)			NO2 = (yHONO) HONO + (1-yHONO) NOX-WALL
XSHC	(varied)	(No T Dependence)			HO. = HO2.
RSI	(Phot. Set = NO2)				HV + #RS/K1 = HO.
ONO2	(Phot. Set = NO2)				HV + #E-NO2/K1 = NO2 + #-1 NOX-WALL

[a] Except as noted, the expression for the rate constant is $k = A\ e^{Ea/RT}\ (T/300)^{B}$. Rate constants and A factor are in cm, molecule, sec. units. Units of Ea is kcal $mole^{-1}$. "Phot Set" means this is a photolysis reaction, with the absorption coefficients and quantum yields given in Table A-3. In addition, if "#(number)" or "#(parameter)" is given as a reactant, then the value of that number or parameter is multiplied by the result in the "rate constant expression" columns to obtain the rate constant used. Furthermore, "#RCONnn" as a reactant means that the rate constant for the reaction is obtained by multiplying the rate constant given by that for reaction "nn". Thus, the rate constant given is actually an equilibrium constant.

[b] The format of the reaction listing is the same as that used in the documentation of the detailed mechanism (Carter 1990).

[c] Rate constants and parameters are averages for the alkane, aromatic, or alkene components of the mineral spirits mixture.

[d] Branched and cyclic alkanes in the mixtures represented by the normal alkane with the same carbon number. Parameters for the lumped aromatic and alkene components of Sample "A" are the same as for the standard mechanism, shown above.

[e] The rate constants and product yield parameters are based on the mixture of species in the base ROG mixture which are being represented.

[f] See Table A-4 for the values of the parameters used for the specific chambers modeled in this study.

Table A-3. Absorption cross sections and quantum yields for photolysis reactions.

WL (nm)	Abs (cm^2)	QY	WL (nm)	Abs (cm^2)	QY	WL (nm)	Abs (cm^2)	QY	WL (nm)	Abs (cm^2)	QY	WL (nm)	Abs (cm^2)	QY
Photolysis File = NO2														
250.0	2.83E-20	1.000	255.0	1.45E-20	1.000	260.0	1.90E-20	1.000	265.0	2.05E-20	1.000	270.0	3.13E-20	1.000
275.0	4.02E-20	1.000	280.0	5.54E-20	1.000	285.0	6.99E-20	1.000	290.0	8.18E-20	0.999	295.0	9.67E-20	0.998
300.0	1.17E-19	0.997	305.0	1.66E-19	0.996	310.0	1.76E-19	0.995	315.0	2.25E-19	0.994	320.0	2.54E-19	0.993
325.0	2.79E-19	0.992	330.0	2.99E-19	0.991	335.0	3.45E-19	0.990	340.0	3.88E-19	0.989	345.0	4.07E-19	0.988
350.0	4.10E-19	0.987	355.0	5.13E-19	0.986	360.0	4.51E-19	0.984	365.0	5.78E-19	0.983	370.0	5.42E-19	0.981
375.0	5.35E-19	0.979	380.0	5.99E-19	0.975	381.0	5.98E-19	0.974	382.0	5.97E-19	0.973	383.0	5.96E-19	0.972
384.0	5.95E-19	0.971	385.0	5.94E-19	0.969	386.0	5.95E-19	0.967	387.0	5.96E-19	0.966	388.0	5.98E-19	0.964
389.0	5.99E-19	0.962	390.0	6.00E-19	0.960	391.0	5.98E-19	0.959	392.0	5.96E-19	0.957	393.0	5.93E-19	0.953
394.0	5.91E-19	0.950	395.0	5.89E-19	0.942	396.0	6.06E-19	0.922	397.0	6.24E-19	0.870	398.0	6.41E-19	0.820
399.0	6.59E-19	0.760	400.0	6.76E-19	0.695	401.0	6.67E-19	0.635	402.0	6.58E-19	0.560	403.0	6.50E-19	0.485
404.0	6.41E-19	0.425	405.0	6.32E-19	0.350	406.0	6.21E-19	0.290	407.0	6.10E-19	0.225	408.0	5.99E-19	0.185
409.0	5.88E-19	0.153	410.0	5.77E-19	0.130	411.0	5.88E-19	0.110	412.0	5.98E-19	0.094	413.0	6.09E-19	0.083
414.0	6.19E-19	0.070	415.0	6.30E-19	0.059	416.0	6.29E-19	0.048	417.0	6.27E-19	0.039	418.0	6.26E-19	0.030
419.0	6.24E-19	0.023	420.0	6.23E-19	0.018	421.0	6.18E-19	0.012	422.0	6.14E-19	0.008	423.0	6.09E-19	0.004
424.0	6.05E-19	0.000	425.0	6.00E-19	0.000									
Photolysis File = NO3NO														
585.0	2.77E-18	0.000	590.0	5.14E-18	0.250	595.0	4.08E-18	0.400	600.0	2.83E-18	0.250	605.0	3.45E-18	0.200
610.0	1.48E-18	0.200	615.0	1.96E-18	0.100	620.0	3.58E-18	0.100	625.0	9.25E-18	0.050	630.0	5.66E-18	0.050
635.0	1.45E-18	0.030	640.0	1.11E-18	0.000									
Photolysis File = NO3NO2														
400.0	0.00E+00	1.000	405.0	3.00E-20	1.000	410.0	4.00E-20	1.000	415.0	5.00E-20	1.000	420.0	8.00E-20	1.000
425.0	1.00E-19	1.000	430.0	1.30E-19	1.000	435.0	1.80E-19	1.000	440.0	1.90E-19	1.000	445.0	2.20E-19	1.000
450.0	2.80E-19	1.000	455.0	3.30E-19	1.000	460.0	3.70E-19	1.000	465.0	4.30E-19	1.000	470.0	5.10E-19	1.000
475.0	6.00E-19	1.000	480.0	6.40E-19	1.000	485.0	6.90E-19	1.000	490.0	8.80E-19	1.000	495.0	9.50E-19	1.000
500.0	1.01E-18	1.000	505.0	1.10E-18	1.000	510.0	1.32E-18	1.000	515.0	1.40E-18	1.000	520.0	1.45E-18	1.000
525.0	1.48E-18	1.000	530.0	1.94E-18	1.000	535.0	2.04E-18	1.000	540.0	1.81E-18	1.000	545.0	1.81E-18	1.000
550.0	2.36E-18	1.000	555.0	2.68E-18	1.000	560.0	3.07E-18	1.000	565.0	2.53E-18	1.000	570.0	2.54E-18	1.000
575.0	2.74E-18	1.000	580.0	3.05E-18	1.000	585.0	2.77E-18	1.000	590.0	5.14E-18	0.750	595.0	4.08E-18	0.600
600.0	2.83E-18	0.550	605.0	3.45E-18	0.400	610.0	1.45E-18	0.300	615.0	1.96E-18	0.250	620.0	3.58E-18	0.200
625.0	9.25E-18	0.150	630.0	5.66E-18	0.050	635.0	1.45E-18	0.000						
Photolysis File = O3O3P														
280.0	3.97E-18	0.100	281.0	3.60E-18	0.100	282.0	3.24E-18	0.100	283.0	3.01E-18	0.100	284.0	2.73E-18	0.100
285.0	2.44E-18	0.100	286.0	2.21E-18	0.100	287.0	2.01E-18	0.100	288.0	1.76E-18	0.100	289.0	1.58E-18	0.100
290.0	1.41E-18	0.100	291.0	1.26E-18	0.100	292.0	1.10E-18	0.100	293.0	9.89E-19	0.100	294.0	8.59E-19	0.100
295.0	7.70E-19	0.100	296.0	6.67E-19	0.100	297.0	5.84E-19	0.100	298.0	5.07E-19	0.100	299.0	4.52E-19	0.100
300.0	3.92E-19	0.100	301.0	3.42E-19	0.100	302.0	3.06E-19	0.100	303.0	2.60E-19	0.100	304.0	2.37E-19	0.100
305.0	2.01E-19	0.112	306.0	1.79E-19	0.149	307.0	1.56E-19	0.197	308.0	1.38E-19	0.259	309.0	1.25E-19	0.339
310.0	1.02E-19	0.437	311.0	9.17E-20	0.546	312.0	7.88E-20	0.652	313.0	6.77E-20	0.743	314.0	6.35E-20	0.816
315.0	5.10E-20	0.872	316.0	4.61E-20	0.916	317.0	4.17E-20	0.949	318.0	3.72E-20	0.976	319.0	2.69E-20	0.997
320.0	3.23E-20	1.000	330.0	6.70E-21	1.000	340.0	1.70E-21	1.000	350.0	4.00E-22	1.000	355.0	0.00E+00	1.000
400.0	0.00E+00	1.000	450.0	1.60E-22	1.000	500.0	1.34E-21	1.000	550.0	3.32E-21	1.000	600.0	5.06E-21	1.000
650.0	2.45E-21	1.000	700.0	8.70E-22	1.000	750.0	3.20E-22	1.000	800.0	1.60E-22	1.000	900.0	0.00E+00	1.000
Photolysis File = O3O1D														
280.0	3.97E-18	0.900	281.0	3.60E-18	0.900	282.0	3.24E-18	0.900	283.0	3.01E-18	0.900	284.0	2.73E-18	0.900
285.0	2.44E-18	0.900	286.0	2.21E-18	0.900	287.0	2.01E-18	0.900	288.0	1.76E-18	0.900	289.0	1.58E-18	0.900
290.0	1.41E-18	0.900	291.0	1.26E-18	0.900	292.0	1.10E-18	0.900	293.0	9.89E-19	0.900	294.0	8.59E-19	0.900
295.0	7.70E-19	0.900	296.0	6.67E-19	0.900	297.0	5.84E-19	0.900	298.0	5.07E-19	0.900	299.0	4.52E-19	0.900
300.0	3.92E-19	0.900	301.0	3.42E-19	0.900	302.0	3.06E-19	0.900	303.0	2.60E-19	0.900	304.0	2.37E-19	0.900
305.0	2.01E-19	0.888	306.0	1.79E-19	0.851	307.0	1.56E-19	0.803	308.0	1.38E-19	0.741	309.0	1.25E-19	0.661
310.0	1.02E-19	0.563	311.0	9.17E-20	0.454	312.0	7.88E-20	0.348	313.0	6.77E-20	0.257	314.0	6.35E-20	0.184
315.0	5.10E-20	0.128	316.0	4.61E-20	0.084	317.0	4.17E-20	0.051	318.0	3.72E-20	0.024	319.0	2.69E-20	0.003
320.0	3.23E-20	0.000												
Photolysis File = HONO														
311.0	0.00E+00	1.000	312.0	2.00E-21	1.000	313.0	4.20E-21	1.000	314.0	4.60E-21	1.000	315.0	4.20E-21	1.000
316.0	3.00E-21	1.000	317.0	4.60E-21	1.000	318.0	3.60E-20	1.000	319.0	6.10E-20	1.000	320.0	2.10E-20	1.000
321.0	4.27E-20	1.000	322.0	4.01E-20	1.000	323.0	3.93E-20	1.000	324.0	4.01E-20	1.000	325.0	4.04E-20	1.000
326.0	3.13E-20	1.000	327.0	4.12E-20	1.000	328.0	7.55E-20	1.000	329.0	6.64E-20	1.000	330.0	7.29E-20	1.000
331.0	8.70E-20	1.000	332.0	1.38E-19	1.000	333.0	5.91E-20	1.000	334.0	5.91E-20	1.000	335.0	6.45E-20	1.000
336.0	5.91E-20	1.000	337.0	4.58E-20	1.000	338.0	1.91E-19	1.000	339.0	1.63E-19	1.000	340.0	1.05E-19	1.000
341.0	8.70E-20	1.000	342.0	3.35E-19	1.000	343.0	2.01E-19	1.000	344.0	1.02E-19	1.000	345.0	8.54E-20	1.000
346.0	8.32E-20	1.000	347.0	8.20E-20	1.000	348.0	7.49E-20	1.000	349.0	7.13E-20	1.000	350.0	6.83E-20	1.000
351.0	1.74E-19	1.000	352.0	1.14E-19	1.000	353.0	3.71E-19	1.000	354.0	4.96E-19	1.000	355.0	2.46E-19	1.000
356.0	1.19E-19	1.000	357.0	9.35E-20	1.000	358.0	7.78E-20	1.000	359.0	7.29E-20	1.000	360.0	6.83E-20	1.000
361.0	6.90E-20	1.000	362.0	7.32E-20	1.000	363.0	9.00E-20	1.000	364.0	1.21E-19	1.000	365.0	1.33E-19	1.000
366.0	2.13E-19	1.000	367.0	3.52E-19	1.000	368.0	4.50E-19	1.000	369.0	2.93E-19	1.000	370.0	1.19E-19	1.000
371.0	9.46E-20	1.000	372.0	8.85E-20	1.000	373.0	7.44E-20	1.000	374.0	4.77E-20	1.000	375.0	2.70E-20	1.000
376.0	1.90E-20	1.000	377.0	1.50E-20	1.000	378.0	1.90E-20	1.000	379.0	5.80E-20	1.000	380.0	7.78E-20	1.000
381.0	1.14E-19	1.000	382.0	1.40E-19	1.000	383.0	1.72E-19	1.000	384.0	1.99E-19	1.000	385.0	1.90E-19	1.000
386.0	1.19E-19	1.000	387.0	5.65E-20	1.000	388.0	3.20E-20	1.000	389.0	1.90E-20	1.000	390.0	1.20E-20	1.000
391.0	5.00E-21	1.000	392.0	0.00E+00	1.000									
Photolysis File = H2O2														
250.0	8.30E-20	1.000	255.0	6.70E-20	1.000	260.0	5.20E-20	1.000	265.0	4.20E-20	1.000	270.0	3.20E-20	1.000
275.0	2.50E-20	1.000	280.0	2.00E-20	1.000	285.0	1.50E-20	1.000	290.0	1.13E-20	1.000	295.0	8.70E-21	1.000
300.0	6.60E-21	1.000	305.0	4.90E-21	1.000	310.0	3.70E-21	1.000	315.0	2.80E-21	1.000	320.0	2.00E-21	1.000
325.0	1.50E-21	1.000	330.0	1.20E-21	1.000	335.0	9.00E-22	1.000	340.0	7.00E-22	1.000	345.0	5.00E-22	1.000
350.0	3.00E-22	1.000	355.0	0.00E+00	1.000									

Table A-3. (continued)

WL (nm)	Abs (cm^2)	QY	WL (nm)	Abs (cm^2)	QY	WL (nm)	Abs (cm^2)	QY	WL (nm)	Abs (cm^2)	QY	WL (nm)	Abs (cm^2)	QY
Photolysis File = CO2H														
210.0	3.75E-19	1.000	220.0	2.20E-19	1.000	230.0	1.38E-19	1.000	240.0	8.80E-20	1.000	250.0	5.80E-20	1.000
260.0	3.80E-20	1.000	270.0	2.50E-20	1.000	280.0	1.50E-20	1.000	290.0	9.00E-21	1.000	300.0	5.80E-21	1.000
310.0	3.40E-21	1.000	320.0	1.90E-21	1.000	330.0	1.10E-21	1.000	340.0	6.00E-22	1.000	350.0	4.00E-22	1.000
360.0	0.00E+00	1.000												
Photolysis File = HCHONEWR														
280.0	2.49E-20	0.590	280.5	1.42E-20	0.596	281.0	1.51E-20	0.602	281.5	1.32E-20	0.608	282.0	9.73E-21	0.614
282.5	6.76E-21	0.620	283.0	5.82E-21	0.626	283.5	9.10E-21	0.632	284.0	3.71E-20	0.638	284.5	4.81E-20	0.644
285.0	3.95E-20	0.650	285.5	2.87E-20	0.656	286.0	2.24E-20	0.662	286.5	1.74E-20	0.668	287.0	1.13E-20	0.674
287.5	1.10E-20	0.680	288.0	2.62E-20	0.686	288.5	4.00E-20	0.692	289.0	3.55E-20	0.698	289.5	2.12E-20	0.704
290.0	1.07E-20	0.710	290.5	1.35E-20	0.713	291.0	1.99E-20	0.717	291.5	1.56E-20	0.721	292.0	8.65E-21	0.724
292.5	5.90E-21	0.727	293.0	1.11E-20	0.731	293.5	6.26E-20	0.735	294.0	7.40E-20	0.738	294.5	5.36E-20	0.741
295.0	4.17E-20	0.745	295.5	3.51E-20	0.749	296.0	2.70E-20	0.752	296.5	1.75E-20	0.755	297.0	1.16E-20	0.759
297.5	1.51E-20	0.763	298.0	3.69E-20	0.766	298.5	4.40E-20	0.769	299.0	3.44E-20	0.773	299.5	2.02E-20	0.776
300.0	1.06E-20	0.780	300.4	7.01E-21	0.780	300.6	8.63E-21	0.779	300.8	1.47E-20	0.779	301.0	2.01E-20	0.779
301.2	2.17E-20	0.779	301.4	1.96E-20	0.779	301.6	1.54E-20	0.778	301.8	1.26E-20	0.778	302.0	1.03E-20	0.778
302.2	8.53E-21	0.778	302.4	7.13E-21	0.778	302.6	6.61E-21	0.777	302.8	1.44E-20	0.777	303.0	3.18E-20	0.777
303.2	3.81E-20	0.777	303.4	5.57E-20	0.777	303.6	6.91E-20	0.776	303.8	6.58E-20	0.776	304.0	6.96E-20	0.776
304.2	5.79E-20	0.776	304.4	5.24E-20	0.776	304.6	4.30E-20	0.775	304.8	3.28E-20	0.775	305.0	3.60E-20	0.775
305.2	5.12E-20	0.775	305.4	4.77E-20	0.775	305.6	4.43E-20	0.774	305.8	4.60E-20	0.774	306.0	4.01E-20	0.774
306.2	3.28E-20	0.774	306.4	2.66E-20	0.774	306.6	2.42E-20	0.773	306.8	1.95E-20	0.773	307.0	1.58E-20	0.773
307.2	1.37E-20	0.773	307.4	1.19E-20	0.773	307.6	1.01E-20	0.772	307.8	9.01E-21	0.772	308.0	8.84E-21	0.772
308.2	2.08E-20	0.772	308.4	2.39E-20	0.772	308.6	3.08E-20	0.771	308.8	3.39E-20	0.771	309.0	3.18E-20	0.771
309.2	3.06E-20	0.771	309.4	2.84E-20	0.771	309.6	2.46E-20	0.770	309.8	1.95E-20	0.770	310.0	1.57E-20	0.770
310.2	1.26E-20	0.767	310.4	9.26E-21	0.764	310.6	7.71E-21	0.761	310.8	6.05E-21	0.758	311.0	5.13E-21	0.755
311.2	4.82E-21	0.752	311.4	4.54E-21	0.749	311.6	6.81E-21	0.746	311.8	1.04E-20	0.743	312.0	1.43E-20	0.740
312.2	1.47E-20	0.737	312.4	1.35E-20	0.734	312.6	1.13E-20	0.731	312.8	9.86E-21	0.728	313.0	7.82E-21	0.725
313.2	6.48E-21	0.722	313.4	1.07E-20	0.719	313.6	2.39E-20	0.716	313.8	3.80E-20	0.713	314.0	5.76E-20	0.710
314.2	6.14E-20	0.707	314.4	7.45E-20	0.704	314.6	5.78E-20	0.701	314.8	5.59E-20	0.698	315.0	4.91E-20	0.695
315.2	4.37E-20	0.692	315.4	3.92E-20	0.689	315.6	2.89E-20	0.686	315.8	2.82E-20	0.683	316.0	2.10E-20	0.680
316.2	1.66E-20	0.677	316.4	2.05E-20	0.674	316.6	4.38E-20	0.671	316.8	5.86E-20	0.668	317.0	6.28E-20	0.665
317.2	5.07E-20	0.662	317.4	4.33E-20	0.659	317.6	4.17E-20	0.656	317.8	3.11E-20	0.653	318.0	2.64E-20	0.650
318.2	2.24E-20	0.647	318.4	1.70E-20	0.644	318.6	1.24E-20	0.641	318.8	1.11E-20	0.638	319.0	7.70E-21	0.635
319.2	6.36E-21	0.632	319.4	5.36E-21	0.629	319.6	4.79E-21	0.626	319.8	6.48E-21	0.623	320.0	1.48E-20	0.620
320.2	1.47E-20	0.614	320.4	1.36E-20	0.608	320.6	1.69E-20	0.601	320.8	1.32E-20	0.595	321.0	1.49E-20	0.589
321.2	1.17E-20	0.583	321.4	1.15E-20	0.577	321.6	9.64E-21	0.570	321.8	7.26E-21	0.564	322.0	5.94E-21	0.558
322.2	4.13E-21	0.552	322.4	3.36E-21	0.546	322.6	2.39E-21	0.539	322.8	2.01E-21	0.533	323.0	1.76E-21	0.527
323.2	2.82E-21	0.521	323.4	4.65E-21	0.515	323.6	7.00E-21	0.508	323.8	7.80E-21	0.502	324.0	7.87E-21	0.496
324.2	6.59E-21	0.490	324.4	5.60E-21	0.484	324.6	4.66E-21	0.477	324.8	4.21E-21	0.471	325.0	7.77E-21	0.465
325.2	2.15E-20	0.459	325.4	3.75E-20	0.453	325.6	4.10E-20	0.446	325.8	6.47E-20	0.440	326.0	7.59E-20	0.434
326.2	6.51E-20	0.428	326.4	5.53E-20	0.422	326.6	5.76E-20	0.415	326.8	4.43E-20	0.409	327.0	3.44E-20	0.403
327.2	3.22E-20	0.397	327.4	2.13E-20	0.391	327.6	1.91E-20	0.384	327.8	1.42E-20	0.378	328.0	9.15E-21	0.372
328.2	6.79E-21	0.366	328.4	4.99E-21	0.360	328.6	4.77E-21	0.353	328.8	1.75E-20	0.347	329.0	3.27E-20	0.341
329.2	3.99E-20	0.335	329.4	5.13E-20	0.329	329.6	4.00E-20	0.322	329.8	3.61E-20	0.316	330.0	3.38E-20	0.310
330.2	3.08E-20	0.304	330.4	2.16E-20	0.298	330.6	2.09E-20	0.291	330.8	1.41E-20	0.285	331.0	9.95E-21	0.279
331.2	7.76E-21	0.273	331.4	6.16E-21	0.267	331.6	4.06E-21	0.260	331.8	3.03E-21	0.254	332.0	2.41E-21	0.248
332.2	1.74E-21	0.242	332.4	1.33E-21	0.236	332.6	2.70E-21	0.229	332.8	1.65E-21	0.223	333.0	1.17E-21	0.217
333.2	9.84E-22	0.211	333.4	8.52E-22	0.205	333.6	6.32E-22	0.198	333.8	5.21E-22	0.192	334.0	1.46E-21	0.186
334.2	1.80E-21	0.180	334.4	1.43E-21	0.174	334.6	1.03E-21	0.167	334.8	7.19E-22	0.161	335.0	4.84E-22	0.155
335.2	2.73E-22	0.149	335.4	1.34E-22	0.143	335.6	-1.62E-22	0.136	335.8	1.25E-22	0.130	336.0	4.47E-22	0.124
336.2	1.23E-21	0.118	336.4	2.02E-21	0.112	336.6	3.00E-21	0.105	336.8	2.40E-21	0.099	337.0	3.07E-21	0.093
337.2	2.29E-21	0.087	337.4	2.46E-21	0.081	337.6	2.92E-21	0.074	337.8	8.10E-21	0.068	338.0	1.82E-20	0.062
338.2	3.10E-20	0.056	338.4	3.24E-20	0.050	338.6	4.79E-20	0.043	338.8	5.25E-20	0.037	339.0	5.85E-20	0.031
339.2	4.33E-20	0.025	339.4	4.20E-20	0.019	339.6	3.99E-20	0.012	339.8	3.11E-20	0.006	340.0	2.72E-20	0.000
Photolysis File = HCHONEWM														
280.0	2.49E-20	0.350	280.5	1.42E-20	0.346	281.0	1.51E-20	0.341	281.5	1.32E-20	0.336	282.0	9.73E-21	0.332
282.5	6.76E-21	0.327	283.0	5.82E-21	0.323	283.5	9.10E-21	0.319	284.0	3.71E-20	0.314	284.5	4.81E-20	0.309
285.0	3.95E-20	0.305	285.5	2.87E-20	0.301	286.0	2.24E-20	0.296	286.5	1.74E-20	0.291	287.0	1.13E-20	0.287
287.5	1.10E-20	0.282	288.0	2.62E-20	0.278	288.5	4.00E-20	0.273	289.0	3.55E-20	0.269	289.5	2.12E-20	0.264
290.0	1.07E-20	0.260	290.5	1.35E-20	0.258	291.0	1.99E-20	0.256	291.5	1.56E-20	0.254	292.0	8.65E-21	0.252
292.5	5.90E-21	0.250	293.0	1.11E-20	0.248	293.5	6.26E-20	0.246	294.0	7.40E-20	0.244	294.5	5.36E-20	0.242
295.0	4.17E-20	0.240	295.5	3.51E-20	0.238	296.0	2.70E-20	0.236	296.5	1.75E-20	0.234	297.0	1.16E-20	0.232
297.5	1.51E-20	0.230	298.0	3.69E-20	0.228	298.5	4.40E-20	0.226	299.0	3.44E-20	0.224	299.5	2.02E-20	0.222
300.0	1.06E-20	0.220	300.4	7.01E-21	0.220	300.6	8.63E-21	0.221	300.8	1.47E-20	0.221	301.0	2.01E-20	0.221
301.2	2.17E-20	0.221	301.4	1.96E-20	0.221	301.6	1.54E-20	0.222	301.8	1.26E-20	0.222	302.0	1.03E-20	0.222
302.2	8.53E-21	0.222	302.4	7.13E-21	0.222	302.6	6.61E-21	0.223	302.8	1.44E-20	0.223	303.0	3.18E-20	0.223
303.2	3.81E-20	0.223	303.4	5.57E-20	0.223	303.6	6.91E-20	0.224	303.8	6.58E-20	0.224	304.0	6.96E-20	0.224
304.2	5.79E-20	0.224	304.4	5.24E-20	0.224	304.6	4.30E-20	0.225	304.8	3.28E-20	0.225	305.0	3.60E-20	0.225
305.2	5.12E-20	0.225	305.4	4.77E-20	0.225	305.6	4.43E-20	0.226	305.8	4.60E-20	0.226	306.0	4.01E-20	0.226
306.2	3.28E-20	0.226	306.4	2.66E-20	0.226	306.6	2.42E-20	0.227	306.8	1.95E-20	0.227	307.0	1.58E-20	0.227
307.2	1.37E-20	0.227	307.4	1.19E-20	0.227	307.6	1.01E-20	0.228	307.8	9.01E-21	0.228	308.0	8.84E-21	0.228
308.2	2.08E-20	0.228	308.4	2.39E-20	0.228	308.6	3.08E-20	0.229	308.8	3.39E-20	0.229	309.0	3.18E-20	0.229
309.2	3.06E-20	0.229	309.4	2.84E-20	0.229	309.6	2.46E-20	0.230	309.8	1.95E-20	0.230	310.0	1.57E-20	0.230
310.2	1.26E-20	0.233	310.4	9.26E-21	0.236	310.6	7.71E-21	0.239	310.8	6.05E-21	0.242	311.0	5.13E-21	0.245
311.2	4.82E-21	0.248	311.4	4.54E-21	0.251	311.6	6.81E-21	0.254	311.8	1.04E-20	0.257	312.0	1.43E-20	0.260
312.2	1.47E-20	0.263	312.4	1.35E-20	0.266	312.6	1.13E-20	0.269	312.8	9.86E-21	0.272	313.0	7.82E-21	0.275
313.2	6.48E-21	0.278	313.4	1.07E-20	0.281	313.6	2.39E-20	0.284	313.8	3.80E-20	0.287	314.0	5.76E-20	0.290
314.2	6.14E-20	0.293	314.4	7.45E-20	0.296	314.6	5.78E-20	0.299	314.8	5.59E-20	0.302	315.0	4.91E-20	0.305
315.2	4.37E-20	0.308	315.4	3.92E-20	0.311	315.6	2.89E-20	0.314	315.8	2.82E-20	0.317	316.0	2.10E-20	0.320
316.2	1.66E-20	0.323	316.4	2.05E-20	0.326	316.6	4.38E-20	0.329	316.8	5.86E-20	0.332	317.0	6.28E-20	0.335
317.2	5.07E-20	0.338	317.4	4.33E-20	0.341	317.6	4.17E-20	0.344	317.8	3.11E-20	0.347	318.0	2.64E-20	0.350
318.2	2.24E-20	0.353	318.4	1.70E-20	0.356	318.6	1.24E-20	0.359	318.8	1.11E-20	0.362	319.0	7.70E-21	0.365

Table A-3. (continued)

WL (nm)	Abs (cm^2)	QY	WL (nm)	Abs (cm^2)	QY	WL (nm)	Abs (cm^2)	QY	WL (nm)	Abs (cm^2)	QY	WL (nm)	Abs (cm^2)	QY
319.2	6.36E-21	0.368	319.4	5.36E-21	0.371	319.6	4.79E-21	0.374	319.8	6.48E-21	0.377	320.0	1.48E-20	0.380
320.2	1.47E-20	0.386	320.4	1.36E-20	0.392	320.6	1.69E-20	0.399	320.8	1.32E-20	0.405	321.0	1.49E-20	0.411
321.2	1.17E-20	0.417	321.4	1.15E-20	0.423	321.6	9.64E-21	0.430	321.8	7.26E-21	0.436	322.0	5.94E-21	0.442
322.2	4.13E-21	0.448	322.4	3.36E-21	0.454	322.6	2.39E-21	0.461	322.8	2.01E-21	0.467	323.0	1.76E-21	0.473
323.2	2.82E-21	0.479	323.4	4.65E-21	0.485	323.6	7.00E-21	0.492	323.8	7.80E-21	0.498	324.0	7.87E-21	0.504
324.2	6.59E-21	0.510	324.4	5.60E-21	0.516	324.6	4.66E-21	0.523	324.8	4.21E-21	0.529	325.0	7.77E-21	0.535
325.2	2.15E-20	0.541	325.4	3.75E-20	0.547	325.6	4.10E-20	0.554	325.8	6.47E-20	0.560	326.0	7.59E-20	0.566
326.2	6.51E-20	0.572	326.4	5.53E-20	0.578	326.6	5.76E-20	0.585	326.8	4.43E-20	0.591	327.0	3.44E-20	0.597
327.2	3.22E-20	0.603	327.4	2.13E-20	0.609	327.6	1.91E-20	0.616	327.8	1.42E-20	0.622	328.0	9.15E-21	0.628
328.2	6.79E-21	0.634	328.4	4.99E-21	0.640	328.6	4.77E-21	0.647	328.8	1.75E-20	0.653	329.0	3.27E-20	0.659
329.2	3.99E-20	0.665	329.4	5.13E-20	0.671	329.6	4.00E-20	0.678	329.8	3.61E-20	0.684	330.0	3.38E-20	0.690
330.2	3.08E-20	0.694	330.4	2.16E-20	0.699	330.6	2.09E-20	0.703	330.8	1.41E-20	0.708	331.0	9.95E-21	0.712
331.2	7.76E-21	0.717	331.4	6.16E-21	0.721	331.6	4.06E-21	0.726	331.8	3.03E-21	0.730	332.0	2.41E-21	0.735
332.2	1.74E-21	0.739	332.4	1.33E-21	0.744	332.6	2.70E-21	0.748	332.8	1.65E-21	0.753	333.0	1.17E-21	0.757
333.2	9.84E-22	0.762	333.4	8.52E-22	0.766	333.6	6.32E-22	0.771	333.8	5.21E-22	0.775	334.0	1.46E-21	0.780
334.2	1.80E-21	0.784	334.4	1.43E-21	0.789	334.6	1.03E-21	0.793	334.8	7.19E-22	0.798	335.0	4.84E-22	0.802
335.2	2.73E-22	0.798	335.4	1.34E-22	0.794	335.6	0.00E+00	0.790	335.8	1.25E-22	0.786	336.0	4.47E-22	0.782
336.2	1.23E-21	0.778	336.4	2.02E-21	0.773	336.6	3.00E-21	0.769	336.8	2.40E-21	0.764	337.0	3.07E-21	0.759
337.2	2.29E-21	0.754	337.4	2.46E-21	0.749	337.6	2.92E-21	0.745	337.8	8.10E-21	0.740	338.0	1.82E-20	0.734
338.2	3.10E-20	0.729	338.4	3.24E-20	0.724	338.6	4.79E-20	0.719	338.8	5.25E-20	0.714	339.0	5.85E-20	0.709
339.2	4.33E-20	0.703	339.4	4.20E-20	0.698	339.6	3.99E-20	0.693	339.8	3.11E-20	0.687	340.0	2.72E-20	0.682
340.2	1.99E-20	0.676	340.4	1.76E-20	0.671	340.6	1.39E-20	0.666	340.8	1.01E-20	0.660	341.0	6.57E-21	0.655
341.2	4.83E-21	0.649	341.4	3.47E-21	0.643	341.6	2.23E-21	0.638	341.8	1.55E-21	0.632	342.0	3.70E-21	0.627
342.2	4.64E-21	0.621	342.4	1.08E-20	0.616	342.6	1.14E-20	0.610	342.8	1.79E-20	0.604	343.0	2.33E-20	0.599
343.2	1.72E-20	0.593	343.4	1.55E-20	0.588	343.6	1.46E-20	0.582	343.8	1.38E-20	0.576	344.0	1.00E-20	0.571
344.2	8.26E-21	0.565	344.4	6.32E-21	0.559	344.6	4.28E-21	0.554	344.8	3.22E-21	0.548	345.0	2.54E-21	0.542
345.2	1.60E-21	0.537	345.4	1.15E-21	0.531	345.6	8.90E-22	0.525	345.8	6.50E-22	0.520	346.0	5.09E-22	0.514
346.2	5.15E-22	0.508	346.4	3.45E-22	0.503	346.6	3.18E-22	0.497	346.8	3.56E-22	0.491	347.0	3.24E-22	0.485
347.2	3.34E-22	0.480	347.4	2.88E-22	0.474	347.6	2.84E-22	0.468	347.8	9.37E-22	0.463	348.0	9.70E-22	0.457
348.2	7.60E-22	0.451	348.4	6.24E-22	0.446	348.6	4.99E-22	0.440	348.8	4.08E-22	0.434	349.0	3.39E-22	0.428
349.2	1.64E-22	0.423	349.4	1.49E-22	0.417	349.6	8.30E-23	0.411	349.8	2.52E-23	0.406	350.0	2.57E-23	0.400
350.2	0.00E+00	0.394	350.4	5.16E-23	0.389	350.6	0.00E+00	0.383	350.8	2.16E-23	0.377	351.0	7.07E-23	0.371
351.2	3.45E-23	0.366	351.4	1.97E-22	0.360	351.6	4.80E-22	0.354	351.8	3.13E-21	0.349	352.0	6.41E-21	0.343
352.2	8.38E-21	0.337	352.4	1.55E-20	0.331	352.6	1.86E-20	0.326	352.8	1.94E-20	0.320	353.0	2.78E-20	0.314
353.2	1.96E-20	0.309	353.4	1.67E-20	0.303	353.6	1.75E-20	0.297	353.8	1.63E-20	0.291	354.0	1.36E-20	0.286
354.2	1.07E-20	0.280	354.4	9.82E-21	0.274	354.6	8.66E-21	0.269	354.8	6.44E-21	0.263	355.0	4.84E-21	0.257
355.2	3.49E-21	0.251	355.4	2.41E-21	0.246	355.6	1.74E-21	0.240	355.8	1.11E-21	0.234	356.0	7.37E-22	0.229
356.2	4.17E-22	0.223	356.4	1.95E-22	0.217	356.6	1.50E-22	0.211	356.8	8.14E-23	0.206	357.0	0.00E+00	0.200
Photolysis File = CCHOR														
260.0	2.00E-20	0.310	270.0	3.40E-20	0.390	280.0	4.50E-20	0.580	290.0	4.90E-20	0.530	295.0	4.50E-20	0.480
300.0	4.30E-20	0.430	305.0	3.40E-20	0.370	315.0	2.10E-20	0.170	320.0	1.80E-20	0.100	325.0	1.10E-20	0.040
330.0	6.90E-21	0.000												
Photolysis File = RCHO														
280.0	5.26E-20	0.960	290.0	5.77E-20	0.910	300.0	5.05E-20	0.860	310.0	3.68E-20	0.600	320.0	1.66E-20	0.360
330.0	6.49E-21	0.200	340.0	1.44E-21	0.080	345.0	0.00E+00	0.020						
Photolysis File = ACET-93C														
250.0	2.37E-20	0.760	260.0	3.66E-20	0.800	270.0	4.63E-20	0.640	280.0	5.05E-20	0.550	290.0	4.21E-20	0.300
300.0	2.78E-20	0.150	310.0	1.44E-20	0.050	320.0	4.80E-21	0.026	330.0	8.00E-22	0.017	340.0	1.00E-22	0.000
350.0	3.00E-23	0.000	360.0	0.00E+00	0.000									
Photolysis File = KETONE														
210.0	1.10E-21	1.000	220.0	1.20E-21	1.000	230.0	4.60E-21	1.000	240.0	1.30E-20	1.000	250.0	2.68E-20	1.000
260.0	4.21E-20	1.000	270.0	5.54E-20	1.000	280.0	5.92E-20	1.000	290.0	5.16E-20	1.000	300.0	3.44E-20	1.000
310.0	1.53E-20	1.000	320.0	4.60E-21	1.000	330.0	1.10E-21	1.000	340.0	0.00E+00	1.000			
Photolysis File = GLYOXAL1														
230.0	2.87E-21	1.000	235.0	2.87E-21	1.000	240.0	4.30E-21	1.000	245.0	5.73E-21	1.000	250.0	8.60E-21	1.000
255.0	1.15E-20	1.000	260.0	1.43E-20	1.000	265.0	1.86E-20	1.000	270.0	2.29E-20	1.000	275.0	2.58E-20	1.000
280.0	2.87E-20	1.000	285.0	3.30E-20	1.000	290.0	3.15E-20	1.000	295.0	3.30E-20	1.000	300.0	3.58E-20	1.000
305.0	2.72E-20	1.000	310.0	2.72E-20	1.000	312.5	2.87E-20	1.000	315.0	2.29E-20	1.000	320.0	1.43E-20	1.000
325.0	1.15E-20	1.000	327.5	1.43E-20	1.000	330.0	1.15E-20	1.000	335.0	2.87E-21	1.000	340.0	0.00E+00	1.000
Photolysis File = GLYOXAL2														
355.0	0.00E+00	1.000	360.0	2.29E-21	1.000	365.0	2.87E-21	1.000	370.0	8.03E-21	1.000	375.0	1.00E-20	1.000
380.0	1.72E-20	1.000	382.0	1.58E-20	1.000	384.0	1.49E-20	1.000	386.0	1.49E-20	1.000	388.0	2.87E-20	1.000
390.0	3.15E-20	1.000	391.0	3.24E-20	1.000	392.0	3.04E-20	1.000	393.0	2.23E-20	1.000	394.0	2.63E-20	1.000
395.0	3.04E-20	1.000	396.0	2.63E-20	1.000	397.0	2.43E-20	1.000	398.0	3.24E-20	1.000	399.0	3.04E-20	1.000
400.0	2.84E-20	1.000	401.0	3.24E-20	1.000	402.0	4.46E-20	1.000	403.0	5.27E-20	1.000	404.0	4.26E-20	1.000
405.0	3.04E-20	1.000	406.0	3.04E-20	1.000	407.0	2.84E-20	1.000	408.0	2.43E-20	1.000	409.0	2.84E-20	1.000
410.0	6.08E-20	1.000	411.0	5.07E-20	1.000	411.5	6.08E-20	1.000	412.0	4.86E-20	1.000	413.0	8.31E-20	1.000
413.5	6.48E-20	1.000	414.0	7.50E-20	1.000	414.5	8.11E-20	1.000	415.0	8.11E-20	1.000	415.5	6.89E-20	1.000
416.0	4.26E-20	1.000	417.0	4.86E-20	1.000	418.0	5.88E-20	1.000	419.0	6.69E-20	1.000	420.0	3.85E-20	1.000
421.0	5.67E-20	1.000	421.5	4.46E-20	1.000	422.0	5.27E-20	1.000	422.5	1.05E-19	1.000	423.0	8.51E-20	1.000
424.0	6.08E-20	1.000	425.0	7.29E-20	1.000	426.0	1.18E-19	1.000	426.5	1.30E-19	1.000	427.0	1.07E-19	1.000
428.0	1.66E-19	1.000	429.0	4.05E-20	1.000	430.0	5.07E-20	1.000	431.0	4.86E-20	1.000	432.0	4.05E-20	1.000
433.0	3.65E-20	1.000	434.0	4.05E-20	1.000	434.5	6.08E-20	1.000	435.0	5.07E-20	1.000	436.0	8.11E-20	1.000
436.5	1.13E-19	1.000	437.0	5.27E-20	1.000	438.0	1.01E-19	1.000	438.5	1.38E-19	1.000	439.0	7.70E-20	1.000
440.0	2.47E-19	1.000	441.0	8.11E-20	1.000	442.0	6.08E-20	1.000	443.0	7.50E-20	1.000	444.0	9.32E-20	1.000
445.0	1.13E-19	1.000	446.0	5.27E-20	1.000	447.0	2.43E-20	1.000	448.0	2.84E-20	1.000	449.0	3.85E-20	1.000
450.0	6.08E-20	1.000	451.0	1.09E-19	1.000	451.5	9.32E-20	1.000	452.0	1.22E-19	1.000	453.0	2.39E-19	1.000
454.0	1.70E-19	1.000	455.0	3.40E-19	1.000	455.5	4.05E-19	1.000	456.0	1.01E-19	1.000	457.0	1.62E-20	1.000

Table A-3. (continued)

WL (nm)	Abs (cm^2)	QY	WL (nm)	Abs (cm^2)	QY	WL (nm)	Abs (cm^2)	QY	WL (nm)	Abs (cm^2)	QY	WL (nm)	Abs (cm^2)	QY
458.0	1.22E-20	1.000	458.5	1.42E-20	1.000	459.0	4.05E-21	1.000	460.0	4.05E-21	1.000	460.5	6.08E-21	1.000
461.0	2.03E-21	1.000	462.0	0.00E+00	1.000									
Photolysis File = MEGLYOX1														
220.0	2.10E-21	1.000	225.0	2.10E-21	1.000	230.0	4.21E-21	1.000	235.0	7.57E-21	1.000	240.0	9.25E-21	1.000
245.0	8.41E-21	1.000	250.0	9.25E-21	1.000	255.0	9.25E-21	1.000	260.0	9.67E-21	1.000	265.0	1.05E-20	1.000
270.0	1.26E-20	1.000	275.0	1.43E-20	1.000	280.0	1.51E-20	1.000	285.0	1.43E-20	1.000	290.0	1.47E-20	1.000
295.0	1.18E-20	1.000	300.0	1.14E-20	1.000	305.0	9.25E-21	1.000	310.0	6.31E-21	1.000	315.0	5.47E-21	1.000
320.0	3.36E-21	1.000	325.0	1.68E-21	1.000	330.0	8.41E-22	1.000	335.0	0.00E+00	1.000			
Photolysis File = MEGLYOX2														
350.0	0.00E+00	1.000	354.0	4.21E-22	1.000	358.0	1.26E-21	1.000	360.0	2.10E-21	1.000	362.0	2.10E-21	1.000
364.0	2.94E-21	1.000	366.0	3.36E-21	1.000	368.0	4.21E-21	1.000	370.0	5.47E-21	1.000	372.0	5.89E-21	1.000
374.0	7.57E-21	1.000	376.0	7.99E-21	1.000	378.0	8.83E-21	1.000	380.0	1.01E-20	1.000	382.0	1.09E-20	1.000
384.0	1.35E-20	1.000	386.0	1.51E-20	1.000	388.0	1.72E-20	1.000	390.0	2.06E-20	1.000	392.0	2.10E-20	1.000
394.0	2.31E-20	1.000	396.0	2.48E-20	1.000	398.0	2.61E-20	1.000	400.0	2.78E-20	1.000	402.0	2.99E-20	1.000
404.0	3.20E-20	1.000	406.0	3.79E-20	1.000	408.0	3.95E-20	1.000	410.0	4.33E-20	1.000	412.0	4.71E-20	1.000
414.0	4.79E-20	1.000	416.0	4.88E-20	1.000	418.0	5.05E-20	1.000	420.0	5.21E-20	1.000	422.0	5.30E-20	1.000
424.0	5.17E-20	1.000	426.0	5.30E-20	1.000	428.0	5.21E-20	1.000	430.0	5.55E-20	1.000	432.0	5.13E-20	1.000
434.0	5.68E-20	1.000	436.0	6.22E-20	1.000	438.0	6.06E-20	1.000	440.0	5.47E-20	1.000	441.0	6.14E-20	1.000
442.0	5.47E-20	1.000	443.0	5.55E-20	1.000	443.5	6.81E-20	1.000	444.0	5.97E-20	1.000	445.0	5.13E-20	1.000
446.0	4.88E-20	1.000	447.0	5.72E-20	1.000	448.0	5.47E-20	1.000	449.0	6.56E-20	1.000	450.0	5.05E-20	1.000
451.0	3.03E-20	1.000	452.0	4.29E-20	1.000	453.0	2.78E-20	1.000	454.0	2.27E-20	1.000	456.0	1.77E-20	1.000
458.0	8.41E-21	1.000	460.0	4.21E-21	1.000	464.0	1.68E-21	1.000	468.0	0.00E+00	1.000			
Photolysis File = BZCHO														
299.0	1.78E-19	1.000	304.0	7.40E-20	1.000	306.0	6.91E-20	1.000	309.0	6.41E-20	1.000	313.0	6.91E-20	1.000
314.0	6.91E-20	1.000	318.0	6.41E-20	1.000	325.0	8.39E-20	1.000	332.0	7.65E-20	1.000	338.0	8.88E-20	1.000
342.0	8.88E-20	1.000	346.0	7.89E-20	1.000	349.0	7.89E-20	1.000	354.0	9.13E-20	1.000	355.0	8.14E-20	1.000
364.0	5.67E-20	1.000	368.0	6.66E-20	1.000	369.0	8.39E-20	1.000	370.0	8.39E-20	1.000	372.0	3.45E-20	1.000
374.0	3.21E-20	1.000	376.0	2.47E-20	1.000	377.0	2.47E-20	1.000	380.0	3.58E-20	1.000	382.0	9.90E-21	1.000
386.0	0.00E+00	1.000												
Photolysis File = ACROLEIN														
250.0	1.80E-21	1.000	252.0	2.05E-21	1.000	253.0	2.20E-21	1.000	254.0	2.32E-21	1.000	255.0	2.45E-21	1.000
256.0	2.56E-21	1.000	257.0	2.65E-21	1.000	258.0	2.74E-21	1.000	259.0	2.83E-21	1.000	260.0	2.98E-21	1.000
261.0	3.24E-21	1.000	262.0	3.47E-21	1.000	263.0	3.58E-21	1.000	264.0	3.93E-21	1.000	265.0	4.67E-21	1.000
266.0	5.10E-21	1.000	267.0	5.38E-21	1.000	268.0	5.73E-21	1.000	269.0	6.13E-21	1.000	270.0	6.64E-21	1.000
271.0	7.20E-21	1.000	272.0	7.77E-21	1.000	273.0	8.37E-21	1.000	274.0	8.94E-21	1.000	275.0	9.55E-21	1.000
276.0	1.04E-20	1.000	277.0	1.12E-20	1.000	278.0	1.19E-20	1.000	279.0	1.27E-20	1.000	280.0	1.27E-20	1.000
281.0	1.26E-20	1.000	282.0	1.26E-20	1.000	283.0	1.28E-20	1.000	284.0	1.33E-20	1.000	285.0	1.38E-20	1.000
286.0	1.44E-20	1.000	287.0	1.50E-20	1.000	288.0	1.57E-20	1.000	289.0	1.63E-20	1.000	290.0	1.71E-20	1.000
291.0	1.78E-20	1.000	292.0	1.86E-20	1.000	293.0	1.95E-20	1.000	294.0	2.05E-20	1.000	295.0	2.15E-20	1.000
296.0	2.26E-20	1.000	297.0	2.37E-20	1.000	298.0	2.48E-20	1.000	299.0	2.60E-20	1.000	300.0	2.73E-20	1.000
301.0	2.85E-20	1.000	302.0	2.99E-20	1.000	303.0	3.13E-20	1.000	304.0	3.27E-20	1.000	305.0	3.39E-20	1.000
306.0	3.51E-20	1.000	307.0	3.63E-20	1.000	308.0	3.77E-20	1.000	309.0	3.91E-20	1.000	310.0	4.07E-20	1.000
311.0	4.25E-20	1.000	312.0	4.39E-20	1.000	313.0	4.44E-20	1.000	314.0	4.50E-20	1.000	315.0	4.59E-20	1.000
316.0	4.75E-20	1.000	317.0	4.90E-20	1.000	318.0	5.05E-20	1.000	319.0	5.19E-20	1.000	320.0	5.31E-20	1.000
321.0	5.43E-20	1.000	322.0	5.52E-20	1.000	323.0	5.60E-20	1.000	324.0	5.67E-20	1.000	325.0	5.67E-20	1.000
326.0	5.62E-20	1.000	327.0	5.63E-20	1.000	328.0	5.71E-20	1.000	329.0	5.76E-20	1.000	330.0	5.80E-20	1.000
331.0	5.95E-20	1.000	332.0	6.23E-20	1.000	333.0	6.39E-20	1.000	334.0	6.38E-20	1.000	335.0	6.24E-20	1.000
336.0	6.01E-20	1.000	337.0	5.79E-20	1.000	338.0	5.63E-20	1.000	339.0	5.56E-20	1.000	340.0	5.52E-20	1.000
341.0	5.54E-20	1.000	342.0	5.53E-20	1.000	343.0	5.47E-20	1.000	344.0	5.41E-20	1.000	345.0	5.40E-20	1.000
346.0	5.48E-20	1.000	347.0	5.90E-20	1.000	348.0	6.08E-20	1.000	349.0	6.00E-20	1.000	350.0	5.53E-20	1.000
351.0	5.03E-20	1.000	352.0	4.50E-20	1.000	353.0	4.03E-20	1.000	354.0	3.75E-20	1.000	355.0	3.55E-20	1.000
356.0	3.45E-20	1.000	357.0	3.46E-20	1.000	358.0	3.49E-20	1.000	359.0	3.41E-20	1.000	360.0	3.23E-20	1.000
361.0	2.95E-20	1.000	362.0	2.81E-20	1.000	363.0	2.91E-20	1.000	364.0	3.25E-20	1.000	365.0	3.54E-20	1.000
366.0	3.30E-20	1.000	367.0	2.78E-20	1.000	368.0	2.15E-20	1.000	369.0	1.59E-20	1.000	370.0	1.19E-20	1.000
371.0	8.99E-21	1.000	372.0	7.22E-21	1.000	373.0	5.86E-21	1.000	374.0	4.69E-21	1.000	375.0	3.72E-21	1.000
376.0	3.57E-21	1.000	377.0	3.55E-21	1.000	378.0	2.83E-21	1.000	379.0	1.69E-21	1.000	380.0	8.29E-24	1.000
381.0	0.00E+00	1.000												

Table A-4. Values of chamber-dependent parameters used in the model simulations of the environmental chamber experiments for this study. [a]

Parm.	Value(s)	Discussion
k(1)	0.173 min^{-1} (first series) 0.207 min^{-1} (second series)	Derived from trend (for first series) or average (for second series) of results of quartz tube NO_2 actinometry measurements carried out around the time of the experiments. The first series consist of the runs carried out in 1996 prior to the change in reaction bags and light banks, and the second series is the set of runs carried out afterwards.
k(O3W)	$1.5x10^{-4}$ min^{-1}	The results of the O_3 dark decay experiments in this chamber are reasonably consistent with the recommended default of Carter et al (1995e) for Teflon bag chambers in general.
k(N25I) k(N25S)	$2.8\ x10^{-3}$ min^{-1}, $1.5x10^{-6}$ - k_g ppm^{-1} min^{-1}	Based on the N_2O_5 decay rate measurements in a similar chamber reported by Tuazon et al. (1983). Although we previously estimated there rate constants were lower in the larger Teflon bag chambers (Carter and Lurmann, 1990, 1991), we now consider it more reasonable to use the same rate constants for all such chambers (Carter et al., 1995e).
k(NO2W) yHONO	$1.6x10^{-4}$ min^{-1} 0.2	Based on dark NO_2 decay and HONO formation measured in a similar chamber by Pitts et al. (1984). Assumed to be the same in all Teflon bag chambers (Carter et al, 1995e).
k(XSHC)	250 min^{-1}	Estimated by modeling pure air irradiations. Not an important parameter affecting model predictions except for pure air or NO_x-air runs.
RS/K1	$3.27x10^{6}$ $e^{-7297/T}$ ppm	Based on model simulations of n-butane - NO_x experiments as discussed by Carter et al (1997a). The temperature dependence is derived from simulating outdoor experiments as discussed by Carter et al. (1995c).
E-NO2/K1	0.03 ppb	Based on model simulations of pure air experiments.

[a] See Table A-2 for definitions of the parameters.

APPENDIX B
GC-MS DATA

The detailed results of the Safety-Kleen and DRI GC-MS analyses of the four mineral spirits samples, and example total ion chromatograms, are given in this Appendix. Figures B-1 through B-4 give the results of the Safety-Kleen GC-MS analyses for, together with the model species assignments for each separated peak. Figures B-5 through B-8 give the results of the DRI analyses, and the model species assigned to each peak. Summaries of these data are given in Tables 4 and 5 in the main body of the report. Examples of total ion chromatograms provided for each sample by Safety-Kleen and DRI are given on Figures B-1 through B-8, with the chromatograms from the two laboratories shown on the same page for each sample, for easier comparison. In all cases, the elution time goes from left to right, and the chromatograms are truncated to show only the periods when significant peaks are observed.

Table B-1. Results of Safety-Kleen GC-MS analysis of Mixture "A", and detailed model species assignments used for ozone impact modeling.

GC-MS Data			GC-MS Assignments			Model Species Assignments	
Ret Time	Area %	Mol Ion	Compound Identified	Class	Car-bons		
8.68	0.01		Methanol	other	1	INERT	[a]
12.34	0.02	86		aliphatic	8	BR-C8	
14.60	0.07		111-TCE	other	2	INERT	[a]
15.94	0.01			aliphatic	8	BR-C8	
17.51	0.02	100		aliphatic	8	BR-C8	
19.89	0.01	98	Methyl cyclohexane	alicyclic	7	ME-CYCC6	
23.44	0.04			aliphatic	8	BR-C8	
24.20	0.12		Toluene	aromatic	7	TOLUENE	
24.37	0.02			aliphatic	8	(C8 Cyc/Ole)	0.950 CYC-C8 0.040 C8-OLE1 0.010 C8-OLE2 [b]
25.49	0.02	112		alicyclic	8	(C8 Cyc/Ole)	[b,c]
27.62	0.20	114	n-Octane	aliphatic	8	N-C8	
28.09	0.02	112		alicyclic	9	(C9 Cyc/Ole)	0.950 CYC-C9 0.040 C9-OLE1 0.010 C9-OLE2 [b]
29.77	0.09		PERC.	other	2	INERT	
30.82	0.01			aliphatic	9	BR-C9	
31.77	0.11	128		aliphatic	9	BR-C9	
32.85	0.09	126		alicyclic	9	(C9 Cyc/Ole)	[b,c]
33.31	0.04	112		alicyclic	9	(C9 Cyc/Ole)	[b,c]
33.83	0.13			alicyclic	9	(C9 Cyc/Ole)	[b,c]
35.55	0.05			alicyclic	9	(C9 Cyc/Ole)	[b,c]
36.28	0.20	126		alicyclic	9	(C9 Cyc/Ole)	[b,c]
36.47	0.11			aliphatic	9	BR-C9	
36.93	0.05	126		alicyclic	9	(C9 Cyc/Ole)	[b,c]
37.18	0.02			aliphatic	9	BR-C9	
37.69	0.15	128		aliphatic	9	BR-C9	
37.84	0.28	128		aliphatic	9	BR-C9	
38.32	0.02	128		aliphatic	9	BR-C9	
38.59	0.02			alicyclic	9	(C9 Cyc/Ole)	[b,c]
39.16	0.40	128		aliphatic	9	BR-C9	
39.38	0.17	106	Xylene	aromatic	8	Xylene Mix	0.50 M-XYLENE 0.50 P-XYLENE
39.75	0.08			alicyclic	9	(C9 Cyc/Ole)	[b,c]
40.57	0.18	126		alicyclic	9	(C9 Cyc/Ole)	[b,c]
40.77	0.08	126		alicyclic	9	(C9 Cyc/Ole)	[b,c]

Table B-1 (continued)

GC-MS Data			GC-MS Assignments			Model Species Assignments	
Ret Time	Area %	Mol Ion	Compound Identified	Class	Car-bons	Model Species	Comments
41.20	0.02			alicyclic	9	(C9 Cyc/Ole)	[b,c]
41.44	0.07	126		alicyclic	9	(C9 Cyc/Ole)	[b,c]
42.01	0.12	126		alicyclic	9	(C9 Cyc/Ole)	[b,c]
42.28	0.24			alicyclic	9	(C9 Cyc/Ole)	[b,c]
42.54	0.07			alicyclic	9	(C9 Cyc/Ole)	[b,c]
42.91	0.34	126		alicyclic	9	(C9 Cyc/Ole)	[b,c]
43.31	0.20	126		alicyclic	9	(C9 Cyc/Ole)	[b,c]
43.62	0.04			alicyclic	9	(C9 Cyc/Ole)	[b,c]
44.04	0.14	106	Xylene	aromatic	8	O-XYLENE	[d]
44.28	0.03	124		alicyclic	9	(C9 Cyc/Ole)	[b,c]
44.79	2.36	128	n-Nonane	aliphatic	9	N-C9	
45.29	0.22	140		alicyclic	10	(C10 Cyc/Ole)	0.950 CYC-C10 0.040 C10-OLE1 0.010 C10-OLE2 [b]
46.36	0.27	126		alicyclic	10	(C10 Cyc/Ole)	[b,c]
46.92	0.44	126		alicyclic	10	(C10 Cyc/Ole)	[b,c]
47.17	0.05			aliphatic	10	BR-C10	
47.52	0.09	126		alicyclic	10	(C10 Cyc/Ole)	[b,c]
47.73	0.04			alicyclic	10	(C10 Cyc/Ole)	[b,c]
48.07	0.07			aliphatic	10	BR-C10	
48.36	0.16			aliphatic	10	BR-C10	
48.75	0.11			alicyclic	10	(C10 Cyc/Ole)	[b,c]
49.15	0.06			aliphatic	10	BR-C10	
49.81	0.94	124		alicyclic	10	(C10 Cyc/Ole)	[b,c]
50.32	0.04	140		alicyclic	10	(C10 Cyc/Ole)	[b,c]
50.62	0.02	120	Cumene	aromatic	9	I-C3-BEN	
50.89	0.15			aliphatic	10	BR-C10	
51.14	0.37	140		alicyclic	10	(C10 Cyc/Ole)	[b,c]
52.12	1.91	142		aliphatic	10	BR-C10	
52.61	0.47	126		alicyclic	10	(C10 Cyc/Ole)	[b,c]
52.95	0.13			aliphatic	10	BR-C10	
53.50	0.23			aliphatic	10	BR-C10	
53.92	0.81			aliphatic	10	BR-C10	
54.32	0.19	140		alicyclic	10	(C10 Cyc/Ole)	[b,c]
54.56	0.17			alicyclic	10	(C10 Cyc/Ole)	[b,c]
54.97	0.13	140		alicyclic	10	(C10 Cyc/Ole)	[b,c]
55.27	0.14			alicyclic	10	(C10 Cyc/Ole)	[b,c]
55.87	0.13	140		alicyclic	10	(C10 Cyc/Ole)	[b,c]
56.06	0.26	140		alicyclic	10	(C10 Cyc/Ole)	[b,c]
56.88	0.53	140		alicyclic	10	(C10 Cyc/Ole)	[b,c]
57.10	0.29			aliphatic	10	BR-C10	

Table B-1 (continued)

GC-MS Data			GC-MS Assignments			Model Species Assignments	
Ret Time	Area %	Mol Ion	Compound Identified	Class	Car-bons	Model Species	Comments
							0.05 C9-BEN1
57.35	0.09	120		aromatic	9	(C9 Arom)	0.25 C9-BEN2
							0.70 C9-BEN3 [f]
58.27	1.04	140		alicyclic	10	(C10 Cyc/Ole)	[b,c]
58.67	1.21	142		aliphatic	10	BR-C10	
58.86	0.14	140		alicyclic	10	(C10 Cyc/Ole)	[b,c]
59.28	1.45			aliphatic	10	BR-C10	
59.68	0.17	120		aromatic	9	(C9 Arom)	[f,g]
60.11	0.15			aliphatic	10	BR-C10	
60.43	0.06			alicyclic	10	(C10 Cyc/Ole)	[b,c]
60.94	1.23	142		aliphatic	10	BR-C10	
61.70	0.18	138		alicyclic	10	(C10 Cyc/Ole)	[b,c]
62.10	0.73	140		alicyclic	10	(C10 Cyc/Ole)	[b,c]
62.56	0.29	138,140		alicyclic	10	(C10 Cyc/Ole)	[b,c]
62.81	0.44	140		alicyclic	10	(C10 Cyc/Ole)	[b,c]
63.07	0.20	140		alicyclic	10	(C10 Cyc/Ole)	[b,c]
63.47	0.24	140		alicyclic	10	(C10 Cyc/Ole)	[b,c]
63.83	0.08	12		aromatic	9	(C9 Arom)	[f,g]
64.54	0.69	140		alicyclic	10	(C10 Cyc/Ole)	[b,c]
64.74	0.53	140		alicyclic	10	(C10 Cyc/Ole)	[b,c]
65.25	0.61	140		alicyclic	10	(C10 Cyc/Ole)	[b,c]
65.54	0.27	140		alicyclic	10	(C10 Cyc/Ole)	[b,c]
65.72	0.21			alicyclic	10	(C10 Cyc/Ole)	[b,c]
66.21	0.14			alicyclic	10	(C10 Cyc/Ole)	[b,c]
66.49	0.44			alicyclic	10	(C10 Cyc/Ole)	[b,c]
67.36	0.60	120		aromatic	9	(C9 Arom)	[f,g]
67.65	0.26	140		alicyclic	10	(C10 Cyc/Ole)	[b,c]
68.70	7.11	142	n-Decane	aliphatic	10	N-C10	
							0.950 CYC-C11
69.15	0.50	140		alicyclic	11	(C11 Cyc/Ole)	0.040 C11-OLE1
							0.010 C11-OLE2 [b]
69.77	0.08			alicyclic	11	(C11 Cyc/Ole)	[b,c]
70.31	0.34			alicyclic	11	(C11 Cyc/Ole)	[b,c]
70.67	0.10			alicyclic	11	(C11 Cyc/Ole)	[b,c]
71.03	0.37			alicyclic	11	(C11 Cyc/Ole)	[b,c]
71.51	0.71			alicyclic	11	(C11 Cyc/Ole)	[b,c]
71.94	0.30			aliphatic	11	BR-C11	
72.44	0.41			aliphatic	11	BR-C11	
72.96	0.19			alicyclic	11	(C11 Cyc/Ole)	[b,c]
73.47	0.55	138		alicyclic	11	(C11 Cyc/Ole)	[b,c]
73.77	0.15			alicyclic	11	(C11 Cyc/Ole)	[b,c]
74.48	2.76	156		aliphatic	11	BR-C11	

Table B-1 (continued)

GC-MS Data			GC-MS Assignments			Model Species Assignments	
Ret Time	Area %	Mol Ion	Compound Identified	Class	Car-bons	Model Species	Comments
							0.05 C10-BEN1
75.15	0.66	120		aromatic	10	(C10 Arom)	0.25 C10-BEN2
							0.70 C10-BEN3 [f]
75.65	0.75			alicyclic	11	(C11 Cyc/Ole)	[b,c]
75.90	0.34			alicyclic	11	(C11 Cyc/Ole)	[b,c]
76.69	0.53	154		alicyclic	11	(C11 Cyc/Ole)	[b,c]
77.46	1.38	140		alicyclic	11	(C11 Cyc/Ole)	[b,c]
77.78	0.24	154		alicyclic	11	(C11 Cyc/Ole)	[b,c]
78.00	0.15			alicyclic	11	(C11 Cyc/Ole)	[b,c]
78.29	0.52			alicyclic	11	(C11 Cyc/Ole)	[b,c]
78.75	0.89			aliphatic	11	BR-C11	
79.05	0.15			alicyclic	11	(C11 Cyc/Ole)	[b,c]
79.41	0.37	154		alicyclic	11	(C11 Cyc/Ole)	[b,c]
79.76	0.28	138,154		alicyclic	11	(C11 Cyc/Ole)	[b,c]
79.98	0.23	138		alicyclic	11	(C11 Cyc/Ole)	[b,c]
80.44	0.24			alicyclic	11	(C11 Cyc/Ole)	[b,c]
81.07	0.76	154		alicyclic	11	(C11 Cyc/Ole)	[b,c]
81.43	0.25			alicyclic	11	(C11 Cyc/Ole)	[b,c]
82.19	0.62			aliphatic	11	BR-C11	
82.73	0.60	134		aromatic	10	(C10 Arom)	[f,g]
83.09	0.19	154		alicyclic	11	(C11 Cyc/Ole)	[b,c]
83.75	0.99	156		aliphatic	11	BR-C11	
84.42	1.15	138		alicyclic	11	(C11 Cyc/Ole)	[b,c]
84.64	0.97	156		aliphatic	11	BR-C11	
84.97	0.31	138		alicyclic	11	(C11 Cyc/Ole)	[b,c]
85.68	1.32			aliphatic	11	BR-C11	
86.27	0.72	152,154		alicyclic	11	(C11 Cyc/Ole)	[b,c]
86.83	0.31			alicyclic	11	(C11 Cyc/Ole)	[b,c]
87.55	1.27	156		aliphatic	11	BR-C11	
87.90	0.18	154		alicyclic	11	(C11 Cyc/Ole)	[b,c]
88.36	0.36			alicyclic	11	(C11 Cyc/Ole)	[b,c]
88.80	0.12			alicyclic	11	(C11 Cyc/Ole)	[b,c]
89.03	0.14			alicyclic	11	(C11 Cyc/Ole)	[b,c]
89.28	0.13	152		alicyclic	11	(C11 Cyc/Ole)	[b,c]
89.60	0.49	154		alicyclic	11	(C11 Cyc/Ole)	[b,c]
90.03	0.71	154		alicyclic	11	(C11 Cyc/Ole)	[b,c]
90.44	0.16	134		aromatic	10	(C10 Arom)	[f,g]
90.76	0.28	152,154		alicyclic	11	(C11 Cyc/Ole)	[b,c]
91.09	0.46			alicyclic	11	(C11 Cyc/Ole)	[b,c]
91.68	0.84	154		alicyclic	11	(C11 Cyc/Ole)	[b,c]
92.10	0.34	134		aromatic	10	(C10 Arom)	[f,g]
92.64	0.97	154		alicyclic	11	(C11 Cyc/Ole)	[b,c]

Table B-1 (continued)

GC-MS Data			GC-MS Assignments			Model Species Assignments	
Ret Time	Area %	Mol Ion	Compound Identified	Class	Car-bons	Model Species	Comments
93.11	0.42	154		alicyclic	11	(C11 Cyc/Ole)	[b,c]
93.42	0.60	152		alicyclic	11	(C11 Cyc/Ole)	[b,c]
94.05	0.27	154		alicyclic	11	(C11 Cyc/Ole)	[b,c]
94.57	0.41			alicyclic	11	(C11 Cyc/Ole)	[b,c]
95.51	8.29	156	n-Undecane	aliphatic	11	N-C11	
							0.950 CYC-C12
96.02	0.40	138		alicyclic	12	(C12 Cyc/Old)	0.040 C12-OLE1
							0.010 C12-OLE2 [b]
96.36	0.11	152		alicyclic	12	(C12 Cyc/Old)	[b,c]
96.59	0.39			aliphatic	12	BR-C12	
96.94	0.35			aliphatic	12	BR-C12	
97.43	0.56			alicyclic	12	(C12 Cyc/Old)	[b,c]
97.84	0.16			aliphatic	12	BR-C12	
98.01	0.12			alicyclic	12	(C12 Cyc/Old)	[b,c]
98.19	0.17			alicyclic	12	(C12 Cyc/Old)	[b,c]
98.67	1.16	152		alicyclic	12	(C12 Cyc/Old)	[b,c]
99.02	0.79			aliphatic	12	BR-C12	
							0.05 C11-BEN1
99.41	0.50	134		aromatic	11	(C11 Arom)	0.25 C11-BEN2
							0.70 C11-BEN3 [f]
99.91	0.34			alicyclic	12	(C12 Cyc/Old)	[b,c]
100.22	0.67			aliphatic	12	BR-C12	
101.09	1.09	170		aliphatic	12	BR-C12	
101.44	0.15			aliphatic	12	BR-C12	
101.77	0.38	168		alicyclic	12	(C12 Cyc/Old)	[b,c]
102.13	0.80	152		alicyclic	12	(C12 Cyc/Old)	[b,c]
102.36	0.35			alicyclic	12	(C12 Cyc/Old)	[b,c]
103.07	0.86	154		alicyclic	12	(C12 Cyc/Old)	[b,c]
103.70	0.78	152,154		alicyclic	12	(C12 Cyc/Old)	[b,c]
103.92	0.32			alicyclic	12	(C12 Cyc/Old)	[b,c]
104.42	0.46			alicyclic	12	(C12 Cyc/Old)	[b,c]
104.77	0.31			alicyclic	12	(C12 Cyc/Old)	[b,c]
105.03	0.13	148		aromatic	11	(C11 Arom)	[f,g]
105.42	0.31			aliphatic	12	BR-C12	
105.60	0.23			alicyclic	12	(C12 Cyc/Old)	[b,c]
105.85	0.13			alicyclic	12	(C12 Cyc/Old)	[b,c]
106.29	0.77	170		aliphatic	12	BR-C12	
106.52	0.70			aliphatic	12	BR-C12	
106.80	0.49	134		aromatic	11	(C11 Arom)	[f,g]
107.25	0.63			aliphatic	12	BR-C12	
107.47	0.31	152,168		alicyclic	12	(C12 Cyc/Old)	[b,c]
108.04	0.96			aliphatic	12	BR-C12	

Table B-1 (continued)

GC-MS Data			GC-MS Assignments			Model Species Assignments	
Ret Time	Area %	Mol Ion	Compound Identified	Class	Car-bons	Model Species	Comments
108.42	0.36			alicyclic	12	(C12 Cyc/Old)	[b,c]
108.75	0.33	132		aromatic	11	(C11 Arom)	[f,g]
108.94	0.14	148		aromatic	11	(C11 Arom)	[f,g]
109.22	0.67			aliphatic	12	BR-C12	
109.70	0.44			alicyclic	12	(C12 Cyc/Old)	[b,c]
110.11	0.30			alicyclic	12	(C12 Cyc/Old)	[b,c]
110.44	0.10			alicyclic	12	(C12 Cyc/Old)	[b,c]
110.60	0.14	148		aromatic	11	(C11 Arom)	[f,g]
110.79	0.16			aliphatic	12	BR-C12	
111.34	0.13			alicyclic	12	(C12 Cyc/Old)	[b,c]
111.60	0.21	168		alicyclic	12	(C12 Cyc/Old)	[b,c]
111.89	0.47	166		aliphatic	12	BR-C12	
112.33	0.61	168	Naphthalen	alicyclic	12	(C12 Cyc/Old)	[b,c]
112.71	0.19			aromatic	10	NAPHTHAL	
112.95	0.22	146		aromatic	11	(C11 Arom)	[f,g]
113.13	0.25	168		alicyclic	12	(C12 Cyc/Old)	[b,c]
113.35	0.14	146		aromatic	11	(C11 Arom)	[f,g]
113.55	0.21	166		alicyclic	12	(C12 Cyc/Old)	[b,c]
114.26	3.15	170	n-Dodecane	aliphatic	12	N-C12	
114.50	0.21	160		aromatic	12	(C12 Arom)	0.05 C12-BEN1 0.25 C12-BEN2 0.70 C12-BEN3 [f]
114.82	0.35	146		aromatic	12	(C12 Arom)	[f,g]
115.30	0.22	166		alicyclic	13	(C13 Cyc/Ole)	0.950 CYC-C13 0.040 C13-OLE1 0.010 C13-OLE2 [b]
115.72	0.13			alicyclic	13	(C13 Cyc/Ole)	[b,c]
116.32	1.30	184		aliphatic	13	BR-C13	
116.83	0.10			aliphatic	13	BR-C13	
117.19	0.16			alicyclic	13	(C13 Cyc/Ole)	[b,c]
117.47	0.15			aliphatic	13	BR-C13	
117.66	0.07			aliphatic	13	BR-C13	
117.88	0.06	148,160		aromatic	12	(C12 Arom)	[f,g]
118.21	0.09			alicyclic	13	(C13 Cyc/Ole)	[b,c]
118.53	0.20	182		alicyclic	13	(C13 Cyc/Ole)	[b,c]
119.26	0.10	166		alicyclic	13	(C13 Cyc/Ole)	[b,c]
119.97	0.07			alicyclic	13	(C13 Cyc/Ole)	[b,c]
120.36	0.10			alicyclic	13	(C13 Cyc/Ole)	[b,c]
120.52	0.13			alicyclic	13	(C13 Cyc/Ole)	[b,c]
120.82	0.17			alicyclic	13	(C13 Cyc/Ole)	[b,c]
121.80	0.13			aliphatic	13	BR-C13	
122.08	0.09			aliphatic	13	BR-C13	

Table B-1 (continued)

GC-MS Data			GC-MS Assignments			Model Species Assignments	
Ret Time	Area %	Mol Ion	Compound Identified	Class	Car-bons	Model Species	Comments
122.72	0.09			aliphatic	13	BR-C13	
123.35	0.09			aliphatic	13	BR-C13	
124.29	0.07			aliphatic	13	BR-C13	
124.60	0.17			aliphatic	13	BR-C13	
124.95	0.02	146		aromatic	12	(C12 Arom)	[f,g]
128.08	0.23	184	n-Tridecane	aliphatic	13	N-C13	
128.99	0.02	142		aromatic	13	(C13 Arom)	0.05 C13-BEN1 0.25 C13-BEN2 0.70 C13-BEN3 [f]
137.10	0.01			aliphatic	14	BR-C14	
139.54	0.05			aliphatic	14	BR-C14	
146.83	0.02			aliphatic	14	BR-C14	
149.52	0.02			aliphatic	14	BR-C14	

[a] Contribution of the low level of this low reactivity compound is assumed to be negligible.

[b] GC-MS cannot distinguish between cycloalkenes and olefins. Assumed to be 95% cycloalkane and 5% olefin model species, based on FIA type analysis data. Alkenes assumed to be 80% terminal and 20% internal based on information provided by Safety-Kleen (O'Donnell, private communication, 1997) that these are primary alkenes.

[c] See assumed distribution for cycloalkane/olefin with same carbon number, above.

[d] Xylene isomers assumed based on relative retention times.

[e] Meta and para isomers do not separate on most GC's. Assume equal amounts of each.

[f] Assume ~5% monosubstitued, ~25% disubstituted, and ~70% tri- or polysubstibuted benzenes based on analyses of a different mineral spirits cample carried out by Safety-Kleen (O'Donnell, private communication, 1997), which indicated a predominance of

[g] See assumed distribution assumed for the aromatic isomer with the same carbon number

Table B-2. Results of Safety-Kleen GC-MS analysis of Mixture "B", and detailed model species assignments used for ozone impact modeling.

GC-MS Data			GC-MS Assignments			Model Species Assignments	
Ret Time	Area %	Mol Ion	Compound Identified	Class	Car-bons	Model Species	Comments
32.86	0.02	126		alicyclic	10	CYC-C10	
36.32	0.03	126		alicyclic	10	CYC-C10	
41.46	0.07	126		alicyclic	10	CYC-C10	
41.99	0.02	126		alicyclic	10	CYC-C10	
42.91	0.04	126		alicyclic	10	CYC-C10	
46.35	0.03	126		alicyclic	10	CYC-C10	
46.72	0.04	126		alicyclic	10	CYC-C10	
46.90	0.04	126		alicyclic	10	CYC-C10	
51.95	0.17			aliphatic	10	BR-C10	
53.92	0.13	140		alicyclic	10	CYC-C10	
56.07	0.06	140		alicyclic	10	CYC-C10	
56.85	0.08			alicyclic	10	CYC-C10	
57.17	0.10	140		alicyclic	10	CYC-C10	
58.16	0.11			alicyclic	10	CYC-C10	
58.50	0.16	140		alicyclic	10	CYC-C10	
58.80	0.07	140		alicyclic	10	CYC-C10	
59.13	0.22	140		alicyclic	10	CYC-C10	
60.81	0.18			aliphatic	10	BR-C10	
62.02	0.11	140		alicyclic	10	CYC-C10	
62.50	0.10	140		alicyclic	10	CYC-C10	
62.72	0.11	140		alicyclic	10	CYC-C10	
63.40	0.05	140		alicyclic	10	CYC-C10	
63.62	0.08	140		alicyclic	10	CYC-C10	
64.45	0.24	140		alicyclic	10	CYC-C10	
64.66	0.08	140		alicyclic	10	CYC-C10	
65.17	0.16	140		alicyclic	10	CYC-C10	
65.47	0.08			alicyclic	10	CYC-C10	
65.98	0.12	140		alicyclic	10	CYC-C10	
66.46	0.07			alicyclic	10	CYC-C10	
66.94	0.06	140		alicyclic	10	CYC-C10	
67.59	0.11	140		alicyclic	10	CYC-C10	
67.96	0.13	140		alicyclic	10	CYC-C10	
68.30	0.00		n-Decane	aliphatic	10	N-C10	
68.39	0.04			alicyclic	11	CYC-C11	
68.95	0.13	140		alicyclic	11	CYC-C11	
70.11	0.08	140		alicyclic	11	CYC-C11	
70.45	0.06	140		alicyclic	11	CYC-C11	
70.87	0.12	140		alicyclic	11	CYC-C11	
71.40	0.11			alicyclic	11	CYC-C11	
71.68	0.05			aliphatic	11	BR-C11	
71.89	0.10			aliphatic	11	BR-C11	
72.36	0.10			aliphatic	11	BR-C11	
72.90	0.06			alicyclic	11	CYC-C11	
73.37	0.25	138		alicyclic	11	CYC-C11	

Table B-2 (continued)

GC-MS Data			GC-MS Assignments			Model Species Assignments	
Ret Time	Area %	Mol Ion	Compound Identified	Class	Car-bons	Model Species	Comments
74.21	0.59	156		aliphatic	11	BR-C11	
74.46	0.11	140		alicyclic	11	CYC-C11	
74.88	0.14			alicyclic	11	CYC-C11	
75.54	0.26			aliphatic	11	BR-C11	
75.81	0.10			aliphatic	11	BR-C11	
76.59	0.08			alicyclic	11	CYC-C11	
77.35	0.63	140		alicyclic	11	CYC-C11	
77.71	0.20	154		alicyclic	11	CYC-C11	
78.20	0.19			alicyclic	11	CYC-C11	
78.63	0.35	154		alicyclic	11	CYC-C11	
79.30	0.09			alicyclic	11	CYC-C11	
79.69	0.14	154		alicyclic	11	CYC-C11	
79.88	0.07			alicyclic	11	CYC-C11	
80.35	0.06			alicyclic	11	CYC-C11	
80.97	0.32	154		alicyclic	11	CYC-C11	
81.39	0.12			alicyclic	11	CYC-C11	
82.11	0.29			aliphatic	11	BR-C11	
82.69	0.20			alicyclic	11	CYC-C11	
83.02	0.14	154		alicyclic	11	CYC-C11	
83.68	0.52	156		aliphatic	11	BR-C11	
84.37	0.91	138		alicyclic	11	CYC-C11	
84.57	0.44	156		aliphatic	11	BR-C11	
84.94	0.16	138		alicyclic	11	CYC-C11	
85.62	0.87			aliphatic	11	BR-C11	
86.19	0.40	154		alicyclic	11	CYC-C11	
86.78	0.13			alicyclic	11	CYC-C11	
87.50	0.85			aliphatic	11	BR-C11	
87.88	0.16	154		alicyclic	11	CYC-C11	
88.27	0.22			alicyclic	11	CYC-C11	
88.76	0.08			alicyclic	11	CYC-C11	
89.03	0.09	154		alicyclic	11	CYC-C11	
89.57	0.33	154		alicyclic	11	CYC-C11	
90.00	0.37	154		alicyclic	11	CYC-C11	
90.72	0.15	154		alicyclic	11	CYC-C11	
91.04	0.21	154		alicyclic	11	CYC-C11	
91.63	0.70	154		alicyclic	11	CYC-C11	
92.07	0.17	154		alicyclic	11	CYC-C11	
92.55	0.56	154		alicyclic	11	CYC-C11	
93.10	0.35	154		alicyclic	11	CYC-C11	
93.43	0.16			alicyclic	11	CYC-C11	
93.57	0.18	152		alicyclic	11	CYC-C11	
94.05	0.24	154		alicyclic	11	CYC-C11	
94.58	0.35	154		alicyclic	11	CYC-C11	
94.99	0.84	154		alicyclic	11	CYC-C11	
95.49	0.52	154		alicyclic	11	CYC-C11	
95.80	0.00		n-Undecane	aliphatic	11	N-C11	
96.03	0.48	138		alicyclic	12	CYC-C12	

Table B-2 (continued)

GC-MS Data			GC-MS Assignments			Model Species Assignments	
Ret Time	Area %	Mol Ion	Compound Identified	Class	Car-bons	Model Species	Comments
96.52	0.49	150		alicyclic	12	CYC-C12	
96.86	0.34			aliphatic	12	BR-C12	
97.41	0.28	152		alicyclic	12	CYC-C12	
97.84	0.23			aliphatic	12	BR-C12	
98.59	1.46	152		alicyclic	12	CYC-C12	
98.75	0.24			aliphatic	12	BR-C12	
99.02	0.60			aliphatic	12	BR-C12	
99.40	0.16	154		alicyclic	12	CYC-C12	
99.65	0.34	164		alicyclic	12	CYC-C12	
100.20	0.74			alicyclic	12	CYC-C12	
101.10	0.99	170		aliphatic	12	BR-C12	
101.49	0.15			aliphatic	12	BR-C12	
101.78	0.30	168		alicyclic	12	CYC-C12	
102.15	1.06	152		alicyclic	12	CYC-C12	
102.41	0.38			alicyclic	12	CYC-C12	
103.12	1.23	154		alicyclic	12	CYC-C12	
103.71	1.12	152,168		alicyclic	12	CYC-C12	
104.47	0.49	152,168		alicyclic	12	CYC-C12	
104.84	0.48	168		alicyclic	12	CYC-C12	
105.48	0.35			aliphatic	12	BR-C12	
105.66	0.38	168		alicyclic	12	CYC-C12	
105.90	0.28	168		alicyclic	12	CYC-C12	
106.38	0.98	170		aliphatic	12	BR-C12	
106.65	1.46	170		aliphatic	12	BR-C12	
106.98	0.31	166,168		alicyclic	12	CYC-C12	
107.39	2.00	170		aliphatic	12	BR-C12	
108.21	1.86	170		aliphatic	12	BR-C12	
108.50	0.72	152,166		alicyclic	12	CYC-C12	
108.84	0.25	168		alicyclic	12	CYC-C12	
109.40	1.82	170		aliphatic	12	BR-C12	
109.55	0.34	166		alicyclic	12	CYC-C12	
109.80	0.60	150,168		alicyclic	12	CYC-C12	
110.20	0.58	166,168		alicyclic	12	CYC-C12	
110.53	0.33	166,168		alicyclic	12	CYC-C12	
110.91	0.64	152		alicyclic	12	CYC-C12	
111.18	0.17			alicyclic	12	CYC-C12	
111.57	0.87	#########		alicyclic	12	CYC-C12	
112.00	0.82	166		alicyclic	12	CYC-C12	
112.13	0.47			alicyclic	12	CYC-C12	
112.44	1.41	168		alicyclic	12	CYC-C12	
113.03	0.54	166		alicyclic	12	CYC-C12	
113.25	0.79	168		alicyclic	12	CYC-C12	
113.65	0.64	166		alicyclic	12	CYC-C12	
113.82	0.18			aliphatic	12	BR-C12	
113.97	0.14			alicyclic	12	CYC-C12	
114.23	1.48	170	n-Dodecane	aliphatic	12	N-C12	
114.50	0.43			alicyclic	13	CYC-C13	

Table B-2 (continued)

GC-MS Data			GC-MS Assignments			Model Species Assignments	
Ret Time	Area %	Mol Ion	Compound Identified	Class	Car-bons	Model Species	Comments
114.65	0.30			alicyclic	13	CYC-C13	
114.92	0.83			alicyclic	13	CYC-C13	
115.39	0.71	166		alicyclic	13	CYC-C13	
115.81	0.90	168		alicyclic	13	CYC-C13	
116.52	3.57	184		aliphatic	13	BR-C13	
116.96	0.53			aliphatic	13	BR-C13	
117.14	0.29			aliphatic	13	BR-C13	
117.32	0.44	166		alicyclic	13	CYC-C13	
117.62	1.17	170		aliphatic	13	BR-C13	
118.35	0.71			alicyclic	13	CYC-C13	
118.65	0.87	182		alicyclic	13	CYC-C13	
118.96	0.31	166		alicyclic	13	CYC-C13	
119.14	0.30			alicyclic	13	CYC-C13	
119.39	0.85	166		alicyclic	13	CYC-C13	
119.64	0.31	166		alicyclic	13	CYC-C13	
120.09	0.59			alicyclic	13	CYC-C13	
120.46	0.65	180,182		alicyclic	13	CYC-C13	
120.69	1.02			alicyclic	13	CYC-C13	
120.96	0.88			alicyclic	13	CYC-C13	
121.34	0.45			aliphatic	13	BR-C13	
121.96	1.45	184		aliphatic	13	BR-C13	
122.25	1.31	184		aliphatic	13	BR-C13	
122.58	0.36			aliphatic	13	BR-C13	
122.91	1.35	184		aliphatic	13	BR-C13	
123.10	0.37	180,182		alicyclic	13	CYC-C13	
123.57	1.75	184		aliphatic	13	BR-C13	
123.79	0.42	182		alicyclic	13	CYC-C13	
123.98	0.35	180		alicyclic	13	CYC-C13	
124.48	1.69	184		aliphatic	13	BR-C13	
124.84	2.43	198		aliphatic	13	BR-C13	
125.10	0.58			aliphatic	13	BR-C13	
125.41	0.28			aliphatic	13	BR-C13	
125.62	0.46			aliphatic	13	BR-C13	
126.10	0.34	180,182		alicyclic	13	CYC-C13	
126.32	0.20	180		alicyclic	13	CYC-C13	
126.61	0.48			alicyclic	13	CYC-C13	
126.89	0.36			alicyclic	13	CYC-C13	
127.28	0.49			alicyclic	13	CYC-C13	
127.47	0.50			alicyclic	13	CYC-C13	
127.93	0.76			alicyclic	13	CYC-C13	
128.23	1.40	184	n-Tridecane	aliphatic	13	N-C13	
128.46	0.34			alicyclic	14	CYC-C14	
128.70	0.35			alicyclic	14	CYC-C14	
128.90	0.51			alicyclic	14	CYC-C14	
129.25	0.29			aliphatic	14	BR-C14	
129.58	0.85			aliphatic	14	BR-C14	
129.91	0.34			aliphatic	14	BR-C14	

Table B-2 (continued)

GC-MS Data			GC-MS Assignments			Model Species Assignments	
Ret Time	Area %	Mol Ion	Compound Identified	Class	Car-bons	Model Species	Comments
130.21	0.39			aliphatic	14	BR-C14	
130.44	0.93			aliphatic	14	BR-C14	
130.85	0.29			aliphatic	14	BR-C14	
131.05	0.32			alicyclic	14	CYC-C14	
131.46	0.29			alicyclic	14	CYC-C14	
131.63	0.25			alicyclic	14	CYC-C14	
131.89	0.17			alicyclic	14	CYC-C14	
132.05	0.16			alicyclic	14	CYC-C14	
132.31	0.26			aliphatic	14	BR-C14	
132.48	0.28			aliphatic	14	BR-C14	
132.75	0.13	180		alicyclic	14	CYC-C14	
132.92	0.21	180		aliphatic	14	BR-C14	
133.13	0.23			alicyclic	14	CYC-C14	
133.82	0.21			alicyclic	14	CYC-C14	
134.09	1.17	182		alicyclic	14	CYC-C14	
134.53	0.52			aliphatic	14	BR-C14	
135.10	0.73			aliphatic	14	BR-C14	
135.67	0.75			aliphatic	14	BR-C14	
135.91	0.19			aliphatic	14	BR-C14	
136.25	0.11			alicyclic	14	CYC-C14	
136.48	0.74			aliphatic	14	BR-C14	
136.88	0.11			alicyclic	14	CYC-C14	
137.19	0.93			aliphatic	14	BR-C14	
137.87	0.22			alicyclic	14	CYC-C14	
138.64	0.21			alicyclic	14	CYC-C14	
138.84	0.11			alicyclic	14	CYC-C14	
139.22	0.16			alicyclic	14	CYC-C14	
139.68	1.71	198	n-Tetradecane	aliphatic	14	N-C14	
140.06	0.26			aliphatic	15	BR-C15	
140.28	0.27			alicyclic	15	CYC-C15	
140.60	0.12			aliphatic	15	BR-C15	
140.79	0.14			alicyclic	15	CYC-C15	
141.27	0.19			aliphatic	15	BR-C15	
143.52	0.08			alicyclic	15	CYC-C15	
144.49	0.10			aliphatic	15	BR-C15	
144.66	0.06			aliphatic	15	BR-C15	
144.97	0.06			aliphatic	15	BR-C15	
145.25	0.10			alicyclic	15	CYC-C15	
145.53	0.06			aliphatic	15	BR-C15	
145.94	0.21			aliphatic	15	BR-C15	
146.77	0.05			aliphatic	15	BR-C15	
149.53	0.22			aliphatic	15	BR-C15	

Table B-3. Results of Safety-Kleen GC-MS analysis of Mixture "C", and detailed model species assignments used for ozone impact modeling.

GC-MS Data			GC-MS Assignments			Model Species Assignmen	
Ret Time	Area %	Mol Ion	Compound Identified	Class	Car-bons	Model Species	Comments
57.14	0.10	140		alicyclic	11	CYC-C11	
62.64	0.14	140		alicyclic	11	CYC-C11	
63.36	0.29	140		alicyclic	11	CYC-C11	
70.85	0.12	140		alicyclic	11	CYC-C11	
74.07	0.15			aliphatic	11	BR-C11	
77.25	0.21	140		alicyclic	11	CYC-C11	
77.66	0.18	154		alicyclic	11	CYC-C11	
78.59	0.28	154		alicyclic	11	CYC-C11	
81.04	0.52	154		alicyclic	11	CYC-C11	
82.07	0.28			alicyclic	11	CYC-C11	
82.71	0.39	154		alicyclic	11	CYC-C11	
83.64	0.41			aliphatic	11	BR-C11	
84.35	1.82	138		alicyclic	11	CYC-C11	
85.58	0.92			aliphatic	11	BR-C11	
86.17	0.62	152,154		alicyclic	11	CYC-C11	
86.79	0.24	152,154		alicyclic	11	CYC-C11	
87.49	0.90			aliphatic	11	BR-C11	
87.86	0.23	154		alicyclic	11	CYC-C11	
88.31	0.37			alicyclic	11	CYC-C11	
89.59	0.69	154		alicyclic	11	CYC-C11	
90.02	0.67	154		alicyclic	11	CYC-C11	
90.74	0.30	154		alicyclic	11	CYC-C11	
91.08	0.35	154		alicyclic	11	CYC-C11	
91.71	1.24	154		alicyclic	11	CYC-C11	
92.12	0.25	154,168		alicyclic	11	CYC-C11	
92.60	1.00	154		alicyclic	11	CYC-C11	
93.15	0.67	154		alicyclic	11	CYC-C11	
93.49	0.55	152		alicyclic	11	CYC-C11	
94.07	0.39	154		alicyclic	11	CYC-C11	
94.63	0.64	154		alicyclic	11	CYC-C11	
95.73	11.71	156	n-Undecane	aliphatic	11	N-C11	
96.08	0.78	138		alicyclic	12	CYC-C12	
96.49	0.28	152		alicyclic	12	CYC-C12	
96.70	0.33			alicyclic	12	CYC-C12	
97.06	0.49			alicyclic	12	CYC-C12	
97.50	0.62			alicyclic	12	CYC-C12	
97.93	0.32			aliphatic	12	BR-C12	
98.29	0.43	154		alicyclic	12	CYC-C12	
98.83	2.09	152		alicyclic	12	CYC-C12	
99.16	1.18	170		aliphatic	12	BR-C12	
99.55	0.37	154		alicyclic	12	CYC-C12	
99.87	0.34			alicyclic	12	CYC-C12	
100.29	1.15			alicyclic	12	CYC-C12	
101.25	2.12			aliphatic	12	BR-C12	

Table B-3 (continued)

GC-MS Data			GC-MS Assignments			Model Species Assignmen	
Ret Time	Area %	Mol Ion	Compound Identified	Class	Car-bons	Model Species	Comments
101.59	0.20			aliphatic	12	BR-C12	
101.90	0.65	168		alicyclic	12	CYC-C12	
102.28	1.55	152		alicyclic	12	CYC-C12	
102.51	0.60			alicyclic	12	CYC-C12	
103.25	2.21	154		alicyclic	12	CYC-C12	
103.85	1.54	154		alicyclic	12	CYC-C12	
104.03	0.36	166,168		alicyclic	12	CYC-C12	
104.55	0.95	168		alicyclic	12	CYC-C12	
104.92	0.82	168		alicyclic	12	CYC-C12	
105.55	0.58	168		alicyclic	12	CYC-C12	
105.72	0.61	168		alicyclic	12	CYC-C12	
105.97	0.49	168		alicyclic	12	CYC-C12	
106.48	1.93	170		aliphatic	12	BR-C12	
106.73	1.51	170		aliphatic	12	BR-C12	
107.05	0.53	168		alicyclic	12	CYC-C12	
107.45	1.84			alicyclic	12	CYC-C12	
107.62	0.84	152,168		alicyclic	12	CYC-C12	
108.30	2.69	170		aliphatic	12	BR-C12	
108.58	0.93			aliphatic	12	BR-C12	
108.89	0.42	168		alicyclic	12	CYC-C12	
109.46	2.42	170		aliphatic	12	BR-C12	
109.63	0.34	166		alicyclic	12	CYC-C12	
109.87	0.70	150168		alicyclic	12	CYC-C12	
110.27	1.01	166,168		alicyclic	12	CYC-C12	
110.59	0.46	166,168		alicyclic	12	CYC-C12	
110.95	0.60	152		alicyclic	12	CYC-C12	
111.50	0.38			alicyclic	12	CYC-C12	
111.68	0.96	152,168		alicyclic	12	CYC-C12	
112.07	0.95	166		alicyclic	12	CYC-C12	
112.19	0.73	168		alicyclic	12	CYC-C12	
112.50	1.86	168		alicyclic	12	CYC-C12	
113.09	0.54	166		alicyclic	12	CYC-C12	
113.30	1.04	168		alicyclic	12	CYC-C12	
113.71	0.83	152,166		alicyclic	12	CYC-C12	
114.75	13.59	170	n-Dodecane	aliphatic	12	N-C12	
114.85	0.20			aliphatic	13	BR-C13	
115.01	0.94			alicyclic	13	CYC-C13	
115.44	0.36	166		alicyclic	13	CYC-C13	
115.60	0.30	166		alicyclic	13	CYC-C13	
115.94	0.79	168		alicyclic	13	CYC-C13	
116.60	3.95	184		aliphatic	13	BR-C13	
116.79	0.18	166		alicyclic	13	CYC-C13	
117.00	0.34			aliphatic	13	BR-C13	
117.19	0.25			aliphatic	13	BR-C13	
117.38	0.39			aliphatic	13	BR-C13	
117.64	0.50			aliphatic	13	BR-C13	
117.79	0.30	166,168		alicyclic	13	CYC-C13	

Table B-3 (continued)

GC-MS Data			GC-MS Assignments			Model Species Assignmen	
Ret Time	Area %	Mol Ion	Compound Identified	Class	Car-bons	Model Species	Comments
118.37	0.41	166,168		alicyclic	13	CYC-C13	
118.74	0.80	182		alicyclic	13	CYC-C13	
119.10	0.37	166		alicyclic	13	CYC-C13	
119.35	0.18			alicyclic	13	CYC-C13	
119.50	0.25	166		alicyclic	13	CYC-C13	
120.09	0.31			alicyclic	13	CYC-C13	
120.68	0.97			alicyclic	13	CYC-C13	
120.95	0.59			alicyclic	13	CYC-C13	
121.89	0.58			alicyclic	13	CYC-C13	
122.15	0.32			aliphatic	13	BR-C13	
122.80	0.31			aliphatic	13	BR-C13	
123.43	0.32			aliphatic	13	BR-C13	
123.93	0.13			alicyclic	13	CYC-C13	
124.35	0.23			alicyclic	13	CYC-C13	
124.67	0.42			aliphatic	13	BR-C13	
128.14	0.53	184	n-Tridecane	aliphatic	13	N-C13	

Table B-4. Results of Safety-Kleen GC-MS analysis of Mixture "D", and detailed model species assignments used for ozone impact modeling.

GC-MS Data			GC-MS Assignments			Model Species Assignments	
Ret Time	Area %	Mol Ion	Compound Identified	Class	Car-bons	Model Species	Comments
77.64	0.04	154		alicyclic	11	CYC-C11	
78.58	0.06			alicyclic	11	CYC-C11	
79.67	0.09			alicyclic	11	CYC-C11	
80.93	0.58	154		alicyclic	11	CYC-C11	
81.90	0.25	154		alicyclic	11	CYC-C11	
82.73	0.16	154		alicyclic	11	CYC-C11	
82.98	0.17	154		alicyclic	11	CYC-C11	
83.66	0.29			aliphatic	11	BR-C11	
84.33	1.16	138		alicyclic	11	CYC-C11	
84.57	0.62			aliphatic	11	BR-C11	
85.62	0.95			aliphatic	11	BR-C11	
86.23	0.68	152,154		alicyclic	11	CYC-C11	
86.81	0.44			alicyclic	11	CYC-C11	
87.57	1.48			aliphatic	11	BR-C11	
88.40	0.46			alicyclic	11	CYC-C11	
89.11	0.44	154		alicyclic	11	CYC-C11	
89.66	0.93	154		alicyclic	11	CYC-C11	
90.10	1.11	154		alicyclic	11	CYC-C11	
90.82	0.50	154		alicyclic	11	CYC-C11	
91.15	0.54	152,154		alicyclic	11	CYC-C11	
91.79	1.43	154		alicyclic	11	CYC-C11	
92.19	0.32			alicyclic	11	CYC-C11	
92.69	1.49	154		alicyclic	11	CYC-C11	
93.24	0.99	154		alicyclic	11	CYC-C11	
93.56	0.87	152,154		alicyclic	11	CYC-C11	
94.16	0.68	154		alicyclic	11	CYC-C11	
95.83	14.33	156	n-Undecane	aliphatic	11	N-C11	
96.06	0.84	138,154		alicyclic	12	CYC-C12	
96.59	0.59	150,152		alicyclic	12	CYC-C12	
96.81	0.58			aliphatic	12	BR-C12	
97.16	0.82			aliphatic	12	BR-C12	
97.56	0.93	152		alicyclic	12	CYC-C12	
98.03	0.54			aliphatic	12	BR-C12	
98.39	0.64	154		alicyclic	12	CYC-C12	
98.92	2.52	152		alicyclic	12	CYC-C12	
99.27	1.73	170		aliphatic	12	BR-C12	
99.47	0.30	166		alicyclic	12	CYC-C12	
99.64	0.55	154,168		alicyclic	12	CYC-C12	
99.96	0.41	164		alicyclic	12	CYC-C12	
100.13	0.33			alicyclic	12	CYC-C12	
100.39	1.40			aliphatic	12	BR-C12	
101.34	2.71			aliphatic	12	BR-C12	
101.62	0.32			aliphatic	12	BR-C12	
101.98	0.84	166,168		alicyclic	12	CYC-C12	

Table B-4 (continued)

GC-MS Data			GC-MS Assignments			Model Species Assignments	
Ret Time	Area %	Mol Ion	Compound Identified	Class	Car-bons	Model Species	Comments
102.34	1.59	152		alicyclic	12	CYC-C12	
102.56	0.77	152		aliphatic	12	BR-C12	
103.30	2.17	154		alicyclic	12	CYC-C12	
103.87	2.21			alicyclic	12	CYC-C12	
104.59	1.08	168		alicyclic	12	CYC-C12	
104.96	0.94	168		alicyclic	12	CYC-C12	
105.58	0.65	168		alicyclic	12	CYC-C12	
105.76	0.60	168		alicyclic	12	CYC-C12	
105.99	0.49	168		alicyclic	12	CYC-C12	
106.51	2.01	170		aliphatic	12	BR-C12	
106.77	1.68	170		aliphatic	12	BR-C12	
107.09	0.54	168		alicyclic	12	CYC-C12	
107.47	1.89			aliphatic	12	BR-C12	
107.64	0.61	168		alicyclic	12	CYC-C12	
108.29	2.50	170		aliphatic	12	BR-C12	
108.60	0.92			aliphatic	12	BR-C12	
108.93	0.53	168		alicyclic	12	CYC-C12	
109.46	2.28	170		aliphatic	12	BR-C12	
109.88	1.00	150,168		alicyclic	12	CYC-C12	
110.26	0.90			aliphatic	12	BR-C12	
110.61	0.42	166		alicyclic	12	CYC-C12	
110.95	0.55			alicyclic	12	CYC-C12	
111.22	0.26			alicyclic	12	CYC-C12	
111.49	0.43	168,182		alicyclic	12	CYC-C12	
111.74	0.68	168		alicyclic	12	CYC-C12	
112.05	0.67	166		alicyclic	12	CYC-C12	
112.17	0.58	168		alicyclic	12	CYC-C12	
112.48	1.26	168		alicyclic	12	CYC-C12	
113.06	0.64	166		alicyclic	12	CYC-C12	
113.28	0.77	168		alicyclic	12	CYC-C12	
113.72	0.70	152,166		alicyclic	12	CYC-C12	
114.62	9.50	170	n-Dodecane	aliphatic	12	N-C12	
114.97	0.64			alicyclic	13	CYC-C13	
115.19	0.19	152,166		alicyclic	13	CYC-C13	
115.53	0.50	166		alicyclic	13	CYC-C13	
115.90	0.67	168		alicyclic	13	CYC-C13	
116.54	3.14	184		aliphatic	13	BR-C13	
116.97	0.29			aliphatic	13	BR-C13	
117.15	0.22			aliphatic	13	BR-C13	
117.34	0.29			aliphatic	13	BR-C13	
117.61	0.44			aliphatic	13	BR-C13	
117.76	0.21	166		alicyclic	13	CYC-C13	
118.33	0.30			alicyclic	13	CYC-C13	
118.69	0.56	182		alicyclic	13	CYC-C13	
119.07	0.25	166		alicyclic	13	CYC-C13	
119.33	0.16			alicyclic	13	CYC-C13	
119.46	0.26	166		alicyclic	13	CYC-C13	

Table B-4 (continued)

GC-MS Data			GC-MS Assignments			Model Species Assignments	
Ret Time	Area %	Mol Ion	Compound Identified	Class	Car-bons	Model Species	Comments
120.07	0.15			alicyclic	13	CYC-C13	
120.63	0.57	168		alicyclic	13	CYC-C13	
120.92	0.36	168		alicyclic	13	CYC-C13	
121.87	0.37			alicyclic	13	CYC-C13	
122.14	0.29			aliphatic	13	BR-C13	
122.79	0.23			aliphatic	13	BR-C13	
123.42	0.20			aliphatic	13	BR-C13	
123.70	0.05			alicyclic	13	CYC-C13	
123.92	0.07			alicyclic	13	CYC-C13	
124.35	0.17			aliphatic	13	BR-C13	
124.65	0.26			aliphatic	13	BR-C13	
128.11	0.21	184	n-Tridecane	aliphatic	13	N-C13	

Table B-5. Results of DRI GC-MS analysis of Mixture "A", and corresponding model species assignments.

Ret Time	Area %	DRI Compound Assignment	Assumed Model Species
11.23	0.06		
11.99	0.01		
12.76	0.12		
13.65	0.07		
14.16	0.03		
14.80	0.12		
15.18	0.15		
15.81	0.02		
16.20	0.01		
16.45	0.36	2-methyl octane	BR-C9
16.83	0.17		
17.09	0.03		
17.47	0.05		
17.73	0.02		
18.11	0.95	2-methyl octene-4	CYC-C9 or C9-0LE
18.74	0.48	methyloctane	BR-C9
19.13	1.13	methyloctane	BR-C9
19.64	0.18		
20.29	2.69	4-octene-3-one	?
21.00	0.89		
21.42	0.63	methyloctene	CYC-C9 or C9-OLE
21.84	0.05		
22.27	2.27		
22.97	3.07	propylcyclohexane	CYC-C9
23.39	1.91	ethylmethylheptane	BR-C10
23.68	0.10		
24.38	1.52		
24.94	6.09	C10H20 Olefin	CYC-C10 or C10-OLE
25.37	3.24	C3-alkylbenzene + C10H22	0.5 C9-BEN 0.5 BR-C10
25.93	2.21	C4 alkyl cyclohexane	CYC-C10
26.49	3.60	C4 alkylcyclohexane	CYC-C10
27.20	10.65	n-Decane	N-C10
27.90	2.62		
28.46	7.91	methyldecane	BR-C11
28.75	1.53	C5 alkylcyclohexane	CYC-C11
29.17	1.04		
29.45	1.36	C5 alkylcyclohexane	CYC-C11
30.87	16.48	decahydronaphthalene	CYC-C10
32.22	6.06	C4 alkylbenzene + ?	C10-BEN
33.11	3.50		
33.79	3.76	Undecanal	?
35.13	2.10		
36.03	1.00		

Table B-5 (continued)

Ret Time	Area %	DRI Compound Assignment	Assumed Model Species
36.48	3.63	C12 Olefin	CYC-C12 or C12-OLE
37.15	0.47		
37.82	3.55	C12H22 olefin + methyl tetrahydronaphthalene	0.5 CYC-C12 or C12-OLE 0.5 CYC-C11
38.94	0.24		
39.84	0.15		
40.73	0.22		
41.41	0.20		
42.08	0.46		
43.42	0.14		
45.89	0.08		
47.24	0.04		
47.91	0.03		
48.36	0.03		
49.03	0.05		
50.37	0.05		
52.17	0.04		
53.74	0.03		
54.86	0.03		
55.31	0.04		
56.20	0.03		
56.87	0.03		
58.22	0.03		
58.67	0.04		
59.79	0.02		
60.24	0.03		
61.80	0.02		
62.48	0.03		
62.93	0.02		
63.82	0.02		
65.17	0.04		

Table B-6. Results of DRI GC-MS analysis of Mixture "B", and corresponding model species assignments.

Ret Time	Area %	DRI Compound Assignment	Assumed Model Species
10.59	0.03		
11.10	0.01		
11.48	0.04		
12.12	0.05		
13.01	0.05		
13.78	0.02		
14.16	0.02		
14.67	0.03		
15.56	0.02		
16.07	0.02		
16.58	0.02		
17.73	0.02		
18.11	0.16		
19.64	0.06		
19.89	0.14		
20.29	0.20	1-ethyl-4-methylcyclohexane	CYC-C9
20.58	0.02		
21.14	0.02		
21.42	0.19		
22.41	0.15		
22.97	0.37	Propylcyclohexane	CYC-C9
23.39	0.44	Ethylmethyl heptane	BR-C9
24.38	0.42	C4-alkylcyclohexane	CYC-C10
24.94	1.19	C10H20 Olefin	CYC-C10 [a]
25.37	0.64	Diethylnonane	BR-C13
25.79	0.67	Diethyhlcyclohexane	CYC-C10
26.63	0.56		
27.06	0.27		
27.34	0.16		
27.90	1.20	C4-Alkylcyclohexane	CYC-C10
28.46	2.09	C11H24 Paraffin	BR-C11
28.75	0.46	C11H24	BR-C11
29.45	1.46	C11H24	BR-C11
30.01	0.80		
30.87	12.29	Decahydronaphthalene	CYC-C10
31.32	1.18		
32.22	3.14	C5-alkylcyclohexane	CYC-C11
33.11	3.90	C5-alkylcyclohexane	CYC-C11
33.78	4.03	Trimethylphenylsilane + C11	BR-C11
34.23	2.16		
35.13	3.89	Pentylcychohexane	CYC-C11
36.48	12.70	C12H26 Paraffin	BR-C12
37.15	1.61	2-methyl-5-(1-methylethenyl) cyclohexane?	?
37.82	4.22	C12H22 Olefin	CYC-C12 [a]

Table B-6 (continued)

Ret Time	Area %	DRI Compound Assignment	Assumed Model Species
38.49	1.44		
39.84	2.15	C13H26 Olefin	CYC-C13 [a]
40.73	3.78	C6H13-Cyclohexane	CYC-C12
41.41	8.53	C13H28 + ?	BR-C13
42.08	11.87	C13H28 Paraffin	BR-C13
42.75	0.05		
43.20	1.61		
44.32	2.36	C14H28-Olefin	CYC-C14 [a]
47.68	0.09		
45.89	2.50	1-Tridecene	CYC-C13 [a]
46.56	2.35	C14H30 Paraffin	BR-C14
48.36	1.31	n-Tetradecane	N-C14
51.05	0.30		
52.84	0.28		
54.86	0.02		
55.53	0.02		
56.42	0.03		
57.10	0.03		
58.44	0.03		
58.89	0.03		
60.46	0.06		
61.13	0.03		
62.47	0.02		
64.04	0.01		

[a] Assumed to be a cycloalkane mis-identified as an alkene.

Table B-7. Results of DRI GC-MS analysis of Mixture "C", and corresponding model species assignments.

Ret Time	Area %	DRI Compound Assignment	Assumed Model Species
10.85	0.04		
11.61	0.03		
12.88	0.04		
21.70	0.03		
22.55	0.05		
24.38	0.30	Dimethyloctane	BR-C10
24.94	0.10		
25.79	0.15		
26.07	0.66	C5-alkylcyclohexane	CYC-C10
26.63	0.20		
27.06	0.09		
27.34	0.05		
27.90	0.26		
28.47	0.58		
29.45	0.93		
30.87	9.16	Decahydronaphthalene	CYC-C10
31.32	1.14		
32.21	3.48	Methyldecane	BR-C11
33.11	5.42	C5-alkylcyclohexane	CYC-C11
33.79	3.15		
34.46	4.11		
35.13	6.59	Pentylcyclohexane	CYC-C11
36.48	9.71	C12H26-Paraffin	BR-C12
37.15	0.92		
37.82	4.25	C12H22 Dodecadiene	CYC-C12 [a]
38.50	43.34	n-Dodecane	N-C12
39.84	1.04	C7-alkylcyclohexane	CYC-C13
40.73	1.11	C12 Olefin	CYC-C12 [a]
41.41	1.17	C13 Olefin	CYC-C13 [a]
42.08	1.20	C13H28 Paraffin	BR-C13
44.32	0.08		
45.89	0.05		
47.01	0.04		
48.13	0.05		
49.93	0.05		
50.82	0.03		
53.96	0.07		
55.76	0.03		
59.34	0.03		
60.01	0.04		
61.58	0.14		
63.82	0.05		
64.94	0.06		

[a] Assumed to be a cycloalkane mis-identified as an alkene.

Table B-8. Results of DRI GC-MS analysis of Mixture "D", and corresponding model species assignments.

Ret Time	Area %	DRI Compound Assignment	Assumed Model Species
11.36	0.07		
12.88	0.06		
17.09	0.06		
18.49	0.05		
20.30	0.07		
21.42	0.04		
22.97	0.08		
28.47	0.05		
30.02	1.69	Ethyl-trimethyl cyclohexane	CYC-C11
30.87	11.08	Decahydronaphthalene	CYC-C10
32.22	13.87	C5-alkylcyclohexane	CYC-C11
33.11	12.07	C5-alkylcyclohexane	CYC-C11
33.79	6.13		
34.46	7.44		
35.13	8.59	Pentylcyclohexane	CYC-C11
37.15	0.81		
36.48	16.33	C12H26 paraffin	BR-C12
37.82	4.72	C12H22 diene	CYC-C12 [a]
38.50	9.44	n-Dodecane	N-C12
39.84	1.12	C13H26 Olefin	CYC-C13 [a]
40.74	0.74	C6H13-cyclohexane?	CYC-C12
41.41	1.01	C13H28 paraffin	BR-C13
42.08	0.81	C13H28	BR-C13
43.43	0.21		
44.32	0.07		
47.46	0.06		
48.36	0.08		
49.70	0.05		
50.82	0.06		
53.96	0.05		
55.76	0.07		
59.56	0.12		
61.58	0.08		
62.25	0.08		
63.82	0.05		
64.72	0.05		
65.17	2.68		

[a] Assumed to be a cycloalkane mis-identified as an alkene.